NTNU
Det skapende universitet

Emisjon av ultrafiolett lys fra positive streamere i sykloheksan

Jarl Øystein Samseth

Master i fysikk og matematikk
Innlevert: juli 2016
Hovedveileder: Steinar Raaen, IFY
Medveileder: Lars Lundgaard, SINTEF Energi

Norges teknisk-naturvitenskapelige universitet
Institutt for fysikk

Summary

Liquid insulation breaks down under high electric stress due to a phenomenon called streamers. Streamers are conducting channels of gas or plasma, and as electric field increases in the bulk, streamers propagate faster. Streamers may swiftly change between different modes of propagation, where the velocity differs by a factor ten.

A suggested mechanism behind the fastest propagation modes (third and/or fourth mode), is photoionisation. This mechanism requires photons with sufficient energy to ionise molecules ahead of the streamer, to be emitted frequently from the streamer. Based on field dependent ionisation potential and the excitation levels of cyclohexane, these photons are expected to be in the UV domain.

In this experiment, positive streamers propagated along the surface of fused silica glass, which is transparent for photons up to $7.7\,\mathrm{eV}$. The light was filtered through different filters, but the main filter was a UV bandpass filter with peak transmittance at $200\,\mathrm{nm}$. The test cell had needle-half-plane electrode geometry and gap distance $4\,\mathrm{mm}$. Square voltage pulses were applied, with amplitudes up to 80 kV.

The hypothesis that streamers emit UV light frequently in third mode, is supported by this experiment. Third mode streamer heads appear to emit UV light continuously, which makes photoionisation possible in third mode, while second mode only emit photons sporadically. The amount of photons increased only slightly with applied voltage where the second propagation mode dominated.

The effect of the glass and electrode geometry on breakdown velocity, is also discussed. The minimum voltage where streamers propagate in fourth mode, was observed to increase drastically from the experimental setup where streamers propagated in the bulk of cyclohexane, to the setup where streamers propagated along the glass. It is argued that shielding effects by different components in the test cell, most likely have caused this change.

Sammendrag

Isolerende væsker for elektriske komponenter, går til gjennomslag ved høyt elektrisk felt grunnet et fenomen kalt streamere. Streamere er elektrisk ledende kanaler av gass eller plasma som propagerer raskere desto høyere den elektriske feltstyrken er. Streamere kan ha brå overganger mellom ulike måter å propagere på, kalt propageringsmoduser, der hastigheten endres med en faktor ti.

Fotoionisering er foreslått som en dominerende mekanisme ved de raskeste (tredje og/eller fjerde) propageringsmodusene. Denne mekanismen forutsetter at streameren utstråler fotoner med tilstrekkelig energi til å ionisere molekylene foran streameren. For sykloheksan er disse fotonenergiene forventet å være i UV området. Dette er basert på det feltavhengige ioniseringspotensialet til sykloheksan i forhold til eksitasjonsnivåene.

I dette eksperimentet propagerer positive streamere langs et vindu som er gjennomsiktig for fotoner opp imot $7.7\,\mathrm{eV}$. Prøvecella består av ei nål plassert over enden til en planelektrode. Gapavstanden var $4\,\mathrm{mm}$. Firkantpulser med amplitude opptil 80 kV, ble påtrykt.

Resultatene underbygger hypotesen om at tredje modus-streamere hyppig utstråler UV lys, hvilket muliggjør fotoionisering som propageringsmekanisme ved denne modusen. Hyppigheten av UV-fotoner sammenfaller nemlig godt med akselerasjonen fra andre til tredje modus. Antallet utstrålte fotoner fra streamerhoder ved andre propageringsmodus, øker litt med økende påtrykt spenning.

Effekten glasset og elektrodegeometrien har på gjennomsnittshastigheten til gjennomslag, blir også diskutert. Konklusjonen er at skjermende effekter fra elektrodene trolig har ført til at fjerde propageringsmodus først inntreffer ved høyere spenning for streamere i dette eksperimentet, enn om streamerne hadde beveget seg lenger unna glasset i et nål-til-planelektrode-oppsett.

Preface

This master thesis is the final work in my applied physics' degree, and is submitted to the Norwegian University of Science and Technology (NTNU). Experimental work has been performed at Sintef Energy with Torstein Grav Aakre as main supervisor. Internal supervisor has been Steinar Raaen.

Five oscilloscopes and several broken glasses later, we have come one step closer to a better detection of streamer UV light. And still there is much left to improve in the lab. To whoever's coming after me: good luck, you'll get stuck, but try a bunch of hours and the victory will be ours (or yours).

I would like to thank Torstein Grav Aakre, my main supervisor, for good cooperation, guidance and help with this experiment, and his collegues at SINTEF; Øystein Hestad, Dag Linhjell and Lars Lundgaard for productive discussions and important information on the topic.

Massive thanks are sent to Magnus Reiersen, my best friend, who prayed for me and made me a computer program needed in both analysis and to properly present some image results. And massive thanks to Bergljot Matre Gåsland, for good discussions, encouragement, working breaks and being a patient listener. I would also like to thank all my friends who patiently have waited as I have arrived too late for anything due to "something I had to finish in the lab".

Contents

Abbreviations and Nomenclature

A list of abbreviations and variables is presented below. The list is sorted alphabetically (latin before greek), first for abbreviations, then for nomenclature.

AV	=	Applied voltage
ETA	=	estimated time of arrival (for a streamer head in Photomultiplier's field of view)
F0	=	The optical system with no additional filter
F1	=	UV bandpass filter - peak at 200 nm
F2	=	longpass filter with cut-off at 280 nm
FOV	=	Field of view, usually referring to the photomultiplier
MCP	=	Microchannel plates
PM	=	Photomultiplier
UV	=	Ultra-violet, as in light domain below 400 nm

d	=	Gap distance between needle and plane electrode
h	=	Entrance window height
h_s	=	Height of the slit
IP	=	Ionisation potential
$MDLI$	=	Mean detected light intensity, according to equation (3.5)
pt	=	passing time - time for streamer head to pass the entrance window
P	=	Radiant power
p	=	Spectral power
S	=	Radiant sensitivity
T	=	Transmittance
$t_{10\%}$	=	10% of applied voltage pulse on its rising edge
$t_{90\%}$	=	90% of applied voltage pulse on its rising edge
t_{BD}	=	90% of applied voltage pulse on its falling edge, due to breakdown
t_{entry}	=	Time of entry in PM's entrance window for a leading streamer head
t_{fs}	=	Time of first spike appearing in the interval [t_{sc}, $ETA(v_{BD}/10)$]
t_{sc}	=	time when reference camera shutter closes
t_{so}	=	time when reference camera shutter opens
V_a	=	Acceleration voltage
V_b	=	Breakdown voltage, where probability of breakdown is 50%
v_{BD}	=	Breakdown velocity - average velocity from streamer inception to breakdown
V_I	=	Measured voltage of the intensity, as recorded by the oscilloscope
x	=	Distance between entrance window frame and streamer head in reference image
λ	=	Wavelength

Chapter 1

Introduction

Liquid is commonly used as electrical insulation of high voltage components, like transformers. The voltage that can be applied across an insulation, is limited by its withstand strength from breaking down, cause when it does, the component is short circuited[1]. A liquid insulation breaks down when a streamer bridges the electrodes on each side of it. Streamers are conducting gas or plasma channels that propagate in liquid under high electric stress[2].

In order to improve insulation liquid properties, the mechanisms behind streamer propagation should be known. That way models and characteristics of streamers can tell what type and mixture of liquids will have the greatest withstand strength against breakdown.

The velocity of streamers determines how wide the equipment's insulation must be in order to not break down during a critical voltage pulse amplitude and duration [1]. The faster the streamer, the wider must the insulation be relative to the voltage pulse duration.

Streamers have been observed to propagate faster with increasing voltage, ranging from 0.1 to several hundred mm/µs [3]. At some voltages the velocity may even increase with a factor of ten during propagation of a single streamer [3]. Each order of velocity is defined as a propagation mode, where different mechanisms are suspected to dominate. Some proposed theories that are believed to explain the slower propagation modes, are Townsend mechanism together with Joule heating [4] . However, the fastest streamers (10-100 km/s corresponding to third and fourth mode) have yet to be understood.

One hypothesised mechanism to cause the acceleration from second to fourth mode streamers, is suggested : Photons emitted from the front of a streamer, ionise the molecules in the volume in front of it. This is called the photo-ionisation mechanism and is expected to enhance the electron avalanche production.

As electric field strength E increases, ionisation potential (IP) decreases [5]. If photo-ionisation is a dominant mechanism in a streamer mode, the field where $IP(E)$ is reduced to the energy of frequently absorbed photons, will coincide with the field where streamers are observed to transition/accelerate into that mode . This will be seen as an acceleration.

It is therefore of interest to find the highest photon energy being emitted frequently from a streamer. The highest excitation energies in many liquids molecules that are relevant in streamer modelling, are found in the ultra violet light (UV) domain[5, 6]. For cyclohexane wavelengths below 180 nm are most relevant. A challenge so far, has been that the relevant photon energies for photoionisation are absorbed by the liquid insulation and has therefore never been measured before.

In this thesis the photo-emission in the UV domain will be studied. The experimental setup is what makes this work unique: A glass window transparent in the UV domain, is put tangent to a positive needle electrode where the streamers are expected to initiate. That way streamers may propagate along the glass. This allows us to detect photons from streamers, that otherwise would have been absorbed by either liquid insulation or glass windows in a test cell.

The purpose of this thesis is to test the following hypotheses:

1. Third mode streamer heads in cyclohexane, emit photons frequently in the UV domain.

2. Fourth mode streamer heads in cyclohexane, emit photons frequently in the UV domain.

Streamer head is another name for the tip of a streamer channel. A correlation study between velocity and the emitted light pulse intensity is also performed on streamers in cyclohexane.

The streamer propagation in cyclohexane along a glass surface is also studied. For streamers along a glass surface, the breakdown velocity distribution over applied voltage pulse amplitudes, is compared with results from an earlier experiment where the streamers propagated inside the liquid.

At the end of this thesis, the radiant power in the UV domain will be estimated based on different spectrum models. Streamer emission spectrum in this domain, is unknown, but desired in an ongoing modelling of streamer propagation with the photo-ionisation mechanism implemented [7].

Chapter 2

Theory

The first section in this chapter, introduces the reader to streamers, propagation modes and light emission characteristic for these modes. The second section explains the proposed mechanisms behind streamer propagation. Third section contains a description of photomultipliers and how they work. In the fourth section a point source model of streamer heads, is deduced in order to calculate its radiant power based on detections of light by a photomultiplier. The last section briefly presents the electric field in two, relevant electrode geometries.

2.1 Streamers

A streamer is defined as a structure visible in shadowgraphic or schlieren images in liquids when stressed by a high electric field [8]. Later it has been discovered that light is refracted through streamers because they appear to be gas or plasma filled filaments in a liquid[2, 4]. These filaments propagate as ionisation waves where the released electrons are believed to cause evaporation at the streamer head [1, 2, 4]. These channels conduct electrons better than the liquid.

A streamer head is the propagating front of a streamer channel. Its tail is the channel in the wake of the head.

Streamers are initiated at protrusions from electrodes or contamination particles in the insulation material, due to the high electric field surrounding them[1, 8].

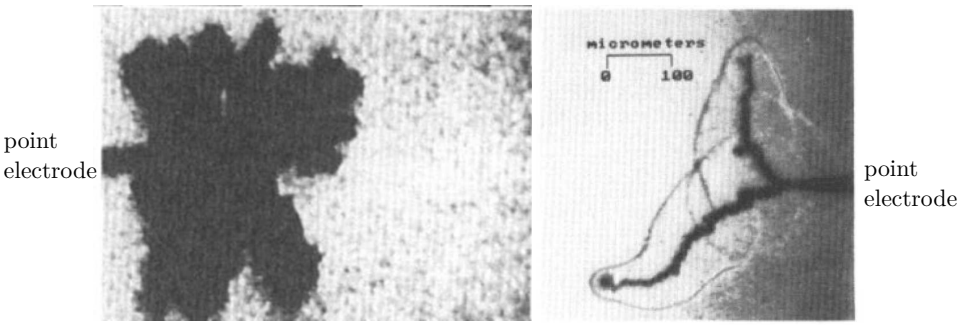

Figure 2.1: Examples of a) first mode streamer in cyclohexane and b) second mode streamer in pentane. Figure a) is copied from [11] and b) from [12]. The ripples around the streamer in b) are shock waves.

Streamers are polarity dependent [9, 10]. In this master thesis only positive streamers are discussed. Positive streamers initiate at the positive electrode.

2.1.1 Streamer Modes

Streamer modes are distinguishable by appearance, velocity, current and light emission [3]. In 1993 Gournay et al. distinguished two types of streamers in cyclohexane and pentane[11]. Later, four streamer modes were defined by their velocities, for oil [3]The propagation velocity between each mode differs with a factor of ten. First mode propagates with velocity of order $0.1\,\mathrm{mm}/\mu\mathrm{s}$, second mode at about $1\,\mathrm{mm}/\mu\mathrm{s}$, and so forth.

First mode streamers are shaped like bushes, while the higher modes are filamentary structured. Examples of first and second mode are depicted in Figure 2.1. First mode streamers are barely luminous in cyclohexane, while light pulses are emitted more intensely and frequently with increasing streamer mode[11].

Second mode streamers in large gaps of oil were observed to initially glow weakly, from numerous channels[3]. After this stage only the streamer head glowed continuously, with periodically occurring re-illuminations[2, 3]. An example of this is depicted in Figure 2.2, where the first glowing stage ends at time t_1. The first stage lasted shorter and shorter as the

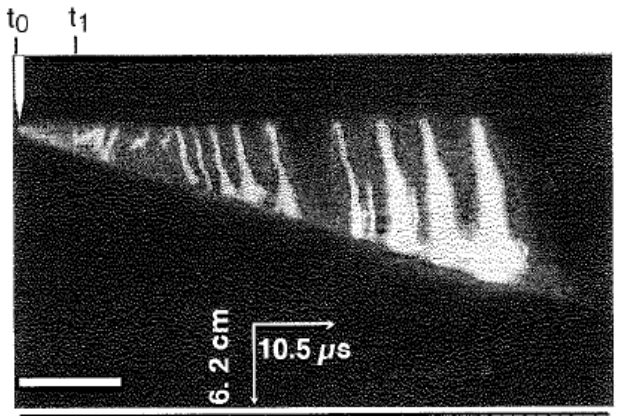

Figure 2.2: A typical streak photo of a second mode streamer in oil. This streamer stops before it reaches the plane electrode. Re-illuminations appear periodically. The photo is copied from [3].

voltage increased, until it disappeared at breakdown voltage. However, in shorter gaps (a few centimeters) the first stage could propagate all the way to breakdown with no re-illumination appearing.

Re-illuminations are depicted in Figure 2.2. Re-illumination is when entire streamer filaments flashes, from head to inception point[2]. It usually occurs periodically in oil[3]. These occur temporarily and each re-illumination coincide with a current pulse[2, 3]. Re-illuminations appear like partial discharges and are assumed to raise the streamer head potential to the same potential as the needle electrode [2].

Third mode in oil is more luminous and branched than second mode, but heads glow and re-illuminations are featured like second mode[3]. A maximum of two highly luminous filaments form the fourth mode streamer in oil [3]. The total light from the streamer, rapidly increases as fourth mode gets closer to the plane electrode.

Several modes during propation

A streamer can transition between modes during propagation. In Figure 2.3 different combinations of modes are marked in the distribution of velocity against voltage pulse amplitudes applied, for positive streamers in transformer oil. Around breakdown voltage [1] second mode streamers crossed the gap from needle to plane electrode. At higher voltages the streamers initiated as third mode and transitioned into second mode during propagation. A steep acceleration started at the acceleration voltage V_a,

[1] Breakdown voltage V_b is the voltage where the breakdown probability is 50%.

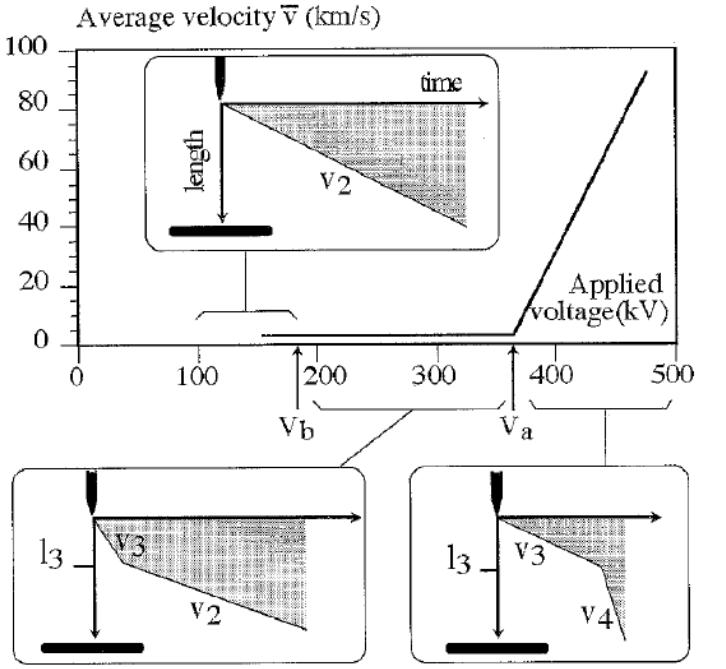

Figure 2.3: Average velocity to breakdown (i.e. breakdown velocity) versus applied voltage in transformer oil, is shown. Different combinations of modes seen in streak photo schematics. Streak photos presents a streamer's position versus time. Gap distance was 10 cm. Figure has been copied from [3].

where third mode streamers transitioned into fourth mode.

Instantaneous velocity

The instantaneous streamer velocity depends on the local electric field relative the physicochemical properties of the liquid [10, 13]. With Nytro10X in a 67 mm gap between the electrodes, Lundgaard et al. observed that the streamer began 5 times faster than it ended at the plane electrode[2]. The streamers propagated with minimum velocity approximately halfway through the gap, as seen in Figure 2.4.

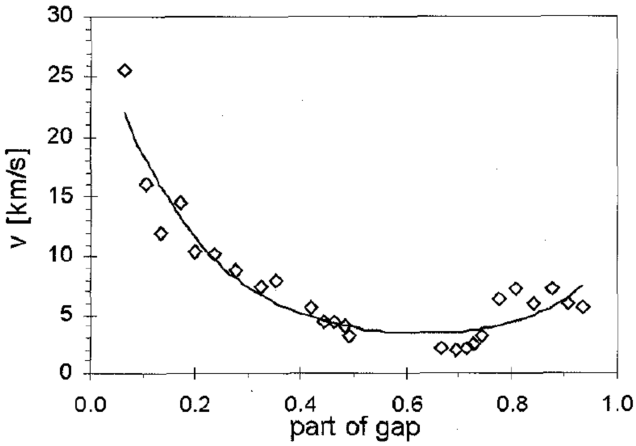

Figure 2.4: Instananeous velocity at different propagated distances for positive streamers in oil, taken from three different streamers at 290 kV. Gap distance was 67 mm. The graph is copied from [2].

Mean velocity

Breakdown velocity is the average velocity during the streamer propagation across the entire gap, from initiation to breakdown. For a mode transition from velocity v_1 to v_2 at time t, breakdown velocity v_{BD} is expected to be

$$v_{BD}(t) = \frac{t}{T}v_1 + (1 - \frac{t}{T})v_2 \tag{2.1}$$

T is the time when breakdown occurs.

If velocities are given, the position x_1 in the gap where the streamer changes mode, can be calculated. Let's assume the average velocity of the in front of and behind this position, are v_1 and v_2, respectively. Then

$$T \cdot v_{BD} = d, \tag{2.2}$$

$$t_1 + t_2 = T, \tag{2.3}$$

$$t_i = \frac{x_i}{v_i} \tag{2.4}$$

$$\text{and} \quad x_1 + x_2 = d \tag{2.5}$$

$$\text{imply} \quad \frac{x_1}{d} = \frac{(\frac{v_2}{v_{BD}} - 1)}{(\frac{v_2}{v_1} - 1)} \tag{2.6}$$

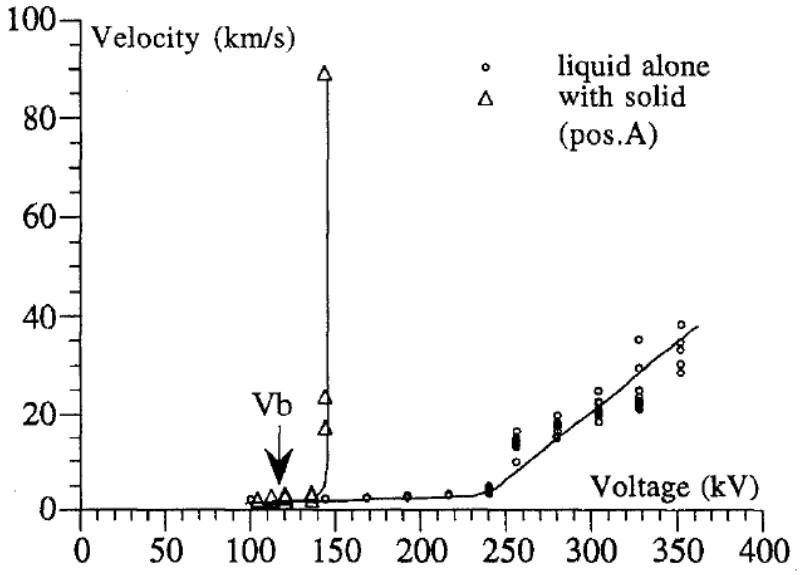

Figure 2.5: Average velocity for streamers crossing a 5 cm gap in mineral oil with and without pressboard aligned with the propagation direction [14].

Here d is the gap distance and x_i is the distance where the streamer propagates with average velocity v_i over a time t_i, $i = \{1, 2\}$. If the transition happens in the first half of the gap, $x_1 < d/2$, then

$$v_{BD} > \frac{2v_1v_2}{v_1 + v_2} \tag{2.7}$$

2.1.2 Streamers along Insulating Surfaces

The presence of a solid insulator, like pressboard, parallel to the electric field, enhances the propagation of streamers in mineral oil [14]. This is shown in Figure 2.5, where streamers accelerate from second mode at a lower voltage once a pressboard is present. The breakdown velocity was, however, unaffected by it. The velocity increased only slightly between V_b and V_a.

Lesaint and Massala proposed an hypothesis that streamer channels shield [2] each other and therefore propagates slowly (at 2- $3\,\mathrm{mm/\mu s}$) be-

[2]Shielding is when the presence of a charge reduces the field at the surface of another

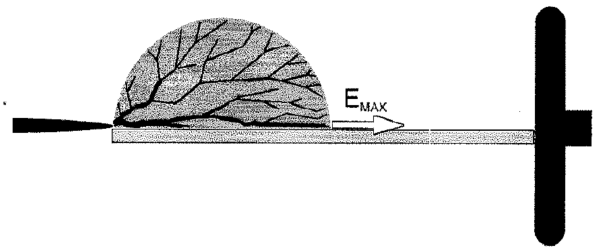

Figure 2.6: Model of streamer along solid insulation. Figure is copied from [2].

tween V_b and V_a [14]. They further proposed that, at V_a, the shielding effect was reduced, and the streamer therefore accelerates. The presence of a solid parallel to the propagating direction, would therefore remove the shielding on half the side of a streamer. This explains why V_a decreased so significantly in the presence of a pressboard. A model of a propagating streamer along a solid insulation, is sketched in Figure **??**.

Lundgaard et al. reported that streamers burned tracks into the pressboard surface when propagating along it[2]. This would enhance the streamer propagation along that surface. Space charges on the surface can also attract soot from the liquid when it has been carbonated.

Allen et al. reported that the streamer velocity along a solid surface in *air* (parallel to the field), depended on the surface material [15]. The streamers along organic insulations like PTFE, were faster than in air alone. Photo-emission has been suggested to contribute with electrons to electron avalanches in gases [15, 16]. Unlike the organic solids, the propagation velocity along a ceramic insulator was similar to the streamers in air alone [15, 17]. These streamers propagated almost invariant of applied voltage amplitude.

Dielectric interface

The effect of introducing a solid insulation in a capacitor, with higher permittivity than the liquid, is that the electric field component orthogonal to the solid-liquid interface increases on the liquid side. And when that high permittivity is installed tangent to a sharp electrode, the field is concentrated around that electrode. This is because the displacement field is con-

object. One example is the accumulation of space charges in front of an electrode. Another example is the use of shields: metal close to or surrounding an electrode with the same electric potential.

served across the interface where the permittivity changes, given that no charge is present on that interface. The argument is deduced as follows.

Gauss law states that

$$\nabla \vec{D} = \rho$$

where ρ is the charge density. $\vec{D} = \varepsilon \cdot \vec{E}$ is the displacement field, with permittivity ε and electric field $\vec{E}$.

With the displacement orthogonal to the interface of two media with different permittivities ε_1 and ε_2, the displacement is conserved: $\varepsilon_1 E_1 = \varepsilon_2 E_2$. The voltage along a displacement field line is

$$V = E_1 d_1 + E_2 d_2, \tag{2.8}$$

where $d = d_1 + d_2$ is an arbitrary distance. Combining these equations the voltage becomes

$$V = E_1 (d_1 + \frac{\varepsilon_1}{\varepsilon_2} d_2). \tag{2.9}$$

Lets assume another case where $\varepsilon_1 = \varepsilon_2$. The field $E = V/d$. For equal voltages V across the same distance d, the fields in the medium 1 can be compared for the two cases:

$$E = E_1 \frac{(d_1 + \frac{\varepsilon_1}{\varepsilon_2} d_2)}{d}. \tag{2.10}$$

Therefore, if $\varepsilon_1 < \varepsilon_2$, then the field $E < E_1$. In other words: With medium 1 alone the field is lower than with a medium of higher permittivity present, at the same voltage.

2.2 Streamer Propagation Mechanisms

First mode streamers are believed to propagate due to Joule heating and Townsend mechanism combined[4]. Joule heating is when a resistive medium is heated due to electric current running through it. As liquid is too dense for Townsend mechanism to explain the observed breakdown voltages in streamers, Joule heating is required to expand the liquid [4]. Electrical discharges may then take place inside the gas or plasma channels created[3]. In

[3]The primary mechanism for electrical discharges in air, is the Townsend mechanism [1].

this way the channel works as a conducting extension of the electrode it originated from, and the potential is moved through a gas cavity towards the opposing electrode.

In this section Townsend mechanism will be described, followed by an explanation of how photo-ionisation is thought to enhance streamer propagation. At last, possible photon energies emitted from cyclohexane molecules, are presented. In appendix C the general processes of ionisation, excitation and photon emittance, are explained in more detail.

2.2.1 Townsend Mechanism

Townsend mechanism describes the propagation of charges by electron avalanches[1]. A positive Townsend discharge starts with a seed electron produced close to an anode. Seed electrons arise as a molecule is ionised, either by background radiation, thermal energy released in the collision between molecules, or due to a high field that reduces the ionisation potential significantly for the electron to tunnel through the potential barrier. Such high fields are typically found near protrusions from electrodes or small, conducting objects within an insulation (contaminations).

The seed electrode then accelerates towards the anode due to the electric field and, depending on the energy it has gained, ionises molecules by inelastic collisions[1]. The sequential multiplication of free electrons form an avalanche.

In the wake of avalanches, positive ions are left in front of the positive electrode[1]. Hence the field is increased ahead of these ions and field ionisation have higher probability of happening.

The electrons gain energy as they are accelerated by the electric field. The longer the (mean) free path is between each collision, the higher energy is attained[1]. The distance between particles is lower in a dense gas, thus the probability of collision increases with decreasing density. In short the energy of electrons in an avalanche depends on the ratio between the electric field and the gas density. A fraction of this energy will then be transferred to a molecule in an inelastic collision, hence the rate of ionisation is proportional to the free electron energy[1].

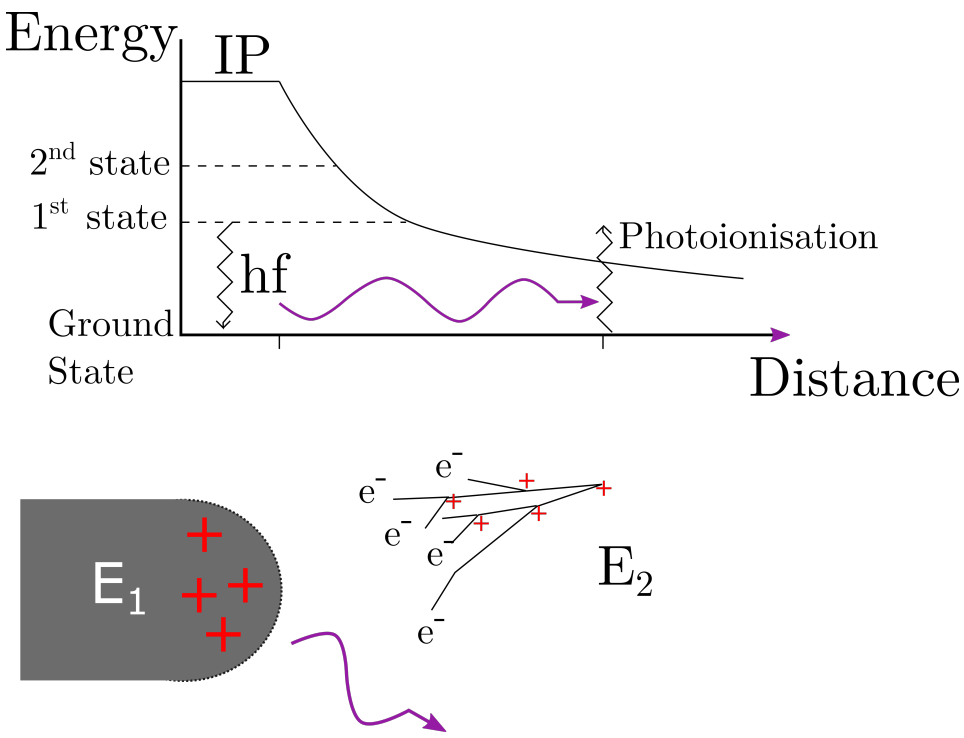

Figure 2.7: A streamer ion de-excites from first excited state. The electric field $\vec{E}_1$ is low due to space charges. The emitted photon with energy hf is absorbed not far from the streamer, where the field strength E_2 is high. Since the ionisation potential $IP(E_2) < hf$, the molecule is ionised and a seed electron is produced.

2.2.2 Photoionisation as Propagation Mechanism

The hypothesised photoionisation mechanism for streamers, is: Liquid molecules ahead of the streamer is ionised by photons emitted from the streamer. This process is illustrated in Figure 2.7. This is possible if photons generated in a low-field region, are absorbed in the high-field region near a streamer[5].

In the wake of an avalanche, the molecules are likely to be excited ions [1]. As they de-excite, the energy is either released as thermal energy or photons are emitted with energy $hf < IP(\vec{E}_1)$[5]. Due to all the space charges in the streamer head, the field $\vec{E}_1$ is reduced there, according to Gauss' law. However, in front of the streamer head the field $\vec{E}_2$ strength is still high and divergent. Hence, if a photon with sufficient energy is emitted from the streamer filament, molecules in the high field nearby, may

be photo-ionised, as illustrated in Figure 2.7.

A stepwise excitation is also possible. A combination of excitation by electron impact and absorption of a photon within the life-time of the excited state, will result in ionisation[5]. Hence partial photoionisation is a also a way that radiation can enhance the electron avalanches in front of a streamer head.

2.2.3 Photoemission from Cyclohexane Streamers

Davari et al. calculated the excited states of cyclohexane, as presented in Figure 2.8. First excited state is $7.0\,\mathrm{eV}$ above ground state, which corresponds to 177 nm wavelength [6]. The IP is reduced from $10\,\mathrm{eV}$ as the electric field increases, which causes the lowest excitation states to disappear in the range 5 to $15\,\mathrm{MV/cm}$ [6].

Absorption and emission spectra for a molecule are expected to be the same [18]. Hence the absorbed wavelength domain of a liquid may coincide well with the domain of emitted photons from a streamer in that liquid. Nytro10XN and cyclohexane absorb UV, with a longpass cut-off at $330\,\mathrm{nm}$ and $220\,\mathrm{nm}$, respectively (see Figure 6.1 in Appendix)[unpublished, SINTEF, Internal communication].

Photo-emission spectrum depends on the energies absorbed by the molecules. In electron avalanches, electron energy is transferred to the molecules when they collide[1]. The probability that a particle's state is occupied, is given by the Maxwell-Boltzmann distribution[19]. This theory describes the probability distribution over kinetic energy (or velocity) of particles in a system, as function of the root mean square velocity v_{rms} of these particles. It was deduced that more of the particles attained higher energies when v_{rms} increased. Electrons are accelerated by the electric field, which is proportional to applied voltage[1]. Hence the energy of emitted photons from streamers and the amount of the photons at these energies, are expected to increase with increasing voltage applied.

2.3 Photomultiplier

There are many designs for photomultiplier tubes (PM tubes) [20]. PMs are generally used because they are highly sensitive photon detectors with fast

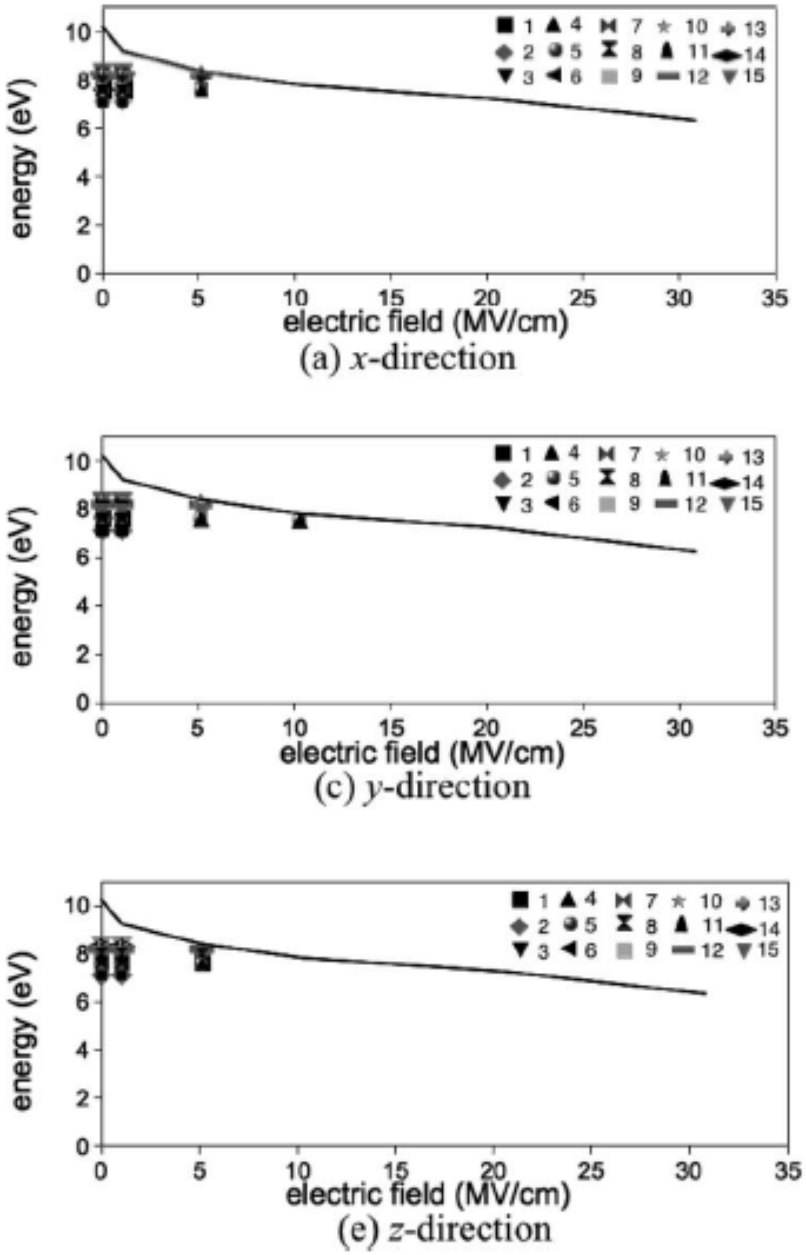

Figure 2.8: The ionisation potential and first excitation levels of cyclohexane with the electric field in different orientations, have been calculated using density function theory (DFT). Cyclohexane molecule is oriented with cylindrical symmetry around the z-axis. The figure is copied from [6].

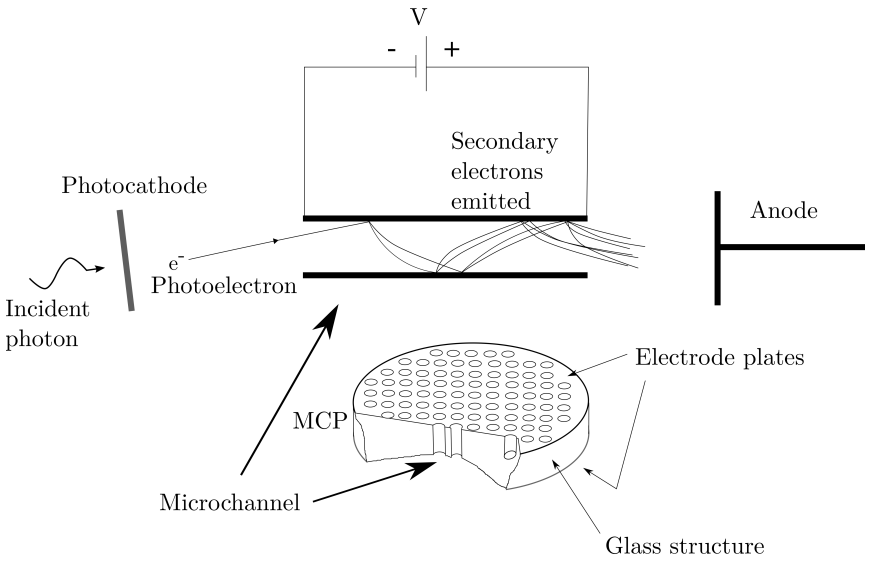

Figure 2.9: The principle of a photomultiplier tube consisting of a microchannel plate in vacuum [20]: The cathode emits electrons when photons collide with it. The photoelectron collides with the walls of a microchannel and secondary electrons are released. The cascade of electrons are collected by the anode. MCPs are resistive components made of glass.

respons time. The general principle is to amplify the intensity of incoming photons, by exciting a photocathode with photons, which then emits electrons that are multiplied and absorbed by an anode [20].

The relevant PM tube for this thesis, consists of a semitransparent photocathode, microchannel plates (MCP) in series and an anode. Microchannels' time responses are fast and have good immunity against magnetic fields [20].

The trajectory of an electron through an MCP PM tube, is sketched in Figure 2.9. A semitransparent photocathode that is hit by a photon, may emit an electron on the other side [20]. This photon-emitted electron (photoelectron) accelerates towards the MCP where it bounces between the walls of a microchannel. The voltage across a photomultiplier tube and the microchannels inside it, accelerates the electrons. Due to this acceleration, secondary electrons are emitted as electrons collide with the microchannel walls. At the end of the MCP a cascade of electrons exits and are absorbed

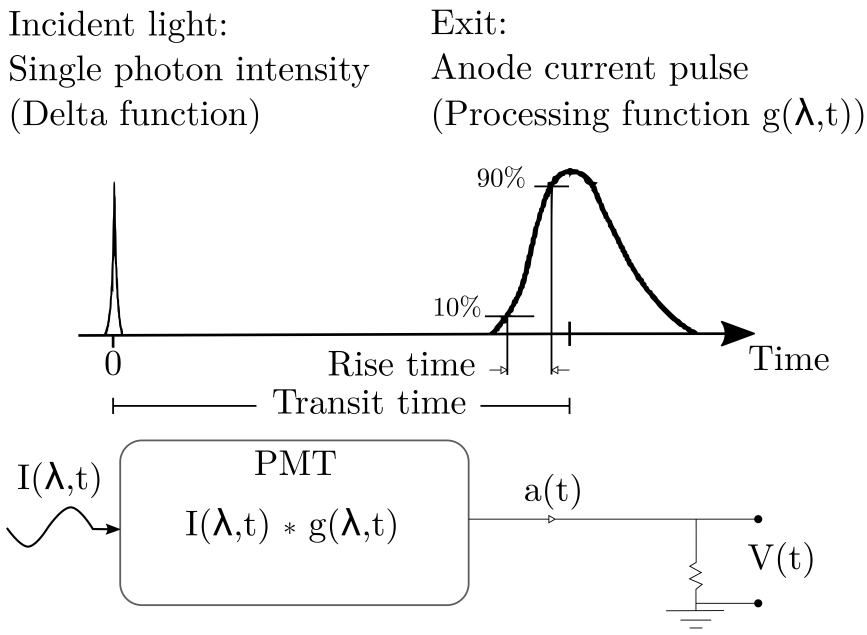

Figure 2.10: The photomultiplier processes the incident light by convolution. A single photon signal will be transformed into the anode current pulse of the shape sketched in this figure. The corresponding voltage is measured across a resistor R.

by an anode. The current through this anode is measured.

2.3.1 Signal Processing

Incident light signal is delayed and changes waveform as it is processed by the PM. This is due to the electron transit time t_t and the anode pulse response time [20]. Transit time is the time for a signal to pass through the PM. A sample pulse of a single photon at 410 nm is shown in Figure 2.10 [21]. It is processed by convolution according to equation (2.11), where the PM's processing function $g(\lambda, t)$ also is illustrated in Figure 2.10.

$$a = I(\lambda, t) * g(\lambda, t) \tag{2.11}$$

a is the anode current and I is the incident intensity as function of wavelength λ and time t.

The PM tube filters the incident signal spectrum in two steps. First the

glass window filters the intensity, given by its transmittance. Then the photocathode responds differently to different frequencies, known as radiant sensitivity . When the supply voltage is high, which it usually is, the differences in photoelectron energies are negligible. Hence the MCP filtering is not perceptible.

Radiant sensitivity S is the ratio of photoelectric current to incident radiant power P, in units Ampere/Watt [20]. This current is magnified through the MCP by a gain G which increases with increasing voltage supplied across the PM. The photomultiplier integrates the incident light power P across all wavelengths λ. The current a exiting the anode is therefore

$$a = G \int P_{(\lambda)} \cdot S_{(\lambda)} \, d\lambda \tag{2.12}$$

.

Quantum efficiency (QE) is the amount of incoming photons divided by photoelectrons exiting the photocathode [20]:

$$QE = S \cdot \frac{hc}{\lambda} = S \cdot \frac{1240\,\mathrm{W} \cdot \mathrm{nm/A}}{\lambda} \cdot 100\% \tag{2.13}$$

hc/λ is the energy of a photon with wavelength λ. h is Planck's constant and c is the speed of light.

Dark current is the anode current when the photomultiplier tube operates in complete darkness [20]. Any noise and offset in this background current may be caused by the high voltage supplied, thermionic emission of electrons, glass scintillation, ionisation of residual gases, ohmic leakage and/or field emission. These possible noise sources in a photomultiplier, are described in more detail, in appendix D.

2.4 Point source model

In this section a point source model of a streamer head, is presented. The relation between the power of light emitted from a point source and the detected intensity at a photomultiplier, is deduced. The light traverse a lens and some filters, so the conservation of light power must be considered. The theory is based on geometrical optics as presented in [19].

2.4.1 Optics

The entrance pupil of an optical system is the image of the aperture stop that defines the marginal rays. The exit pupil is the image of the entrance pupil on the other side of the system. Entrance window and exit window are images of the field stop through the optical system. The field stop defines the chief ray through a system.

The location and height of an object and its image, can be calculated to first order approximation by lens-maker equation

$$\frac{1}{f} = \frac{1}{s_1} + \frac{1}{s_2}, \tag{2.14}$$

and the magnification M of the object through the optical system[19]:

$$M = \frac{s_2}{s_1} = -\frac{y_1}{y_2}. \tag{2.15}$$

Here, s_2 is the distance from an image with height y_1, to the principal plane of a lens (or set of lenses) with focal length f. s_1 is the distance from the object to the principal plane H_1. Object height is y_2.

Marginal ray

All rays of light that traverse the optical system, are confined within entrance window and pupil of a system. Marginal rays are defined as the rays that intersect the optical path at the entrance window and touches the entrance pupil edges.

The angle between two conjugate, marginal rays is defined as the numerical aperture (NA) and indicates how much of the light from a point at the entrance window, will traverse the optical system. With an entrance window located a distance z from the entrance pupil with diameter D, the numerical aperture becomes

$$NA = 2 \cdot \arctan \frac{D/2}{z}. \tag{2.16}$$

Power conservation and transmittance

Let's assume perfect imaging, where all light from a point in the object plane is focused onto the same point in the image plane, regardless of the

ray's angle relative to the optical path. Then the radiant power is conserved between image and object as long as no light is absorbed on the way.

Now, consider an optical system of lenses and filters with total transmittance T. Transmittance is the ratio of transmitted and incoming intensity. Hence the total transmittance of a series of filters will be the product of their transmittances. Power is related to intensity as follows: $P = \int_0^A I dA$. With a uniform transmittance distributed over a cross section A of light beams, the final power $P_f = TP_i$, where P_i is the radiant power incident to the set of lenses and filters. With this in mind and perfect imaging between entrance and exit window, the power at the exit window will be

$$P = T \cdot P_0, \tag{2.17}$$

regardless of the magnification. P_0 is the radiant power in the entrance window.

2.4.2 Radiant Power of Point Source

Let a point source of be placed in the entrance window, on the optical axis. Further, let's assume that this source emits light isotropically, with radiant power P_s. Then the fraction of light emitted through the system will be given by the solid angle of the marginal rays, relative to a sphere.

The solid angle of a circular entrance pupil with diameter D, a distance z away from a point source, is

$$\Omega = \int_0^{NA} \int_0^{NA} \sin\theta \, d\theta \, d\phi = 2\pi(1 - \cos(NA/2)) \tag{2.18}$$

where NA is given by equation (2.16).

Ultimately the radiant power P at the exit window of an optical system, becomes

$$P = T \cdot \frac{1}{2}(1 - \cos(NA/2)) \cdot P_s \tag{2.19}$$

relative to the P_s is the point source radiant power.

From point source to detector

The emitted light from a point on the optical axis in an entrance window, will traverse filters with total transmittance T and enter the detector, i.e. a

photomultiplier. Photomultipliers have a probability of detecting a photon with wavelength λ, which is represented by radiant sensitivity S in units mA/W.

The current from a photomultiplier anode is measured across a resistor R. The measured voltage, also called intensity voltage V_I, is therefore related to the spectral power $p_s(\lambda)$ from a point source at the entrance window, as given by equation (2.20).

$$V_I = R \cdot G \int S_{(\lambda)} \cdot T_{(\lambda)} \cdot \frac{1}{2}(1 - \cos(NA/2)) \cdot p_{s\,(\lambda)}\, d\lambda, \tag{2.20}$$

according to equations (2.12) and (2.19). Note that spectral power is radiant power per wavelength: $p_s(\lambda) = \frac{dP_s}{d\lambda}$.

2.5 Electric Field and Electrode Geometry

The electric field at the tip of a hyperbolic shaped (needle) electrode above an infinite plane, is calculated using the hyperbolic approximation

$$E_{hyp} = \frac{2V}{r \cdot \ln(\frac{4d}{r})}, \tag{2.21}$$

with tip radius r and applied constant voltage V [11, 22]. The gap distance d is the distance between needle tip and plane in this needle-plane electrode geometry.

Now, let's move the needle electrode to a position above the edge of a finite, plane electrode. The field increases with increasing curvature. An infinite plane may be seen as a surface with zero curvature. If one bends it at one point, a sharp edge is created, with greater curvature. The field close to the corner of a half-plane is therefore greater than the field at a plane electrode. Also, the electric field in the middle of the gap is lower in a needle-half-plane geometry than in a needle-plane geometry. This is because the integrated electric field between the electrodes must be the same in both cases, for voltage to be conserved.

Chapter 3

Experimental Setup and Procedure

In this chapter the experimental setup is described, then the sample liquids are presented, followed by the procedure used to attain the results in the laboratory. The last section will explain the analysis performed on the recorded data. The section on the experimental setup is divided into the subsections about the test cell, the optical system used to focus the light from streamers onto a photomultiplier, the reference camera and at last the pulse from the voltage source is presented.

3.1 Setup

The experimental setup is presented in Figure 3.1. It contains a test cell with a reference camera on one side and a photomultiplier (PM) on the other, a high voltage (HV) impulse generator and an oscilloscope. The signals from the photomultiplier and the probed voltage impulse are recorded by an oscilloscope: Tektronix TDS 540A during Nytro10XN measurements and Tektronix DPO 4104 during measurements using cyclohexane. The voltage impulse generator supplies the test cell with negative HV pulses at the plane electrode. The needle is grounded.

The setup in Figure 3.1 is an improved version of the setup in preliminary tests where Nytro10XN was the sample liquid. During preliminary tests the reference camera was Pixellink.It was replaced with Proxitronic NCA-C to gain shorter shutter times and higher light sensitivity. Another improvement was to replace the oscilloscope Tektronix TDS 540A with

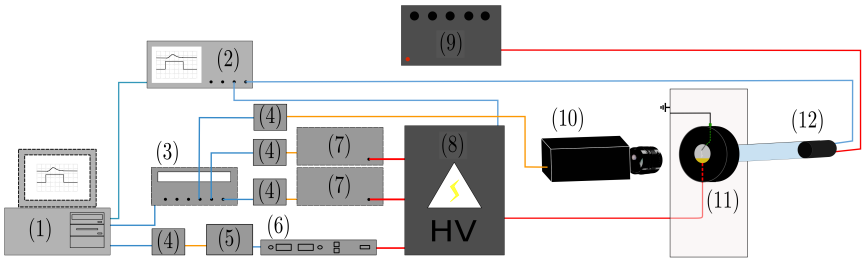

Figure 3.1: The setup: (1) A computer controls and collects data from (2) the oscilloscope Tektronix DPO 4104. The computer also controls (3) the delay generator Stanford Research System DG535 and (6) the HVDC Spellman SL 150 battery via fiber optics (between (4) an optic sender and (5) reciever Blackbox SP380AE). (8) The HV impulse generator is charged by the battery and triggered by two (7) Thyrapulses on each flank of the square voltage pulse it produces. The HV impulse generator was made by Sintef Energy employers (see [23] for setup). The voltage pulse is applied across (11) a needle-plane test cell inside a grounded locker. Light from streamers that occur in the testcell, is detected by (10) a Proxitronic NCA-C camera with a focusing lens on one side, and the (12) photomultiplier PMT MCP R2286U-02 from Hamamatsu Photonics K.K. with an optical system of lens, filters and a slit in a tube. The PMT was supplied by (9) an HVDC generator made at Sintef AS [23].

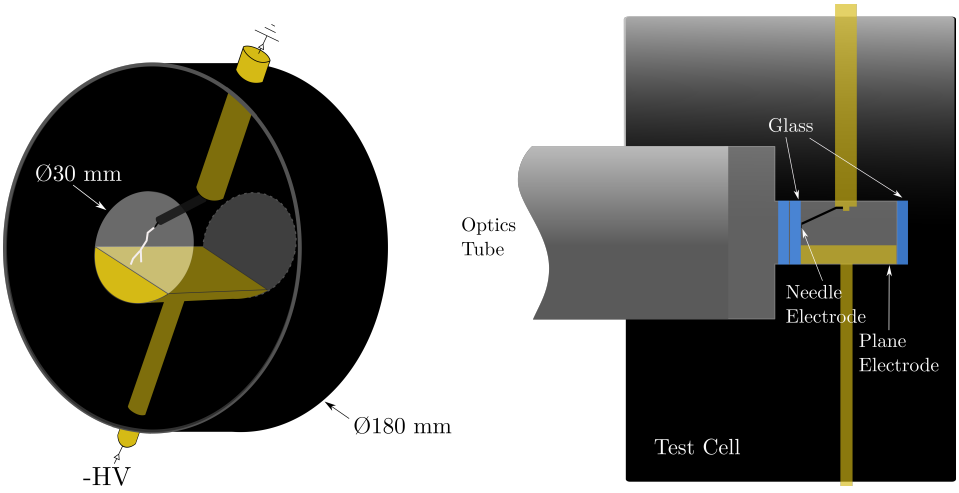

Figure 3.2: The test cell is shown from two angles. It consists of a plane electrode and a needle that was pushed against a window surface. The electrode geometry is called needle-half-plane.

Tektronix DPO 4104 because the latter had faster sampling rate (up to 5GS/s) and frequency (cut-off) respons. A wider slit was installed to ensure that no streamer could go to breakdown around PM's field of view. More shielded coax-cables and lower induction groundings where also installed between the preliminary tests and the cyclohexane measurements. This way the measurement precision increased.

The PM could easily be replaced with a blitz. This way shadowgraphic measurements could be made as the blitz lit through the test cell towards the camera. Preparatory measurements with shadowgraphic images gave an understanding of the velocity distribution and applied voltage versus streamer structure.

3.1.1 Test Cell

The test cell consists of a hollow cylinder made of Polyoxymethylene (POM) containing the sample liquid between two windows, a needle and a plane electrode. It is sketched in Figure 3.2. The plane electrode is semi-cylindrical to fit the inner cylinder, and made of brass. The plane has dimensions $29.4\,\mathrm{mm} \times 35\,\mathrm{mm}$.

A brass feedthrough (20 mm diameter) connects the needle to ground. The feedthrough was typically located $11 - 13$ mm above the plane electrode, depending on the canulla length. The needle is made of $100\,\mu\mathrm{m}$ thick tungsten wire protruding about 1 mm out from a steel canulla, and directed along the glass.

The windows are made of 4 mm thick fused silica glasses. The relative permittivity of the fused quartz silica glass (Corning 7980) is 3.8 [24]. Preliminary works showed that single glass windows crack due to streamers close to them. In order to avoid these cracks, a double set of glasses where inserted as a window. This was implemented after the Nytro10XN series.

The optic tube is the tube containing the optical system that focuses light from the test cell onto the photomultiplier. The tube is bolted to the test cell on the same side as the double glass window. It is grounded by aluminium tape to the test cell locker, to ensure low induction. It is located about 35 mm from the needle along its optical axis, and is 43 mm in diameter.

The test cell is placed in a crib on a metal shelf in a grounded locker. The optics tube and the test cell locker are sealed to be pitch dark.

3.1.2 Photomultiplier

The photomultiplier PMT MCP R2286U-02 consists of a semitransparent photocathode made of bialkali, three microchannel plates (MCP) in series and an anode.

The measured voltage $V_I(t) = R \cdot a$ in the oscilloscope corresponds to PM's anode current a measured across a resistor $R = 50\,\Omega$.

The rise time of PM's processing function g in (2.11), is $0.3\,\mathrm{ns}$ for PMT R2286U-02, and its width at half height is about 1 ns and the transit time is $t_t = 3.8\,\mathrm{ns}$ [20, 21].

Transit time varies with frequency and decreases with increasing supply voltage. PMT MCP R2286U-02 fluctuates with only 30 ps full width at half maximum of the frequency distributed transit time[21].

3.1.3 Optical System

The optical system in front of the photomultiplier is sketched in Figure 3.3. A metal tube containing the optical components (called optics tube) with

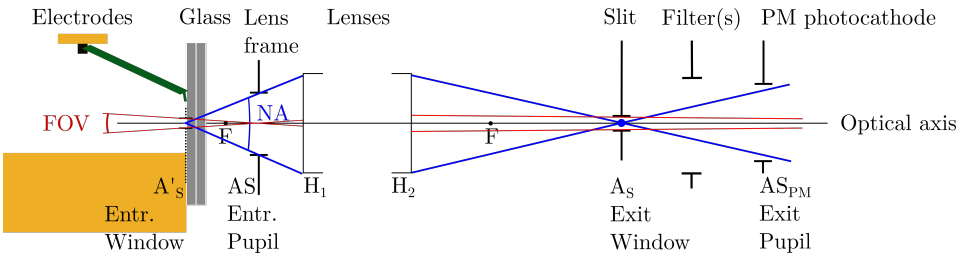

Figure 3.3: The entrance window for the optical system, A'_s, is placed where streamers are expected to propagate: along the glass surface. It is the image aperture of the slit A_s. Marginal and chief rays from streamers are traced (illustratively) through the double set of fused silica glass, the lens (denoted by its principal planes H_1 and H_2), via the image plane at the slit, through any filter present and into the PM entrance.

the PM at its end, is bolted to the test cell to fix the optical axis. The glass-liquid interface in the test cell, forms the object plane where streamers are expected to propagate along. The image plane of this interface is located where the slit is.

The slit acts as the exit window of the system. It defines the spatial resolution for the photomultiplier. It has a rectangular shape, with its 3 mm width parallel to the plane electrode. Its height h_s is changeable and its vertical location can be shifted by a screw gauge of 0.01 mm precision. The filters' diameters are larger than the PM photocathode's diameter of $18\,\mathrm{mm}$.

The Lens is the entrance pupil of the system. Hence PM's optical system has numerical aperture $NA = 13°$. The B.Halle OUV 1.4.15 lens is apochromatic with 60 mm focal length.

PM's field of view (FOV) is dependent on the dimensions of the entrance window, which is the slit's image through the lens. The entrance window is located at the glass-liquid interface.

Transmittance

All filters and optical components' transmittances are presented in Figure 3.4. The radiant sensitivity for PMT R2286U-02 photocathode is also presented in said figure.

The interesting domain in this experiment is below 200 nm, which

has not been documented by the Hamamatsu Photonic company for PMT R2286U-02. They did however document a general transmission spectrum in this domain for sapphire, as presented in 3.4. On this basis, together with the bialkali photocathode radiant sensitivity as measured by Wisa down to 120 nm (also presented in Figure 3.4 [25]), an extension of the total radiant sensitivity for PMT R2286U-02 was estimated. The estimated extension is the product of its components' transmittances and radiant sensitivity, scaled to the documented radiant sensitivity point at 200 nm.

The transmittance for the lens is also extended below 190 nm, estimated as the scaled product of its components' transmittance presented in Figure 3.4. The lens consists of fused silica glass and Calcium fluoride (CaF_2). Note that there are many quartz qualities, so the fused silica lens component may have a higher frequence at 50% transmittance than the fused silica glass transmittance, which was used in the estimation.

Figure **??** displays the total radiant sensitivity of the optical measurement system in the cases where different filters are present. The total radiant sensitivity is the product of PM photocathode's radiant sensitivity S and the optic tube's total transmittance I_f/I_0, given by (**??**). The optic tube's components in the "No filter" case consists of two fused silica glasses and the lens. The three other cases contain the named filter (same as in 3.4) in addition.

3.1.4 Reference Camera

The camera used during the preliminary tests with Nytro10XN, was Pixellink. Its shutter time was too long. In order to determine when the leading streamer head appears in the photomultiplier's field of view and how many streamer channels that appears simultaneously with it, Proxitronic NCA-C was installed for the cyclohexane measurements. It is light sensitive and has shutter time down to 5 ns.

Its shutter time and trigger time was set for each voltage with the aim of capturing the streamer as it passed the slit. This way the one-pixel signals from the PM could be better understood and the amount of streamer heads entering the PMs field of view at the same time, could be counted.

The shutter time and gain of Proxitronic must be set at the Proxitronic Pulse Control box.

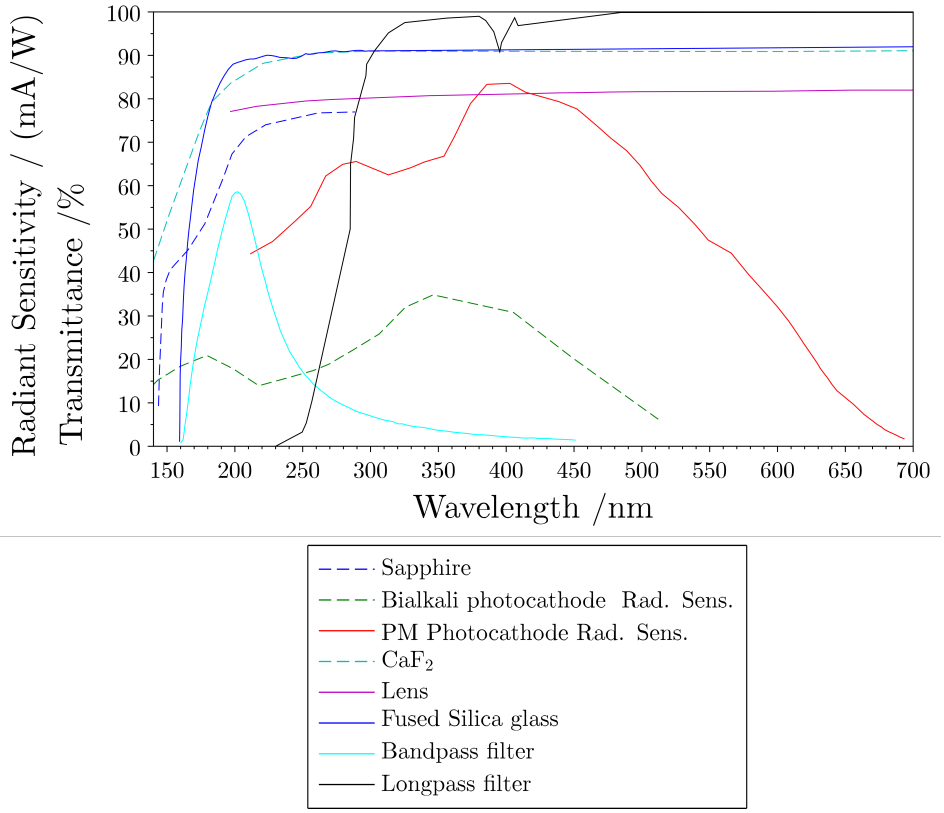

Figure 3.4: Transmittance and radiant sensitivity of all components in the optic tube. Data from sources: Sapphire [20], Bialkali photocathode [26], PM[21], CaF2 [27], B. Halle OUV 1.4.15 Lens [28], Edmund Optics Fused Silica glass [29], Acton UV bandpass filter (peak at 200 nm) [30] and Edmund Optics Longpass filter with cut-off 280 nm [31].

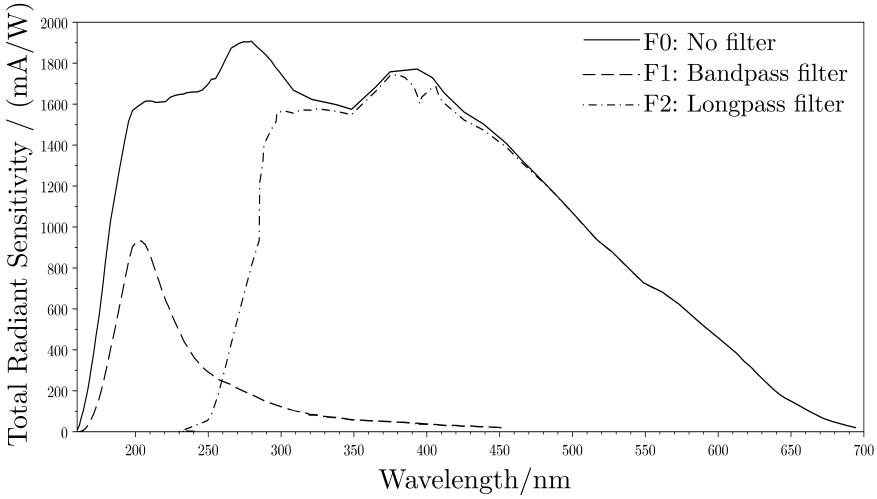

Figure 3.5: The total radiant sensitivity ($T \cdot S$) of the optical measurement system is the transmittance through all the optic tube's components and PM photocathode's radiant sensitivity. The "No filter" case has the minimum amount of components in the optic tube.

Proxitronic Shutter

Timing of the Proxitronic shutter open (t_{so}) and close (t_{so}) must be accurate in order to estimate the streamer heads' time of arrival in the entrance window. The delay of the Proxitronic camera was set at the delay generator via Labview. There was an additional delay due to the circuit between the delay generator (DG) and the camera shutter: optic sender and transmitter, the Proxitronic pulse control box and a trigger signal amplifier inside the camera. The Proxitronic camera was documented with a 30 ns after the trigger monitor point, due to the amplifier[32].

The delay between DG and Proxitronic camera's trigger monitor was measured to be 162 ns with jitter <1 ns. This delay was measured by comparing the direct signal from the delay generator to the oscilloscope, with the monitored trigger output from the camera. Different coax cable lengths between monitor and oscilloscope, and between delay generator and oscilloscope, was accounted. The delay per meter through a coax cable was measured to be $4.8\,\mathrm{ns/m}$.

The rise time of the trigger signal monitored in the Proxitronic camera, was 4.4 ns. The shutter times at 25 ns and 1 us settings on the Proxitronic pulse control box, were infact measured to be $(29 \pm 4)\,\mathrm{ns}$ and 1.0406 µs (between 90% on rising and falling edge).

3.1.5 Voltage Source

The voltage impulse is probed and this current is integrated in order to record the voltage signal across the probe capacitor.

A high voltage square pulse of width $50\,\mu\mathrm{s}$ (if no breakdown occurs) is applied across the test cell. Figure **??** shows typical probed voltage pulses. The pulses' rise time increases from $(16.5 \pm 0.1)\,\mathrm{ns}$ at 50 kV to $(19.9 \pm 0.7)\,\mathrm{ns}$ at 80 kV. Rise time is defined as the time $t_{90\%} - t_{10\%}$ between 10% and 90% of a pulse's amplitude on its rising edge. If breakdown occurs, the time of breakdown t_{BD} is defined as 90% of a pulse's amplitude at its falling edge. The high voltage impulse generator was limited to $80\,\mathrm{kV}$ due to self-ignition of its spark gap. Its setup has been presented in earlier studies [23]. The probed voltage pulse amplitude fluctuated slightly from applied voltage AV set at the HV battery. The relative, standard deviation of the probed pulses' global amplitude maximum, was 0.015 at the most.

The applied voltage time of trigger had a jitter of about STD($t_{10\%}$) 9 ns

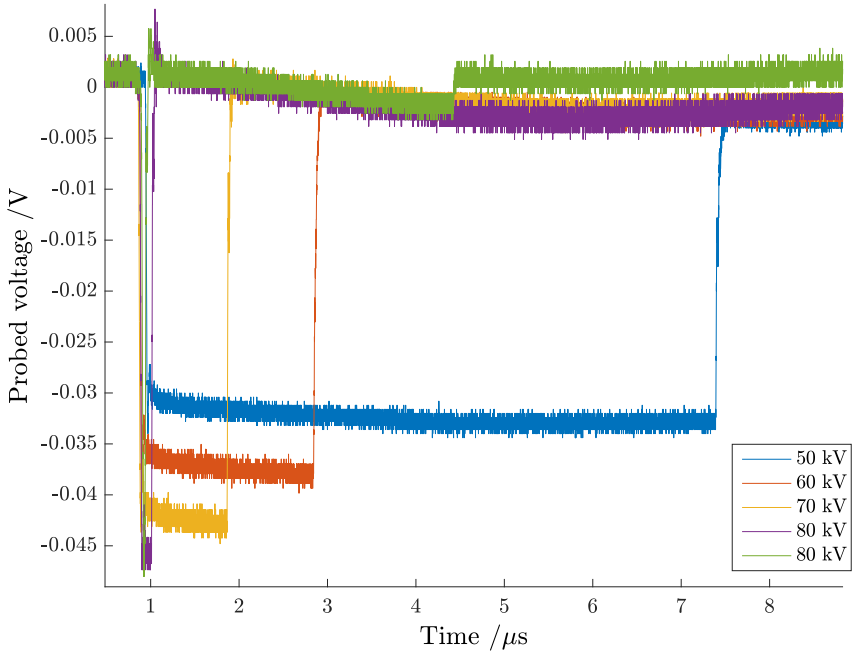

Figure 3.6: These are typical voltage square pulses that were applied across the test cell. Breakdown is occuring in all these cases.

at $AV = 80$ kV and 15 ns at $AV = [60, 70]$ kV and 20 ns at $AV = 50$ kV.

3.2 Sample Liquids

Nytro10XN and cyclohexane were the sample liquids. Nytro10XN is a transformer oil known to emit light quite intensely from its streamers and was therefore considered to be a good preparatory sample in which to measure the UV emission.

Cyclohexane is one of the simple compositioned liquids SINTEF use to study the streamer mechanism. The molecular setup is known, which makes it an ideal liquid for modelling. The cyclohexane from VWR Prolabo Chemicals was initially 100.0% percent pure. Its relative permittivity is $\epsilon_r = 2.0$ at room temperature [33].

3.3 Experimental Procedure

A labview procedure controlled many of the parameters. It triggered a voltage pulse generator, an oscilloscope and a camera via the delay generator, and stored the data from the oscilloscope.

The procedure for Nytro10XN (the preliminary series) was: 15 voltage pulses were applied per voltage, below 30 kV where the glass started to break. Waiting time between pulses, was 3 minutes.

The procedure for cyclohexane was: 20 voltage impulses applied per voltage, for a selection of voltages giving at least one voltage per breakdown velocity decade. A three minute break between each pulse was set to let the liquid recover. The same procedure was performed for all the transmission filters.

Parameters that varied during the experiment, are presented in table 3.1. The PM gain G was $3.0 \cdot 10^7$ for all cyclohexane experiments, and $4.7 \cdot 10^7$ under Nytro10XN experiments.

The field of view in vertical orientation under the cyclohexane measurements, was $FOV = 0.06°$.

Series #	Liquid	Filter	d mm	d_w mm	h mm	M #	t_s ns
4	Nytro10XN	F1	4.37 ± 0.03	2.2	0.66	5.0	-
23	Cyclohexane	F1	4.13 ± 0.05	2.07	0.076(4)	5.52(7)	29 and 1041
26	Cyclohexane	F2	4.14 ± 0.05	2.07	0.076(4)	5.52(7)	29
27	Cyclohexane	F0	4.14 ± 0.05	2.07	0.076(4)	5.52(7)	29

Table 3.1: The important parameters that varied during this experiment. Only the series discussed in this report, are presented. d_w is the entrance window distance from needle. d is the gap distance between the electrodes. h is entrance window height, M is magnification (between needle plane and its image plane at the slit, t_s is Proxitronic shutter time ($= t_{sc} - t_{so}$) and HV_{PM} is the PM voltage supply. Filters - F0: No filter, F1: UV bandpass filter - peak at 200 nm, F2: longpass filter with cut-off at 280 nm.

3.3.1 Preparatory Procedures

The Proxitronic camera was focused onto the needle and shifted vertically to get the entrance window in the center of the image. Next the PM and its optical system was installed.Preparatory images with the slit enlightened, were used to find the slit position in the images, and the camera resolution.

The gap distance and slit opening was measured by aiming a crosshaired binocular at the needle or plane electrode, and shifting the binocular vertically between these targets using a screw gauge. The screw gauge had precision $0.01\,\mathrm{mm}$. The binocular line of sight was parallel to the plane electrode. The position of each target was measured minimum four times in order to reduce measurement errors.

The image plane of the glass-liquid interface was found by adjusting the lens' position until the needle tip and plane electrode was focused onto a paper sheet in the slit opening. The magnified gap distance was measured by moving the slit with a screw gauge between needle and plane electrode. Each electrode position was measured minimum three times in order to reduce measurement errors. The magnification is found by measuring the gap distance between needle and plane electrode, in both image and object plane, according to (2.15).

For both liquids a preliminary shadowgraphic measurement series was made. Based on these shadow-graphic images , the best position of the slit was chosen to be in the middle of the gap.

A test was performed on cyclohexane to ensure that the space charges would be drained with 3 minutes waiting time between the voltage pulses: A series with one hour waiting time was performed and the breakdown velocities were compared to a series with 3 minutes waiting time. No significant difference was discovered. The conclusion of this preparatory test was that 3 minutes is sufficient waiting time for the liquid to self-heal and space charges to drain from both liquid and glass surface. [1]

3.4 Data Analysis

3.4.1 General Parameters

The time it takes for a streamer to pass the entrance window, called passing time, is

$$pt = \frac{h}{v}. \tag{3.1}$$

The entrance window has the height $h = h_s/M$. v is the velocity at time of entry into the field of view.

The passing time pt was set by the breakdown velocity $v_{BD}$and the entrance window height h of the measurement, according to equation (3.2).

The breakdown velocity is calculated as

$$v_{BD} = \frac{d}{t_{BD} - t_{10\%}}, \tag{3.2}$$

where d is the gap distance between needle and plane electrode, $t_{10\%}$ is the time at 10% AV on the rising edge of the voltage pulse and t_{BD} is the time at 90% AV on its falling flank./$t_{10\%}$ and t_{BD} are the times at $10\%AV$ on the rising edge and $90\%AV$ on falling flank of the applied voltage pulse, respectively.

From the raw data recorded by the oscilloscope, the absolute intensity voltage is defined as

$$|V_I| = -(V_I - offset). \tag{3.3}$$

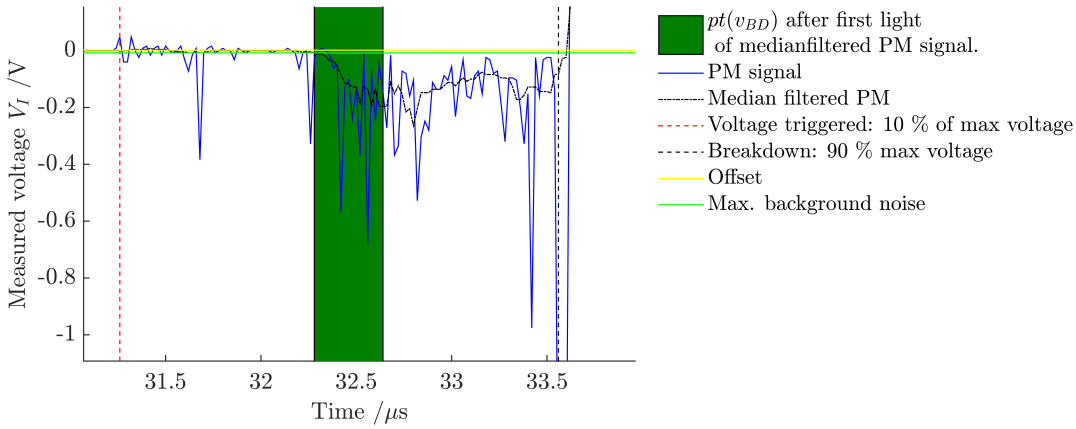

Figure 3.7: The voltage which is below the line of maximum background noise and within the passing time $pt(v_{BD})$. This time domain starts where the streamer head is interpreted to enter PM's FOV: When the median filtered voltage is below maximum background noise.

3.4.2 Nytro10XN Data Analysis

In Nytro10XN streamer heads were assumed to glow continuously. An assumption like this was necessary in lack of reference images with short enough shutter time to aid in the estimated time of arrival (ETA) in the entrance window, for a streamer. Since the entrance window was high, noisy background oscillations and spikes were filtered out using median filter of order 10. Continuous light was left in this filter, and therefore the first sign of continuous light could be interpreted as the time t_{entry} when a leading streamer head entered PM's field of view (FOV). An analysed measurement is presented in Figure 3.7 as an example.

Mean intensity voltage is the measured (unfiltered) voltage V_I integrated over the domain t_{entry} to $t_{entry} + ptv_{BD}$, and divided by ptv_{BD}.

[1]It was otherwise assumed that cyclohexane and Nytro10XN have the same self-healing properties as pentane (milliseconds) [12].

3.4.3 Cyclohexane Data Analysis

Streamer heads' appearance is not assumed for cyclohexane measurements. Instead the reference images are analysed to estimate the time for a leading streamer head to appear in PM's entrance window. Hence, ETA from the time when the reference camera shutter is closed (t_{sc}), is the distance between leading head and the frame of the entrance window in the reference image.

Some streamers are hardly visible in the reference image. These images have been processed using ImageJ [2], to get more contrast.

In order to investigate the UV light intensity emitted from a leading streamer head, one must know for sure when it appears in the photomultiplier signal. Therefore four criteria were set to determine when the streamer head is appearing in the signal, as certain as possible with the data available. Let's call them the head detection criteria. An analysed example is presented in Figure 3.8 to illustrate these head detection criteria.

The first criterium is that the leading head passes or will pass the PM's field of view alone, and exit before any second streamer head appears. This is to make sure that only one head will be represented in each statistic of detected light from the time frame when it appears in the PM's field of view.

The second criterium is that the head is relatively close to the entrance window when the reference image was taken. This minimises the error of estimating the time when the head will appear in the PM's field of view, and thereby maximise the certainty that the detected light in the PM signal, originate from the head and not its tail's or any noise like pre-spike (pre-spikes will be discussed in section 4.3.3).

The estimated time for a leading streamer head to arrive in PM's field of view, ETA is given by the velocity v it has to travel the distance x between PM's entrance window frame and its position observed in the reference image (see example in Figure 3.8a).

$$ETA(v) = \frac{x}{v} + t_{sc} \tag{3.4}$$

t_{sc} is the time when the reference camera shutter closed.

The third criterium requires there to be any sign of light more intense than background noise, between the time when the reference camera closes and $ETA(v_{BD/10})$ presented in equation (3.4), and quite close to $ETA(v_{BD})$.

[2] Download at https://imagej.nih.gov/ij/index.html, anno 2016.

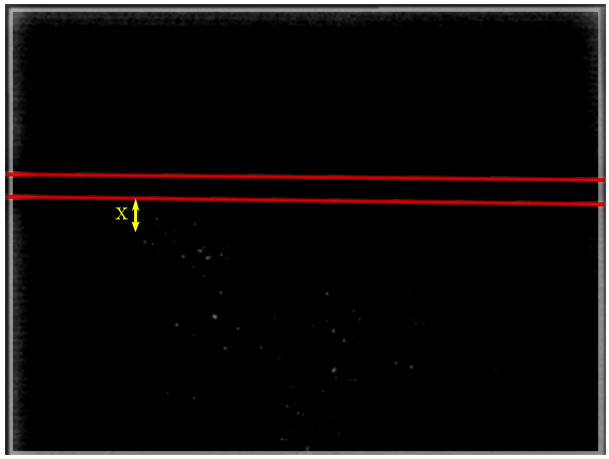

(a) Reference image: Red lines are located at PM's entrance window frames.

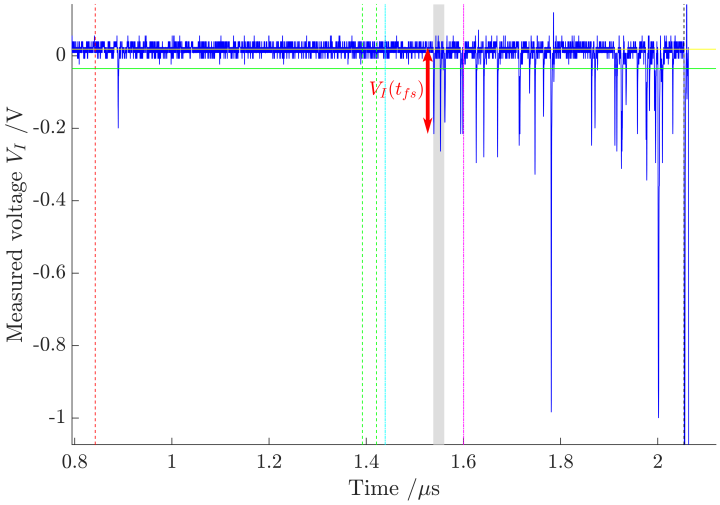

(b) Photomultiplier recording

Passing time: $[t_{fs}, t_{fs} + pt(v_{BD})]$
PM signal
Voltage triggered: $t_{10\%}$
Breakdown: t_{BD}
Offset
Max. background noise
Ref. Camera shutter open and close
$ETA(v_{BD})$
$ETA(v_{BD}/10)$

Figure 3.8: Head detection criteria are fulfilled in this example: 1. One leading streamer head will appear alone in the PM's entrance window. 2. Distance x is short. 3. The first spike between Ref. camera shutter closes (t_{sc}) and $ETA(v_{BD/10})$, appears at a reasonable time t_{fs} for a streamer that has propagated with velocity of about $1/2 \cdot v_{BD}$ after the image was taken. 4. No re-illumination appear.

This gives room for one change of streamer mode along the distance l or that the streamer propagates slower than the breakdown velocity in the middle of the gap.The criterium also rules out any measurement where no light from the head is detected.

The fourth criterium rules out any re-illuminations. Re-illuminations are so intense that the oscilloscope range and usually the photomultiplier are saturated. Fourth criterium therefore states that no re-illumination can appear together with the streamer head appearance in the PM's recordings.

By definition, the first spike in the interval between the t_{sc} and $ETA(v_{BD}/10)$ of a PM recording, appears at the time t_{fs}. Correspondingly $|V_{I(t_{fs})}|$ is the measured voltage amplitude of this spike, as illustrated in Figure 3.8b. A spike is defined as a local maximum in the measured voltage $|V_I(t)|$ of the PM's signal.

The mean detected light intensity is the mean of only the samples in the PM recording that are more intense than the background noise. This statistic was calculated on cyclohexane measurements, because light often appeared as separated spikes. In a sense, the mean detected light intensity is to compress the signal from a chosen interval, by removing the samples where no light has been recorded.

Mathematically mean detected light intensity can be expressed as follows:

$$MDLI(a,b) = \frac{\int_a^b |V_I(t)| \cdot H(|V_I(t)| - L)\, dt}{\int_a^b H(|V_I(t)| - L)\, dt} \tag{3.5}$$

Here $H(x)$ is the Heaviside function. L is the limit, which is set by the maximum background noise measured before the voltage pulse is applied, relative to the offset of the signal V_I. The definition of $|V_I|$ is presented in (3.3).

3.4.4 Point Source Power Model

The spectral power emitted from the streamer, is estimated by assuming it to be a point source at located on the entrance window.

PM's anode current is measured across a $50\,\Omega$ resistor in the oscilloscope. The measured voltage, called intensity voltage V_I, of the spectral power p_s from a point source at the entrance window, is

$$V_I = R \cdot G \int S_{(\lambda)} \cdot T_{(\lambda)} \cdot \frac{1}{2}(1 - \cos(NA/2)) \cdot p_{s\,(\lambda)}\, d\lambda, \tag{3.6}$$

as deduced in 2.4 (see equation (2.20)). The PM gain G was $3.0 \cdot 10^7$ for all cyclohexane experiments, and $4.7 \cdot 10^7$ under Nytro10XN experiments.

Since the transmittance and radiant sensitivity of the optical system and photomultiplier, are wavelength dependent, and the spectrum of the source is unknown in the UV domain, a couple of model spectra will be used. These are based on (A) the energies of emitted photons due to de-excitation in from the first excited states to ground state in a cyclohexane molecule, (B) the absorbance spectrum of cyclohexane (as presented in Appendix A). Spectrum model (C) is a delta function $\delta(x)$ at 200 nm, the peak value of filter F1. This model therefore defines the lower bound for the radiant power.

The spectral power of spectrum models (A) and (B), are constants $p_{s(\lambda)} = K/(b-a)$ in the wavelength domains $[a, b] = [160, 177]$ nm and $[160, 220]$ nm, respectively, and zero otherwise. Spectrum model (C) is $p_{s(\lambda)} = K \cdot \delta(\lambda - 200\,\mathrm{nm})$. From a known, measured voltage V_I in the equation (3.6), the radiant and spectral power of these models, can be calculated. The radiant power is $P_s(a, b) = \int_a^b p_{s(\lambda)} d\lambda$.

Chapter 4

Results and Discussion

This chapter is divided into three sections. First a preliminary study on the light intensity from streamers in Nytro10XN. The second section is about the breakdown velocity for cyclohexane versus applied voltage. In that section the acceleration voltage of cyclohexane streamers along the glass surface is compared with a test where streamers propagated in the bulk of the liquid. The last section is the main section, where detected light intensity from streamers in cyclohexane, is discussed. This section begins with a discussion on the hypothesis that UV light is emitted from streamer heads. Then it goes on to study how frequently light pulses are detected, and whether the intensity of these light pulses correlates with the streamer velocity. The last result presented, is an estimation of the radiant power from cyclohexane streamer heads. Sources of errors and uncertainties are also discussed at the end.

4.1 UV emission from Streamers in Nytro10XN

Ultraviolet (UV) light is emitted from streamers in Nytro10XN. Figure 4.1 show one typical example of such UV measurements. PM recordings of visible light (using filters F0 or F2), showed the same trend as this example. The first oscillations at the time when voltage pulse was triggered ($t_{10\%}$), appeared in these preliminary tests as a result of the voltage pulse generator affecting the ground potential of the photomultiplier. These were later damped by reducing the inductance in the ground circuit. This was

one of the improvements peformed before streamers in cyclohexane were tested.

The example also depicts what is interpreted as a pre-spike. It occurs at time $31.8\,\mu s$ in Figure 4.1, before the continuum of light and is therefore believed to be some sort of noise. Pre-spikes are discussed in section 4.3.3.

The entrance window height was 0.66 mm, so the streamer head is recorded together with a large fraction of its tail. The PM recording in Figure 4.1, shows a continuum of light with frequent spikes superimposed. This is expected if the streamer head emits light continuously as it passes the entrance window, which Lundgaard et al. stated that Nytro 10X transformer oil does [2]. Due to this, the passing time of the streamer head should fit the duration of the continuous light. From Figure 4.1 one can see that the upper envelope of the continuous light lasts for $0.5\,\mu s$, while the passing time estimated from the breakdown velocity is $pt(v_{BD}) = 0.30\,\mu s$, according to (3.1). Hence the streamer head appear to be propagating slightly slower than breakdown velocity, which seems reasonable because a multi-branched streamer in oil has been measured to propagate at its slowest about half way across the gap (in a large gap setup) [2]. The streamer appear to enter PM's field of view just before half-time to breakdown, which corresponds well with a streamer having its maximum velocity close to the needle electrode.

Some of the spikes recorded during the time when the streamer head was appearing in the PM's field of view, are most likely emitted from the tail. Once the streamer head exit the PM's field of view, the measured intensity voltage V_I from the tail still emit light pulses at the same rate. The amount of leading heads appearing simultaneously in the PM's field of view, is unknown due to the long shutter time of the Pixellink reference camera.

From this preparatory experiment one can conclude that the heads of second mode streamers in Nytro10XN emit UV light constantly. How photoemission may vary with propagation modes, has not been recorded, as all measurements of Nytro10XN were second mode streamers ($v_{BD} = 1-2\,\mathrm{mm}/\mu s$).

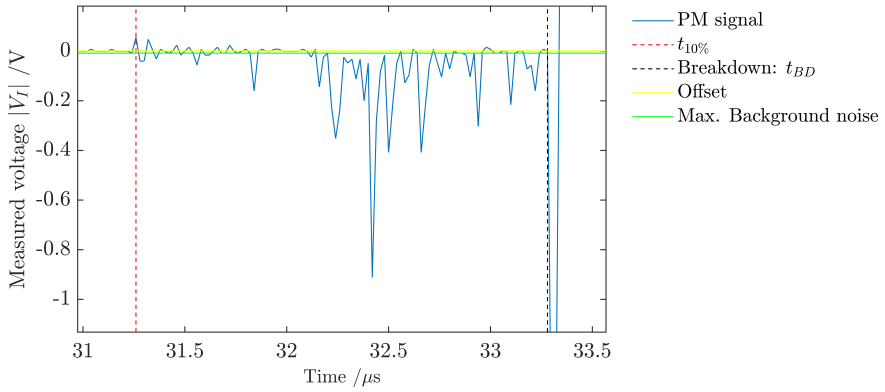

(a) PM recording

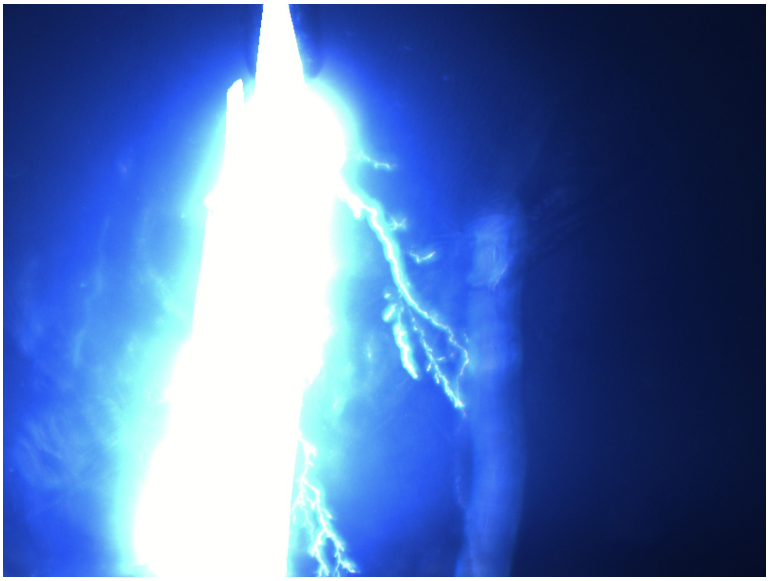

(b) Reference image of breakdown

Figure 4.1: Typical streamer with breakdown velocity $2.2\,\mathrm{mm/\mu s}$. The reference image mainly shows breakdown light. Liquid: Nytro10XN. Filter: F1.

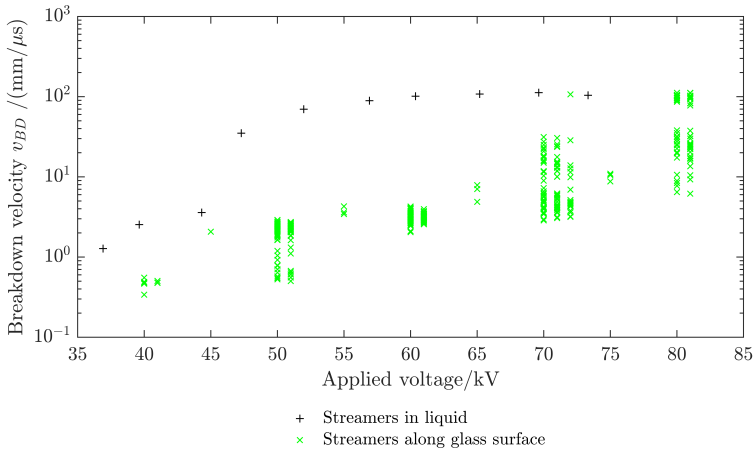

Figure 4.2: Breakdown velocities v_{BD} for cyclohexane with and without a glass present. Streamers along the glass surface were measured in present experiment. Streamers in the bulk of the liquid (+) are averaged measurements performed in a different test cell [unpublished, internal communications SINTEF Energy AS]. In that setup the needle was located in the liquid, 4 mm above the center of the plane electrode and at least 15 mm from the container walls. The square voltage pulse duration was the same as in present experiment.

4.2 Cyclohexane Streamers' Velocity Distribution

In this section the breakdown velocity of streamers along a glass surface will be compared with some measurements of streamers in the bulk of liquid cyclohexane. The latter experiment was performed by Torstein Grav Aakre at Sintef Energy AS [unpublished, internal communication]. Figure 4.2 shows velocity distribution for streamers propagating along the glass surface and streamers propagating in the bulk of cyclohexane. The measurements of streamers that propagated in the bulk, were performed in a different experiment, with a needle-plane electrode geometry. These streamers were observed to accelerate swiftly from second to fourth mode between 45 and 50 kV.

In present experiment, where streamers propagated along the surface of fused silica glass and the electrode geometry is needle-half-plane, a dif-

ferent velocity distribution was observed. The acceleration from second to fourth mode became gentler relative to the streamers in the bulk of the liquid, and at 70 and 80 kV the streamers' breakdown velocities vary from second to fourth mode. Conclusively the acceleration voltage increased from 35 kV to about 80 kV as the test cell changed. Here, acceleration voltage is defined as the voltage where the velocity increases from second mode.

4.2.1 Increased Acceleration Voltage

In this section the reasons for the observed acceleration voltage increase, will be discussed. But first, some factors are presented, which would enhance the streamer propagation along solid insulation surfaces relative to streamers in the bulk of the liquid.

The acceleration voltage is expect to decrease due to the presence of a medium with higher permittivity close to the needle. Since fused silica has about twice the permittivity of cyclohexane, its presence in the test cell increases the electric field around the needle, according to equation 2.10. Hence the required initiation field for avalanches will be met at a lower voltage when fused silica is present. Streamer heads close to the surface experience the same field concentration as a needle. The velocity distribution will correspondingly shift to lower voltages.

Conducting trails of soot or other charged particle did not affect the streamers along the glass. Glass is inorganic, and soot from cyclohexane deterioration had mostly settled on peripheral locations of the glass. The main surface area where streamers propagated, was excavated by the streamers. In addition, neither reference images nor preparatory shadowgraphic images showed any sign of any repetitive streamer trajectory. Hence conducting trails were not formed in present experiment.

It has been reported that the presence of ceramic did not change the propagation velocity of air-streamers significantly [17]. Since glass also is inorganic, it will probably behave in a similar ways, and not enhance streamer propagation in the way that the organic insulation pressboard do [2, 14]. On this basis the propagation of liquid streamers is not expected to change when glass is installed.

In theory the glass properties could prevent electron avalanches from appearing in almost half the volume around the needle and streamer head. Fused silica glass is transparent in the UV domain. The ionisation potential

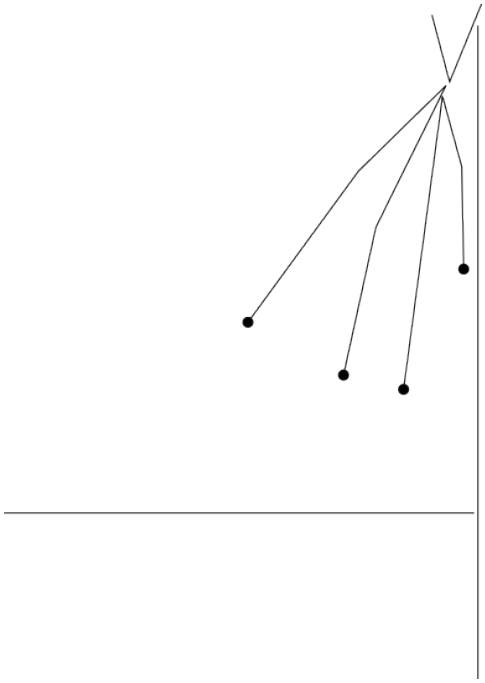

Figure 4.3: Channels racing between needle and plane electrodes along a solid surface. One channel falls behind the other channels due to some decelerating properties of the solid surface. The other channels are unaffected by the solid surface, and hence the breakdown velocity is unchanged for a multi-channel streamer when such a surface is introduced.

of cyclohexane molecules will be reduced in high electric fields, below the energy of UV photons [5]. Now, let's assume that the photoionisation mechanism is driving fourth propagation mode[1] Then streamers in the bulk of cyclohexane, will emit photons that ionise the molecules in the bulk around them. However, when the streamer propagate along a glass surface, most of the ionising photons will traverse the glass. Consequently only half of the volume around the streamer head is available to be ionised. Hence if photoionisation is the main reason for streamer acceleration from second to fourth mode, the presence of glass alone will prevent acceleration and shift the acceleration voltage to higher voltages.

The glass *alone* has not caused the acceleration voltage to increase. In multi-channel streamers the channels shield each other. In the race towards the plane electrode, any channel that falls behind is left behind. It will slow down and eventually stop because it is shielded by channels ahead of it. This holds in general, also when a solid insulation is in the gap.

Now, let's assume that the glass has some property that reduces the

[1]The hypothesised mechanism is described in section 2.2.2.

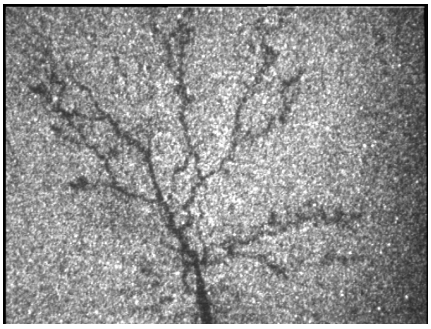

(a) Multiple channels observed in shadow-graphic with $AV = 50$ kV. $v_{BD} = 2.3\,\mathrm{mm/\mu s}$.

(b) Multiple channels observed in reference image with $AV = 60$ kV. $v_{BD} = 2.5\,\mathrm{mm/\mu s}$.

Figure 4.4: Most of the streamers observed at 60 kV had multiple channels glowing in the reference image. At 50 kV some reference images showed a single channel streamer glow which was not slower than the multi-channel streamers in the reference image. The two shadowgraphics that showed streamers at $AV = 50$ kV looked alike.

propagation velocity of streamer channels as they travel along its surface. In the case of a multi-channel streamer, the channels that are close to the surface, will fall behind the other channels, like illustrated in Figure 4.3. But because the channels further away from the glass are unaffected by any decelerating properties of the glass, the breakdown velocity of a multi-channel streamer will be unaffected by the presence of a glass surface.

Streamers in the bulk of cyclohexane, accelerated from second to fourth mode at voltage $V_a = 45$ kV, according to Figure 4.2. Given that photoionisation or any other field dependent mechanism causes the acceleration, the streamer channels further away from a glass are expected to propagate in fourth mode at voltages above $V_a = 45$ kV. However, in present experiment streamers were observed to have multiple channels at 50 and 60 kV applied voltage, but still propagated in second mode along the glass surface. Examples of multi-channel streamers along the glass surface, are shown in Figure 4.4. Since at least one of these channels are believed to propagate in the bulk of the liquid, the glass alone cannot be the cause for the increased acceleration voltage.

The field is suspected to be lower in present test cell than in the test cell that produced the "streamers in liquid" data, for a fixed voltage in Figure

4.2. The geometry of electrodes in the two experimental systems differ a lot. Three main factors in present experiment's setup are the needle location relative to the edge of the plane electrode, the location of the brass holder of the needle relative to the electrode and the grounded optic tube being close to the needle.

Needle-half-plane electrode geometry consists of a needle located above the edge of a plane electrode.The electric field is enhanced around sharp edges. Therefore the field somewhere else along the line between needle and the edge, must be reduced when the voltage is conserved. Consequently the field in the middle of a needle-half-plane will be lower than the field in the middle of a needle-plane setup, at the same voltage.

The needle in this experiment is shielded quite extensively by its own feedthrough. The closest part of the feedthrough is only about 11 mm away from the needle tip. The feedthrough is closer to both plane electrode and needle tip in this geometry than it was in the needle-plane setup. This shielding is expected to both reduce the electric field strength at the needle tip, and rotate the direction of the field component towards the glass. The needle is also shielded by the grounded optic tube in this experiment.

Conclusively, the increase in acceleration voltage is believed to be caused by the difference in electrode geometry between the two setups. On top of this, the glass' transparency in the UV domain may decelerate third and fourth mode streamer channels that travel along its surface. This latter case is plausible given that photoionisation is a contributing mechanism to streamer propagation, and that all channels propagate close to the glass surface.

4.2.2 Errors and Deviations

The variation in the velocity at each voltage in Figure 4.2, is mainly explained by the fact that streamer propagation is a quite stochastic process. The relative standard deviation of the corresponding times to breakdown, were between 12% (at 50 kV) and 55% (at 60 kV) within a single measurement series, which illustrates how stochastic this process was. A couple of negligible deviations relative to this process, are presented below.

The maximum difference in gap distance between the different measurement series that together form the velocity distribution in Figure 4.2, was about 0.07 mm. When the tip radius is assumed to be half the needle width, i.e. $50\,\mu\mathrm{m}$, or smaller, the relative voltage deviation becomes

$\Delta V/V \leq 3‰$ due to this gap distance deviation. It was approximated by the use of equation (2.21). This deviation is negligible relative to the stochastic variation of streamer propagation.

The needle was worn down by streamers with about 0.01 mm during several series (Series 22 to 25, containing about 4-500 voltage pulses), i.e. a relative change of $2‰$. The breakdown velocity v_{BD} was calculated in equation (3.2) under the assumption that the gap distance stayed constant during a series. Since v_{BD} is proportional to the gap distance, this error is negligible relative to its stochastic variations.

The same liquid was used for several series (more than 500 voltage pulses applied). When the test cell was cleaned and refilled with pure cyclohexane, a change in the streamer propagation velocities was observed. The mean velocity had dropped with about $1\,\mathrm{mm/\mu s}$ at 50 and 51 kV applied voltage. In addition the stochastic variations had increased, with standard deviation increasing at 51 kV from 0.2 to $0.8\,\mathrm{mm/\mu s}$ and from 0.67 to $0.75\,\mathrm{mm/\mu s}$ at 50 kV. This shows the propagation velocity is dependent of the liquid deterioration in this experiment. It is therefore recommended to run the liquid through a filter or change it more often, in future experiments.

All breakdown velocities presented in this thesis, including the "Streamers in liquid" presented in Figure 4.2, approximates the time of streamer inception t_{inc} with the time of voltage trigger $t_{10\%}$. An inception delay is expected, hence these are all negatively biased. The inception delay has not been measured, so let us assume that t_{inc} may be as late as 40 ns after $t_{10\%}$ for second mode streamers, and 20 ns for third mode streamers. Hence when inception delay is corrected for, the breakdown voltage should be shifted to 101% and 111% of v_{BD} presented in this thesis, respectively.

4.3 UV emission from Streamers in Cyclohexane

Only a fraction of the UV bandpass filtered measurement (in series 23) could be used to locate the light pulses emitted from streamer heads, with good certainty. This is important when distinguishing head light from tail light. These data were selected on the basis that their reference images showed a leading head located close to or in PM's field of view. The known camera shutter closing time, t_{sc}, can therefore give a good estimated time of arrival (ETA) for the head appearance in the PM's recordings. The hypothesis that a streamer head emits UV, is tested against these selected measurements[2].

4.3.1 UV light detected from Streamer Heads

The hypothesis that UV light is emitted from streamer heads, is supported by this experiment. First one must determine whether light emitted from the streamer's (leading) head, has been detected. From series 23, where the UV bandpass filter (F1) was applied, Figure 4.5 show two typical examples with $AV = 60$ and 80 kV and with breakdown velocities $4.13\,\mathrm{mm/\mu s}$ and $20.03\,\mathrm{mm/\mu s}$, respectively. These examples show reference images of a streamer as it is about to enter or already has entered PM's field of view. Since the times t_{so} and t_{sc} for the reference camera shutter are very accurate (jitter <1 ns), and light pulses appear at these times, there is no doubt that light has been detected from the streamer head.

Secondly and finally one must determine whether UV light has been detected. The light transmitted through bandpass filter F1 is most likely UV light. Though the entire wavelength domain of this filter includes visible light (400 to 450 nm), maximum 3% of any visible light have been transmitted through it. Hence light detected with filter F1 is regarded as mainly UV, even though the spectrum of the light source is unknown. It is also likely that most of this light has wavelength below 320 nm, because F1 is above 5% of maximum radiant sensitivity between 160 and 320 nm.

The emission spectrum measured through filter F1, is probably constricted to wavelengths below 260 nm. This is based on the fact that possi-

[2]The selected data meet the head detection criteria described in section 3.4, and are presented in Appendix B.

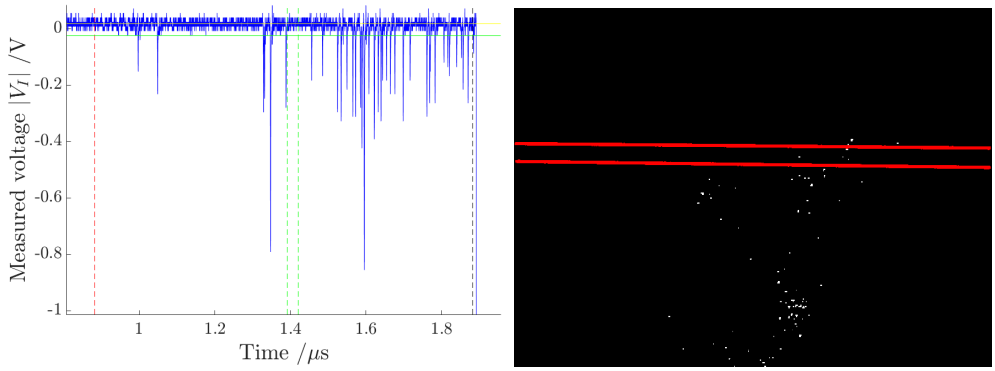

(a) PM recording (left) and reference image (right), AV=60 kV, series 23, v_{BD}= 4.1 mm/µs. Liquid: Cyclohexane. Filter: F1.

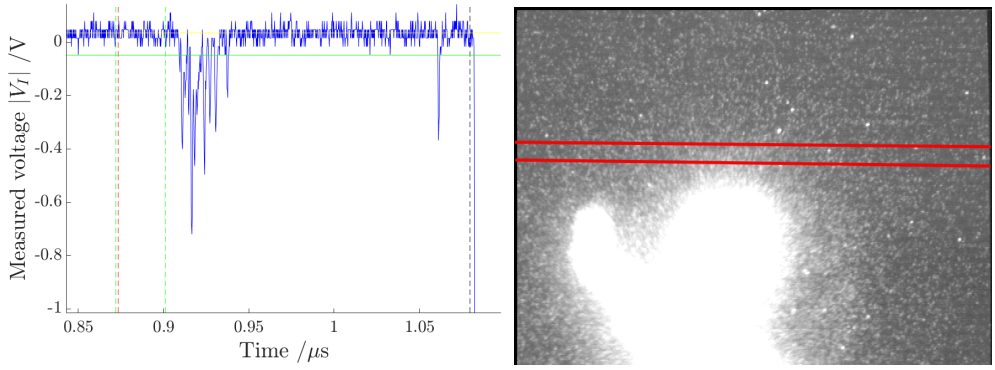

(b) PM recording (left) and reference image (right), AV=80 kV, series 23, v_{BD}= 20.0 mm/µs. Liquid: Cyclohexane. Filter: F1.

PM signal
Voltage triggered: $t_{10\%}$
Breakdown: t_{BD}
Offset
Max. background noise
Ref. Camera shutter open and close

Figure 4.5: The PM's signal show that UV light is detected at the time when the streamer head passes the entrance window. The entrance window frame was located at the two, red lines in the reference image.

ble wavelengths absorbed by a molecule usually coincide with the emitted wavelengths possible [18]. The measured absorption spectrum for cyclohexane is presented in appendix A.

The energy of photons detected through filter F1 is somewhere between 2.7 eV and 7.7 eV. Davari et al. calculated that the first excitation energy of cyclohexane, is 7 eV above ground state. They also calculated the ionisation potential, and found that if photons with energy above 7 eV are

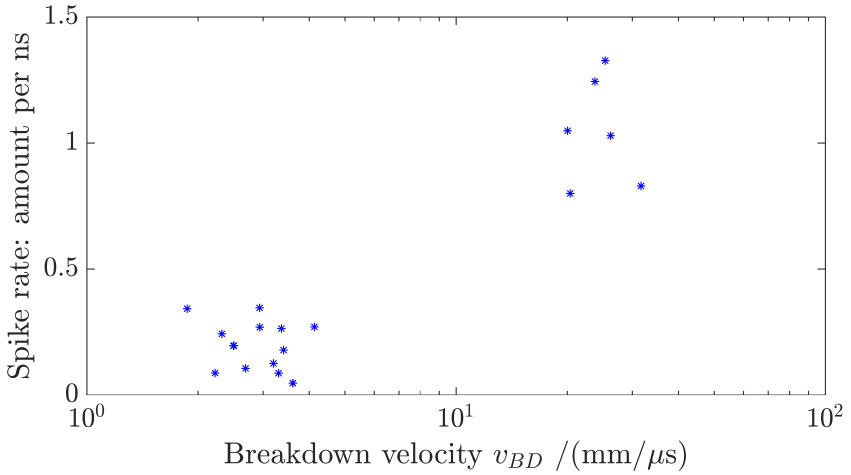

Figure 4.6: The amount of spikes (light pulses) in the PM signal during $pt(v_{BD})$, versus breakdown velocity. $pt(v_{BD})$ is the estimated time it takes for the streamer to pass the PM's field of view. A spike is defined as a peak (or local maximum) in the measured voltage $|V_I|$ of the PM's recordings. The data in this figure have been selected on the head detection criteria, which are described in section 3.4. The light has been filtered with UV bandpass filter F1 in front of the PM.

absorbed by cyclohexane molecules in an electric field above $15\,\mathrm{MV/cm}$, then these photons will be ionising [6].

The electric field in front of the streamer is unknown for a needle-half-plane electrode geometry. However, a very rough approximation can be made. Let's assume that a streamer head is an hyperbolically shaped electrode above an infinite plane. Then equation (2.21) can be used to estimate the electric field at its tip. Gournay et al. found that second mode streamers in cyclohexane behaved as if their electrode tip radius was $6\,\mu\mathrm{m}$ [11]. Based on this radius and a 4 mm gap distance in a needle-plane setup, the applied voltage must be 35 kV in order to have a $15\,\mathrm{MV/cm}$ electric field strength at the streamer tip. It is therefore believable that the ionisation potential is reduced below the upper limit (7.7 eV) of detectable photons in this experiment, when the applied voltage is raised up to 80 kV.

Frequently emitted photons

UV light is emitted much more frequently from the head of third mode streamers than slower streamers in cyclohexane. This is demonstrated in Figure 4.6, where the rate of emitted UV light pulses is plotted against breakdown velocity.

Both UV light and visible light is emitted sporadically from second mode streamers. At velocities below $10\,\mathrm{mm/\mu s}$ and with AV below 80 kV, both the photomultiplier and reference camera detect single light pulses appearing sporadically from anywhere in the streamer channel. The reference camera detects light in the visible domain. The duration of the light pulses in PM's signal, are typically one to a couple of nanoseconds, which corresponds to the photomultiplier's response time of single photons.

Streamer heads with velocities around $20\,\mathrm{mm/\mu s}$ glows quite continuously. Many reference images showed that the reference camera's pixels had been saturated with light from where the streamer had travelled, as seen in Figure 4.5b. One cannot state from the images how much of the streamer is glowing, because its head moves fast enough to cross the image during the shutter time. However, the PM does almost never measure UV light from the tail , with the exception of some re-illuminations or smaller spikes. This indicates that the streamer head emits UV light continuously, while its tail is mostly dark.

Now, how much of the streamer's front is glowing? Two of the selected data in Appendix B show single channels about to enter PM's field of view. One of them is presented in Figure 4.7. Duration and timing of these continuous light pulses correspond to a streamer point source passing the entrance window with approximately breakdown velocity. The duration is 1.6 ns and 2.6 ns for these two examples, where two and three spikes are visible on top of a constant signal (as seen by the upper envelope). This shows that successive photons are detected more frequent than PM's response time for a single photon. The extent of the channel's glowing part is bounded by the resolution of the entrance window, which was 76 nm in this experiment.

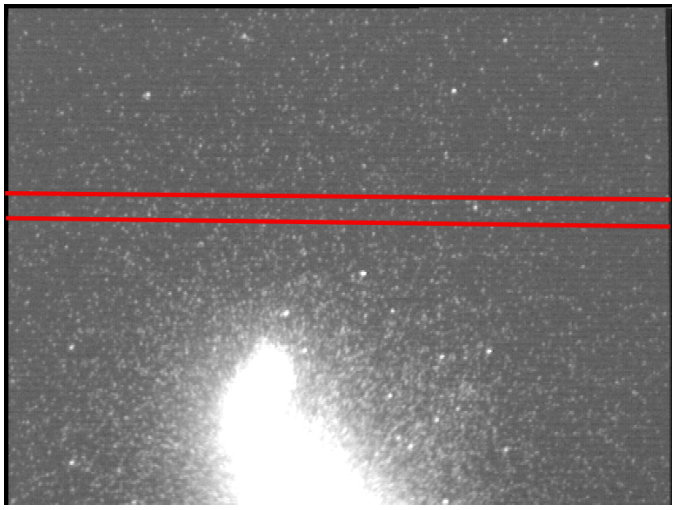

(a) Reference image: Red lines are located at PM's entrance window frames.

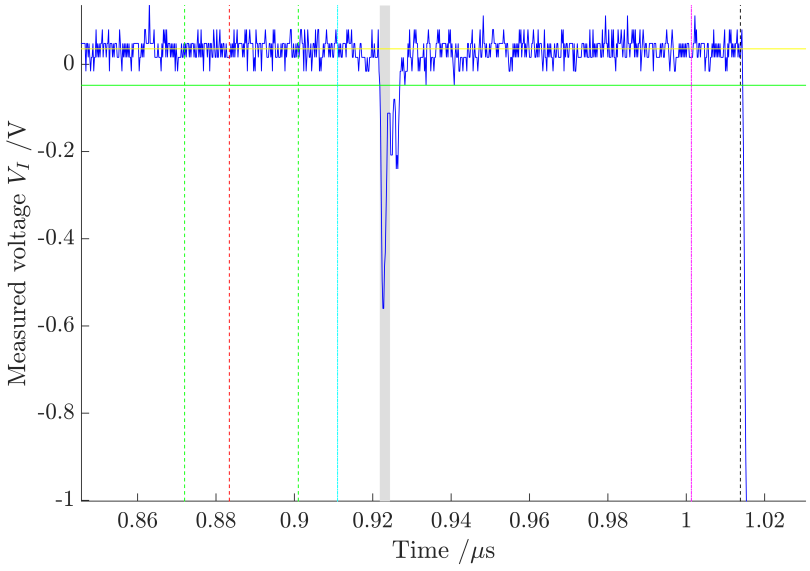

(b) Photomultiplier recording

Passing time: $[t_{fs}, t_{fs} + pt(v_{BD})]$
PM signal
Voltage triggered: $t_{10\%}$
Breakdown: t_{BD}
Offset
Max. background noise
Ref. Camera shutter open and close
$ETA(v_{BD})$
$ETA(v_{BD}/10)$

Figure 4.7: PM recording and reference image of streamer, AV=80 kV, series 23, v_{BD}= 31.7 mm/µs. This example shows one streamer head of third mode glowing quite continuously, while no light is detected from the tail. Liquid: Cyclohexane. Filter: (F1) UV bandpass - peak at 200 nm.

In order for photoionisation to be a dominating factor in streamer propagation, the streamer is required to radiate sufficiently in the wavelength domain that will ionise molecules ahead of it. Hence the acceleration is expected to correlate with an increase in how frequently ionising photons are emitted from the streamer. The measurements in this experiment shows this correlation, as the photoemission is observed to change from sporadically appearing light pulses in second mode, to continuously photoemission from in third mode streamers. These results therefore supports the hypothesis that acceleration from second mode streamers, is caused by photoionisation.

The spike rate distribution in Figure 4.6 cannot determine whether the rate increases together with propagation mode or with increasing applied voltage regardless of the propagation mode. In order to test whether a step in the spike rate correlated with a change in propagation mode, measurements of streamers with different propagation modes at a fixed voltage, could be used. In series 23 both second and third mode streamers were observed with $AV = 70$ kV. Unfortunately non of these measurements met the head detection criteria. It would therefore be hard to determine whether the (few) spikes that appeared, originated from the streamer head or its tail or any pre-spike. It is highly recommended in future work to focus on collecting measurements where the voltage is fixed while the observed propagation modes vary. A high accuracy in determining when the head appears in the PM's field of view, is also required.

Light was not always detected

UV light from streamer *heads* was not always detected. This is shown in several measurements at both 60 and 80 kV with velocities ranging from 4 to $100\,\mathrm{mm/\mu s}$. Figures 4.8a and 4.8b clearly show streamers that already have entered or passed the field of view when the reference image was taken, without any corresponding light pulses in the PM signal. A couple of examples like this, were found for $AV = 60$ kV. At 80-81 kV, 6 out of 20 measurements with velocities above $80\,\mathrm{mm/\mu s}$, and one with velocity $35\,\mathrm{mm/\mu s}$, showed no light at all before breakdown light.

At 60 kV, streamer heads with velocities of about $4\,\mathrm{mm/\mu s}$ do not glow continuously, but emit light pulses sporadically. This is the case in both reference image and the photomultiplier signal for all measurements at and below this voltage and velocity. Hence it would seem that light pulses

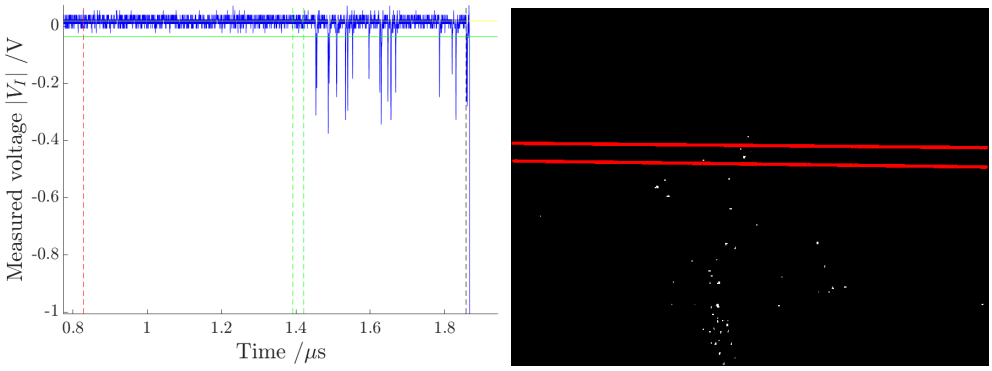

(a) PM recording (left) and reference image (right), AV=60 kV, series 23, v_{BD}= 4.0 mm/µs. Liquid: Cyclohexane. Filter: F1.

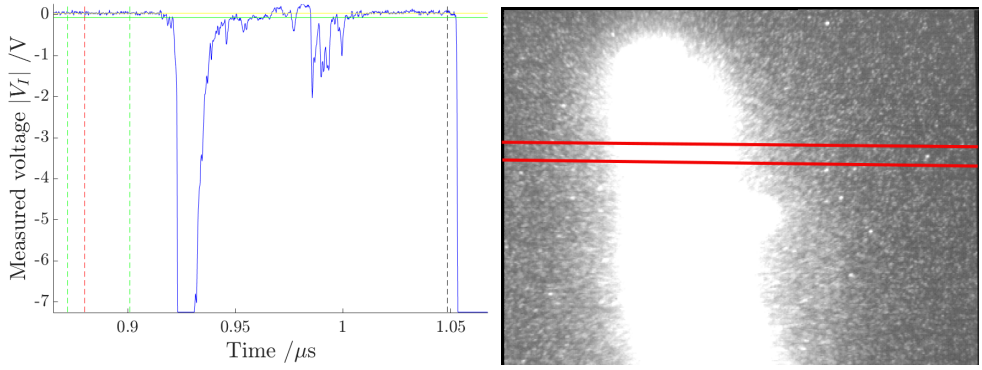

(b) PM recording (left) and reference image (right), AV=81 kV, series 23, v_{BD}= 24.5 mm/µs. Liquid: Cyclohexane. Filter: F1.

- PM signal
- Voltage triggered: $t_{10\%}$
- Breakdown: t_{BD}
- Offset
- Max. background noise
- Ref. Camera shutter open and close

Figure 4.8: No UV light is detected from the leading head of these streamers. This is seen as no light appear in the PM's signal before Ref. camera shutter closes, while the streamer head has passed the PM's entrance window in the reference image. Note also that re-illumination was measured after camera shutter closed. The entrance window frame was located at the two, red lines in the reference image.

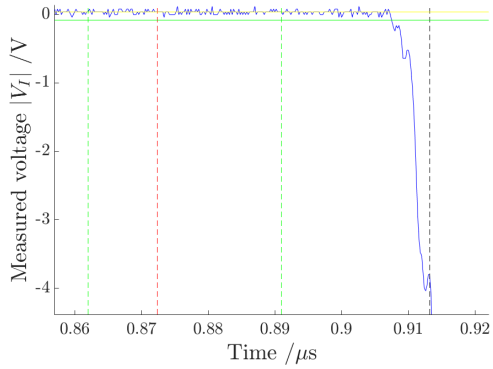

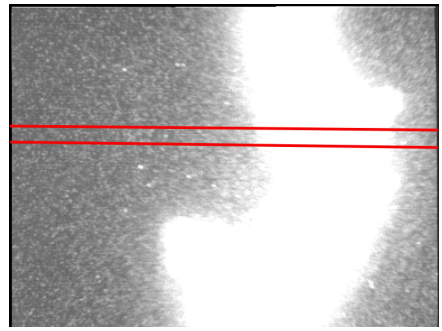

Figure 4.9: No light (visible nor UV) has detected by the PM when the reference image shows a glowing streamer channel, in this example. PM recordings (left) and reference images (right), AV=80 kV, v_{BD}= 101.4 mm/µs. Liquid: Cyclohexane. Filter: (F0) No filter. The needle is located below the image.

sometimes are emitted less frequently than once every 29 ns (the reference image shutter time). Note, however, that the excitation of the PM's photocathode is a quantum statistic phenomenon, which implies that there is a probability for it to detect incident light. For our PM's photocathode, this quantum efficiency is below 40%. Therefore more than every second incident photon will not be detected. Hence in the cases where emission is weak, light pulses may be emitted more frequently than the PM's signal show.

Something in the experimental setup seem to prevent light emitted from streamer heads, from entering the photomultiplier. The reference image in Figure 4.9 definitely shows visible light being emitted as the streamer passes the entrance window, without appearing in the PM signal at all. 11 out of 20 measurements from series 27 at 80-81 kV with velocities between 82 and 111 mm/µs, showed the same. The error seem to be velocity dependent, as all measurements with breakdown velocities above 80 mm/µs in both series 23 and 27, show this trend. This error implicates that the hypothesis of whether fourth mode streamers emit UV light, could not be tested in this work.

Note that these streamers glow very intensely in the reference image,

which corresponds a large amount of photons. Hence the PM's photocathode is expected to be excited.

It is possible that the streamer heads where no light is detected in the PM signal, emit light less frequently than required to detect them as they pass the PM's entrance window. The passing time pt (see (3.1)) for streamers with velocity $80\,\mathrm{mm/\mu s}$, is 0.95 ns. Hence, if the streamer head emits light less frequently than once every nanosecond, it is not likely to be detected by the PM. If this is the case, then it can be tested in the future simply by increasing the entrance window height.

One could argue that the entrance window was too small relative to the sampling rate of the oscilloscope. The sampling rate was 5GS/s in these series. If the instant velocity was more than $200\,\mathrm{mm/\mu s}$, passing time pt would correspond to less than one sample in the oscilloscope recording, with the risk that a continuously glowing streamer head would pass the entrance window without being recorded. However, the photomultiplier response to a single photon, lasts for 1-2 ns regardless of the velocity of its origin. This corresponds to more than 5 samples. The PM detects light independent of the oscilloscope sampling rate, hence any continuously glowing light source will be detected.

One possible factor that may prevent emitted light from being detected by the photomultiplier, is scattering of light. The glass was excavated by streamers in a non-smooth fashion, which will scatter the light. The worst case scenario would be that the surface was angled in such a way that it directed all light outside the marginal rays of PM's optical system. However, this scenario is less likely, as the numerical aperture was wide. Hence a sharp refraction angle would be necessary if all beams of light were to miss the entrance pupil of PM's optical system.

Intensity of emitted light

The intensity of emitted UV light from streamer heads increases with applied voltage, but not with breakdown velocity for second mode streamers. In Figure 4.10 this is observed by the step increase in mean detected light intensity from 50 to 60 kV applied voltage. This is expected because higher electric field strength implies higher electron energy and hence more excited molecules after collisions. When the applied voltage is fixed and the breakdown velocity increases for second mode streamers, the mean detected light intensity is constant.

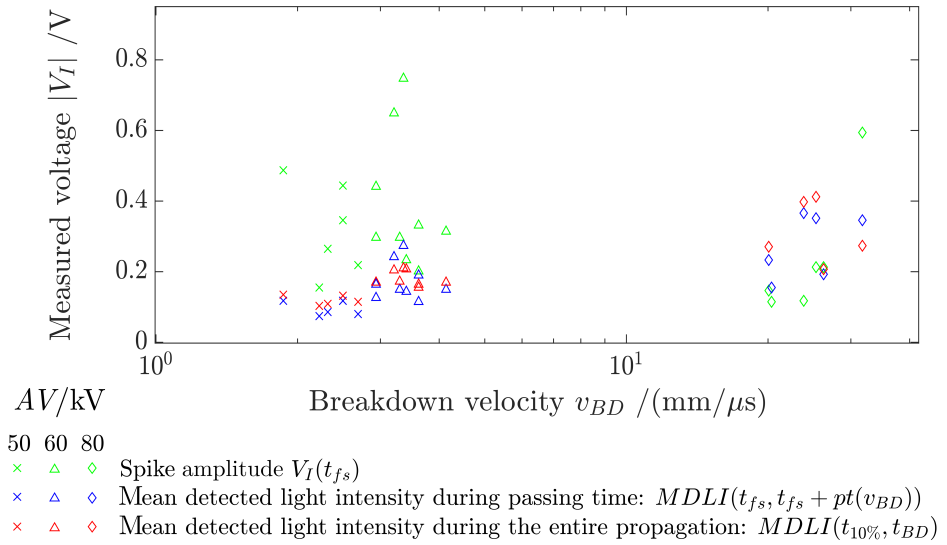

Figure 4.10: Spike amplitude is the intensity of a light pulse most probably emitted from the head. Passing time pt is defined as the time it takes for a streamer head to pass the PM's field of view, hence the time domain $[t_{fs}, t_{fs} + pt(v_{vBD})]$ is when the streamer head appear in PM's recording. $t_{10\%}$ is the time when applied voltage pulse was triggered and t_{BD} is the time of breakdown. Mean detected light intensity $MDLI$ is explained in section 3.4 and equation (3.5). The data behind the statistics in this figure, has been selected from series 23 based on the head detection criteria (described in section 3.4). All selected data are presented in Appendix B.

On average the emitted UV intensity increases slightly from second mode streamers at $AV = 60$ kV, to third mode streamers with $AV = 80$ kV. This is seen by the mean detected light intensity in the interval where the head is estimated to pass the entrance window, $MDLI(t_{fs}, t_{fs} + pt(v_{BD}))$, in Figure 4.10. However, the first spike when a streamer head is believed to enter PM's field of view (t_{fs}), is just as intense for streamers with velocities below $10\,\mathrm{mm/\mu s}$ as above it.

It is possible that the emission spectrum has changed as the applied voltage increases. As voltage increases, the electron energy released in collisions is expected to increase, which results in higher excitation and thus higher photon energies emitted from a molecule. This may imply that the emission spectrum shifts into a domain where more of the emitted light would be absorbed by the bandpass filter (F1). Consequently the radiant power from a streamer may have increased more from second to third mode than it appears by the measured voltage $|V_I|$ in Figure 4.10.

One interesting observation in Figure 4.10 is that the intensity of light pulses emitted from streamers, varies more when the breakdown velocity is of order $10\,\mathrm{mm/\mu s}$ than of order $1\,\mathrm{mm/\mu s}$. One possible explanation for this, is that streamers can propagate in a combination of modes across a gap. If this is the case, then different streamer modes may be observed as streamers enter the PM's FOV, even though their breakdown velocity is almost the same.

Unfortunately, no data in series 23 with streamers propagating in fourth mode, met the criteria for streamer head detection, as described in the analysis section 3.4. Even though some reference images captured the streamer head close to the PM's entrance window, no sign of UV light appeared before breakdown. As discussed earlier, there appears to be some kind of error preventing the photomultiplier from detecting the light from fourth mode streamers .

It is not necessary for the intensity to increase with the streamer modes, in order for the hypothesis about photoionisation to hold. Photoionisation as a dominating propagation mechanism only requires that the streamer frequently emit photons in the correct wavelength domain. However, more molecules will be ionised if the amount of emitted photons increases, resulting in an enhanced propagation, if photoionisation is a driving mechanism. Increased detected light intensity corresponds to more photons detected.

Heads and tails of streamers with velocities between 0.4 and $4\,\mathrm{mm/\mu s}$ appear to emit equally intense light. A comparison between the detected

light intensity across the entire PM-signal, $MDLI(t_{10\%}, t_{BD})$, and the detected light intensity from the streamer as it passes the entrance window, $MDLI(t_{fs}, t_{fs} + pt(v_{v_BD}))$, is presented in Figure 4.10. Since these statistics are almost equal at velocities around $4\,\mathrm{mm/\mu s}$, one can argue that the emitted intensity from the tail does not differ much from the head of a streamer. This is supported by the fact that the spike amplitudes from anywhere in a signal, vary within the same range, when studying each PM recording of measurements with $AV \in [40, 60]$ kV.

4.3.2 Radiant Power from Streamer Head

The detected light appeared continuously from streamer heads in cyclohexane, with 80 kV applied voltage (see section 4.3.1). These streamers had breakdown velocity of about $20\,\mathrm{mm/\mu s}$. In this section the radiant power of emitted light from these streamer heads, are estimated based on the point source model presented in section 3.4.

The radiant power of UV light emitted from a third mode streamer head, is $\geq 9 \times 10^{-8}\,\mathrm{W}$, as integrated across the wavelength domain from 160 to 450 nm. This is based on a mean detected light intensity of $V_I = 0.4\,\mathrm{V}$ in the point source model equation (3.6), with the spectrum model (C).

The radiant power from a streamer head in the UV domain, is credibly of the order 10^{-7} to 10^{-6} W, when based on the models (B) and (A), respectively. This is credible because the spectrum is expected to correlate with the energy levels of cyclohexane molecules. The rough assumption is however that emitted photon energies are equally represented at any time, resulting in a uniform distribution of emitted intensity across these energy levels. A more correct model would be to represent the occupied states and correspondingly the photon energies emitted, with a Maxwell-Boltzmann distribution across these wavelength.

Model (A) is based on the calculated excitation energies of cyclohexane molecules, by Davari et al. [6]. Model (B) is based on the measured absorption spectrum of cyclohexane, as presented in Appendix A. These spectra reflects the available excitation energies of cyclohexane and are therefore expected to represent the emitted energies possible.

The main source of uncertainty is the wavelength dependent transmittance relative to the source's spectrum, because the source's emission spectrum is unknown. As shown, the radiant power varies a lot with the emission spectrum models. The more a spectrum was weighted at wavelengths

where the transmittance is low, the higher will the radiant power be relative to the detected power at the photomultiplier. In order to attain a more accurate estimation of the radiant power, it is recommended that the transmittance is as uniformly distributed across the wavelengths, as possible.

The intensity voltage $|V_I|$ that was used in the estimation of radiant power, was assumed to represent emission from a streamer located in the entrance window at the optical axis[3]. The solid angle would decrease if the point source was located further into the liquid or on the window frames instead of the window's centre. Hence a less fraction of the light would have entered PM's optical system. Therefore the minimum radiant power estimated with a point source in the the entrance window's centre, is also the lower limit of radiant power given any other point source location on the window or inside the liquid (i.e. when absorption of light by the liquid, is neglected). Hence this is the minimum radiant power from a streamer regardless of the streamer's location in the entrance window.

4.3.3 Errors and Uncertainties

One significant error is the use of breakdown velocity v_{BD} as an approximation to the instantaneous velocity of the leading streamer head anywhere in the gap. This error affects the timing of a streamer head's appearance in PM's signal (given by ETA (3.4)), the true passing time pt (see (3.1)) and the comparison between light intensity and velocity. ETA was used in a head detection criterium to estimate when the streamer head would appear in the PM signal. pt was used to define the time frame that the streamer head was recorded by the PM, and therefore defined how much of the channel front that would be regarded as the streamers head. These parameters will all be discussed in the paragraphs below.

The statistics of light detected from the streamer head as it passed the PM's entrance window, were plotted against breakdown velocity. The hypothesis that streamers in third mode emit UV light frequently, was tested under the assumption the breakdown velocity was a good representation of the propagation mode. This assumption is relatively good, as the dominating mode is most likely to be mode that will be recorded as the streamer head passes the PM's entrance window. However, since streamers are able

[3]Remember that the PM's entrance window is the image of the slit, and is located in the same plane as the glass surface that streamers are assumed to propagate along

to transition between modes during propagation, there is a possibility that the statistics spike rate and spike amplitude were based on light pulses that originated from a streamer in a different mode than the breakdown velocity would indicate. In the future this possible error could be avoided by using the position and time of the streamer given in the reference image, to the better estimate the streamer head's velocity as it passes the PM's entrance window.

The most important source of uncertainty when determining whether the streamer head emits UV light, is that the head's appearance in the PM's signal had to be estimated. By the head detection criteria , data were selected on the demand that spikes had to appear relatively close to $ETA(v_{BD})$ (3.4). An assumption still had to be made that the head would appear as the first sign of light between the time when the image was taken and the $ETA(v_{BD}/10)$. This large time range was used in case a mode transition occured between the streamer position in the image, and the entrance window.

To get this estimated time ETA right, is crucial because it determines whether the streamer head light was considered instead of its tail or any pre-spikes(see pre-spikes in section 4.3.3). It is therefore good to know that the ETA was quite certain in this experiment. Light pulses appeared from second mode streamers no later than $ETA(v_{BD}/3)$, which makes sense as streamers that propagate as a single mode, are expected to propagate slower in the center of the gap than the mean velocity to breakdown v_{BD} [2]. In addition these streamers showed no light pulse that could be distinguished from the others. Therefore the error of representing spikes from the tail instead of the head, is negligible. And for third mode streamers there were mainly one continuous light signal in the PM recording, and these light signals appeared approximately at $ETA(v_{BD})$.

ETA in (3.4) also depends on the distance x between the PM's entrance window and streamer head in the reference image, and the velocity across that distance. The entrance window frames [4] in the preparatory reference images where hard to define accurately, hence distance x became inaccurate. The relative resolution error is equal to $\Delta x/x = \Delta\tilde{h}/\tilde{h} = 0.3$, where $\tilde{h}$ is the entrance window height as measured in the preparatory reference image. In addition second mode streamers appeared only as weak light

[4] Remember that the entrance window is the image of the slit at the glass-liquid interface where the streamers propagated.

spots in some images, which made it harder to locate the leading streamer head. Still, these errors are negligible relative to the error of approximating the velocity in the ETA, with breakdown velocity.

The estimated passing time $pt = h/v$ (3.1) also depends mainly on the streamer velocity v. The entrance window height, h, was accurate ($\Delta h/h = 5\%$). The statistics spike rate and mean detected light intensity presented in Figure 4.6 and 4.10, depended on the estimated passing time, as they were describing different features of the streamer's head. The error in estimating the passing time by using a breakdown velocity v_{BD}, mainly had the effect of defining how much of the streamer channel is regarded as its head. For instance, if the streamer propagated slower than v_{BD} when it passed the PM's entrance window, it would only mean that less than the distance h would be regarded as the streamer's head. $h = 0.076$ mm is already a large fraction of the streamer head, so it is an improvement if a less part of the streamer head is considered. Conclusively any error in the passing time estimation does not affect the result noteworthy.

The sensitivity of the photomultiplier is given by its dark current. In this work the background noise observed in the dark current, increased during the series 23, from $0.02\,\mathrm{V}$ at $AV = 40$ and 50 kV, to $0.06\,\mathrm{V}$ at $AV = 60$ and 70 kV, and finally $0.11\,\mathrm{V}$ at 80 kV. A similar development was seen in series 27. Hence the light could be sensed quite well in this experiment. It is mainly the quantum efficiency that limits how many emitted photons that will be detected by the photomultiplier.

Excavated glass

The double set of fused silica glass tangent with the needle electrode, was gradually excavated by streamers propagating along its surface. The excavated surface is rough and therefore expected to scatter the light emitted through it, towards the photomultiplier.The question is how much this scattering distorts the image at the photomultiplier. That will be a task for future studies.

One suggested reason for the cracks in a single glass and excavation of a double glass, is the pressure/shock waves from the rapid expanding channels[12].When channels are further away from the glass, the pressure at the glass is believed to be reduced. This coincides with the fact that this window deterioration was not observed when the needle was located further away from the glass.

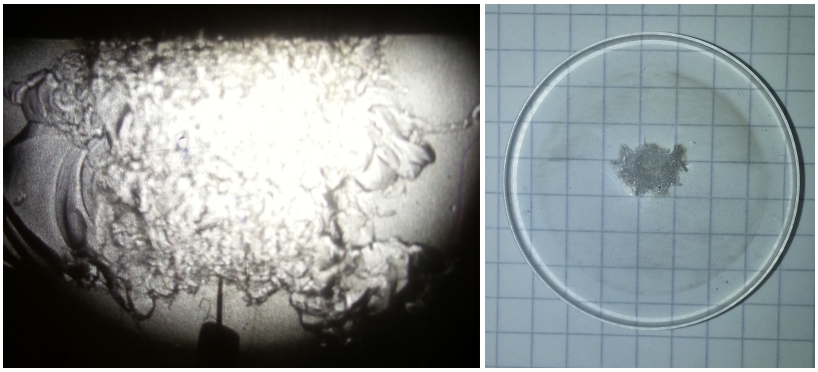

(a) Background light through the testcell and excavated glass.

(b) After experiment: Cavity was 5 mm wide and 1 mm deep.

Figure 4.11: Excavated glass has a rough surface in the cavity.

Light scatters at rough surfaces. With permittivity two times higher in the glass than in the liquid, the light refracts. With many small edges and surfaces, the glass would act as many small prisms. Figure 4.11a depicts shadows in the image of the glass tangent to the needle. When removed from the test cell, the glass reflects a lot of light from its cavity when light from the front, and barely transmit light, as Figure 4.11b shows.

Transmittance uncertainties

The absorption of light in the liquid is regarded as negligible. The distance between streamer and the glass is unknown, but based on the excavated glass, it appears to have propagated along the surface. Also, streamers initiated at the glass surface where the needle was located, and they are likely to take the shortest distance across the electrode gap.

The air in the optic tube might have affected the results more than assumed. The air content in the optic tube was unknown, but the majority of air is usually nitrogen (78%) [34], which absorbs negligibly at wavelengths above 173 nm[35]. H_2O and O_2 absorbs highly below 190 nm, and can therefore not be regarded as negligible. [36]. However, CO_2 is negligible in both molar content of air and its absorption coefficient, for wavelengths above 170 nm [36]. Conclusively, the air have most likely absorbed UV light significantly, so this error should be removed in the future. It is possible either to vacuum the optic tube, or to flush it with a gas that do not

absorb light in the wavelength domain of interest.

This experiment did not focus on finding a fine resolved emission spectrum from a streamer in the domain below 200 nm. The transmittance was only had to be above zero in the important domain, which is below 180 nm for cyclohexane. In the future the focus should be on a more precise measurement of the photons emitted below 180 nm. This is discussed in the chapter on Future Work 5.

The extrapolation of the lens transmittance below 200 nm is a significant uncertainty in the emitted power estimation. The lower limit might be higher because the quality of quartz in the lens was assumed to be as high as the fused silica glasses in the test cell. The quality of quartz glass varies, and so will the transmittance. The error of extrapolating the radiant sensitivity below 190 nm for the photomultiplier is regarded as less significant because the glass and photocathode content is known. The producer presented the transmittance of this glass[20]. The bialkali photocathode's radiant sensitivity was reported in [26].

There is a possibility that the photomultiplier's gain given by the producer is out of date. The gain should drop with accumulated counts, as electrons are scrubbing the microchannel walls [25]. Therefore the estimated radiant power in the point source model may be higher than calculated.

Pre-spikes

A phenomenon called pre-spikes caused uncertainties in the estimation of when a leading streamer head appeared in the PM's field of view. Pre-spikes are light pulses appearing in the PM signal before the streamer has entered the PM's field of view. The existence of pre-spikes in present measurements was verified by comparing the reference camera (Proxitronic) and its known shutter opening time t_{so} with the PM signal. These spikes appeared in the PM signal when UV bandpass filter F1 was used and when the longpass filter F2 was used. Hence if these spikes originates from the test cell, then they are photons in UV and visible domain. Figure 4.12 shows an example of pre-spikes in the visible light domain. Pre-spikes appeared usually for measurements where applied voltage was in the range 50 to 70 kV. Pre-spikes were definitely detected in 9 out of 20 PM recordings at 60 kV and 15 out of 20 recordings at 70 kV of series 23. They could appear equally intense as the light pulses that originated from the streamer channel in the PM's field of view. All in all pre-spikes are hard to distinguish from any

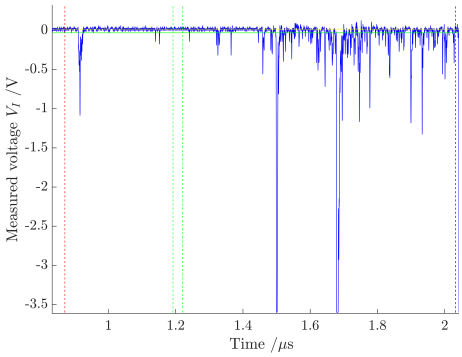

(a) PM recording

PM signal
Voltage triggered: $t_{10\%}$
Breakdown: t_{BD}
Offset
Max. background noise
Ref. Camera shutter open and close

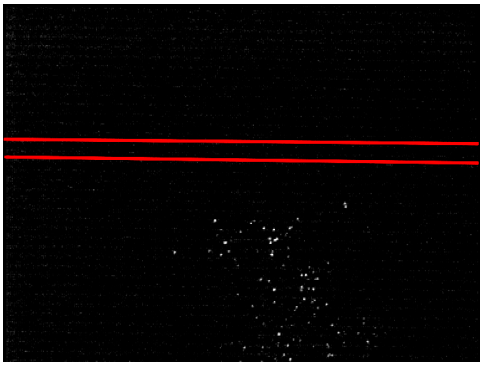

(b) Reference image. Red horisontal lines mark the PM's entrance window frames.

Figure 4.12: The photomultiplier signals show spikes appearing prior to the time when the image was taken (pre-spikes). These can not be light pulses from a streamer channel appearing *in* the PM's field of view, because the reference image shows that the streamer has not passed any of the PM's entrance window frames yet. AV=71 kV, Liquid: Cyclohexane. Filter: F2. The needle is located below the image.

light pulse that originate from a streamer channel appearing in the PM's field of view.

The pre-spikes are not noise pulses in the photomultiplier tube[5]. This statement is based on the measurements of the PM signal taken $3, 6, 9$, etc. minutes after the last applied voltage in a series. No spike above background noise was observed in tens of such dark current measurements.

The origin of pre-spikes, is unknown. No external light source is likely to have penetrated the sealed test locker. One suggestion is that light emitted from outside PM's field of view, is reflected off of the lens and back to the fused silica glass. If the angles are correct, the reflection would only show in the PM signal as long as the ray is within the margins of the optical setup. This requires that the photons reflect at the fused silica glass surface

[5] In Appendix D some possible sources of noise in the dark current, are presented.

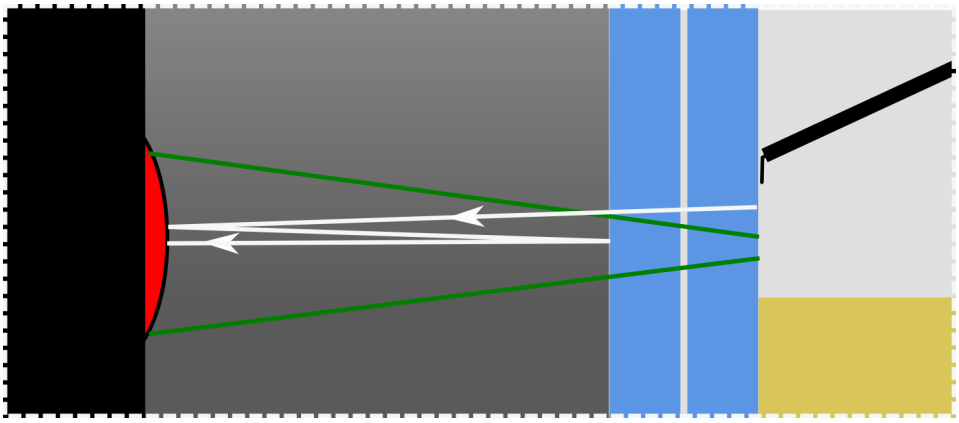

Figure 4.13: The white line illustrates a ray from a part of the streamer not within the PM's field of view. It is reflected at the (red) lens and the (blue) glass, and the final trajectory ends up within the (green) marginal ray with a wider angle than the marginal ray.

within the PM's FOV and travels in a direction within the numeric aperture (NA). An illustration of how light could be reflected, is presented in Figure 4.13. However, this suggestion requires a high fraction of light to be reflected at both the fused silica surface and the lens surface, which is low in the visible and UV domain (light is mostly transmitted). Conclusively this explanation does not seem to be true, Because pre-spikes have been observed to be just as intense as light pulses that have not been reflected, but originate from the streamer. Nor is it likely that any light reflected at any surface within the sample liquid volume would be visible in the UV bandpass filtered PM recordings, because cyclohexane absorbs strongly below $230\,\mathrm{nm}$. The search for the origin of pre-spikes should be performed in the future.

Chapter 5

Future Work

In this section some important improvements are suggested. The objective of these tasks are the same as the superior objective has been for this thesis: to aid and finally test the hypothesis about photoionisation as a dominating mechanism for third and/or fourth mode streamers. Solutions to some challenges on the way to this objective, will be presented.

First and foremost the goal was to measure how much and how frequently photons of high energy are emitted from streamers up to fourth mode. In this experiment a UV bandpass filter (F1) was used. Its wavelength domain of non-zero transmittance was wide and could only indicate that UV (wavelength below 400 nm) was emitted from the streamer. The more interesting domain is however below 180 nm for cyclohexane and many other liquids relevant for streamer modelling. These wavelengths corresponds to the excitation energies of these liquids, as calculated by Davari et al. [5]. It is at these high energies the ionisation by photons seems most likely to first occur as applied voltage is increased. The most important improvement will therefore be to invest in, and implement, a filter that absorbs higher wavelengths than about 180 nm.

Another approach to study a narrower wavelength domain around 200 nm, is to subtract detected, longpass filtered intensity from the unfiltered intensity of a streamer. Generally, the challenge of comparing measured intensity voltages of different filters, is that they filter differently depending on the wavelength of incident light. One must therefore calculate the incident power to both filters, which has been shown in this thesis to not be precise. Fortunately, the No filter (F0) and longpass filter (F2) total radi-

ant sensitivities are approximately equal in the wavelength domain between 280 and 700 nm. And the longpass filter (F2) has a quite sharp cut off (0 to 90 % transmittance from 230 to 280 nm). Hence, when subtracting the measured intensity voltage of F2 from F0, the remainder is approximately equal to the unfiltered (or F0 filtered) light detected in the domain 160 to 280 nm.

A combination of filters that is recommended, is to put the bandpass (F1) and longpass (F2) filters in series[1]. The transmittance of this combination will then be approximately equal to F1 in the wavelength domain 260 to 450 nm. The measured intensity through this combination can therefore be subtracted from measured light through F1 alone. Since the wavelength dependence of these transmittances are almost the same, no assumption has to be made about the streamer's spectrum.

There is, however, a catch to this method. As results have shown during this thesis, the measured intensity from streamer to streamer may vary quite a lot, specially at 80 kV in cyclohexane. To subtract the mean intensity of many different streamers, therefore seems quite imprecise. One suggested solution to increase the precision, is to install a second photomultiplier that observes the same as the main photomultiplier . If the second PM observes the unfiltered light while the main photomultiplier is recording longpass filtered light, the remainder will be the light detected from a single streamer within the desired wavelength domain. This requires to split the light beam with for instance a prism or a semi-transparent mirror [37]. The requirement of UV-transparency down to 150 nm may cost, but it might be worth it.

One challenge on the way to increase the resolution in the UV domain, is to know the lower bound of the total radiant sensitivity of PM and its optical system, more accurately. Neither the lens nor the photomultiplier used, had transmittance or radiant sensitivity documented below 200 nm. To calibrate the lens may be doable, but the photomultiplier is harder to calibrate as it is so sensitive to light. This improvement is therefore desirable, but may not be possible to attain.

The absorption of light by air below 200 nm is also an unknown factor. To study this will improve the accuracy of the measurements, but has a lower priority than to find the lower bound of the optical system's total

[1] Some data were recorded with this filter combination, but almost no reference image met the head detection criteria.

radiant sensitivity. This is because it is suspected to absorb negligibly.

During this experiment, a couple of errors occured where the origin is unknown. It appears that in order to measure light intensity from fourth mode streamers, the cause that prevents such emitted light from entering the photomultiplier, must be found. The origin of the pre-spikes should also be investigated.

The objective of acquiring the light emitted from the head and distinguish it from the rest of a streamer, is to study where most collisions happen and hence where radiation is expected to origin. How intense and how frequently photons are emitted from the head, will be important in the test of the hypothesis about photoionisation as a mechanism in streamer propagation. In order to study streamer heads more accurately, it is recommended to strengthen the statistics of streamer heads. In the laboratory, this is done either by recording a lot of measurements, improve the timing of the reference camera or increase the resolution of the intensity measurement (the PM) without reducing the sensitivity too much. An equipment upgrade is therefore desirable. One possibility is to invest in a multi-anode photomultiplier tube [2]. With higher spatial and time resolution, the streamer head can be traced as it propagates across the gap. The cheaper, but less accurate solution is to perform more measurements with the equipment at hand. When doing this, it is highly recommended to set the reference camera's shutter time closer to when the head appears in PM's entrance window. That way more of the data can accurately pinpoint when the head appears in the photomultiplier's recordings.

The arrival of a streamer head in PM's entrance window can be estimated better in the data analysis. In this thesis the breakdown velocity was used as an approximation of the streamers instantaneous velocity between the heads position in the reference image and the estimated arrival in PM's entrance window. This ETA will be improved with more data on the streamers whereabouts as it crosses the gap. The next iteration should therefore be to add the streamer head's position and time from the reference image, in the calculations of ETA.

The reference images could be clearer. This is done by increasing the Proxitronic gain or shutter time at the lower voltages with slower streamers, and decreasing the gain for higher voltages. Unfortunately, both gain

[2]Multianode photomultiplier tubes by Hamamatsu: `https://www.hamamatsu.com/resources/pdf/etd/PMT_handbook_v3aE-Chapter9.pdf`

and shutter time must be tuned manually on the Proxitronic control box, and will therefore require the presence of person measurement series over several modes and voltages.

As it turned out, the head did not stand out from its tail's signal in the PM for second mode streamers in cyclohexane. And for third mode streamers, only light from the head was detected, with the exception of some re-illuminations. One may therefore question the need of detecting the head light in particular, when studying emitted light intensity. In this thesis, the mean detected light intensity of the entire PM recording to breakdown, deviated negligibly from the mean detected light intensity during the time when the head was in PM's entrance window (see Figure 4.10).

The uncertainties in the measurements by using breakdown velocity to represent the streamers' velocity anywhere in the gap, has been discussed in section 4.3.3. The instantaneous velocity of a streamer can be estimated more accurately if more data on the streamer's whereabout at various times, is collected. As a first iteration, the position and time of the streamer head in the reference image can be used in the estimation.

The precision of the measured intensity may have been affected by light being scattered in the excavated glass. It is suggested to study the effect of the glass cavity on the detected intensity. This could also be done by replacing the PM with the reference camera for a moment, to see the spatially resoluted image of a streamer through that glass.

In this thesis the intensity has been presented in terms of mean detected light intensity in order to compare the continuous light detected in $AV = 80$ kV measurements, with the single light pulses detected when for example 60 kV was applied in these series. The maximum of a delta function (that represents an incident photon to the PM) is represented in the maximum value of any function convoluted with it, like the response function of the photomultiplier (as presented in Figure 2.10 in the Theory chapter). Hence the photon intensity is best represented in the data by the maximum value of each spike in the PM signal. However, the challenge when analysing the data, is to find a local maximum in a light pulse containing many, closely succeeding photons, like the ones measured at 80 kV AV. In the future it may increase the accuracy of the results if the raw data V_I is inverse convoluted (or deconvoluted [3]) with PM's response function.

[3]Deconvolution is available in Matlab, as shown on webpage `http://se.mathworks.com/help/matlab/ref/deconv.html`.

One of the main sources of uncertainty when calculating the power of emitted light based on measured intensity voltage, is that the total radiant sensitivity is highly wavelength dependent, while the sources spectrum is unknown. If a more accurate calculation of the power is desired, one good option is to improve this calculation is either by decreasing the filter's transmittance width substantially, thus increasing resolution in the wavelength domain. Another possibility is to obtain a total radiant sensitivity of the optical system that is as square shaped as possible. That way all wavelengths are "scaled" equally through the optical system, within the filters wavelength domain. The consequence is that the calculated power becomes wavelength independent.

In this work, the breakdown velocity distribution across applied voltages, changed significantly relative to measurements performed for streamers in the bulk of the liquid. Some possible experiments can be made to test the effect of the glass and of the electrode geometry, on the streamer propagation. The effect of the electrode geometry may be tested by replacing the glass with another solid insulation where the streamer velocity along its surface, is known from needle-plane experimental setups. The glass' effect on the streamer may be tested by putting glass up against the needle in the experimental setup that was used to measure the breakdown velocity of streamers in the bulk of the liquid. This would only require to make a stable holder for the glass, put it inside the test cell against the needle, and fill the rest of the test cell with liquid.

Chapter 6

Conclusion

The hypothesis that third mode streamers emit UV light frequently, is supported by this experiment. Streamer heads in cyclohexane appear to emit UV light more frequently in third propagation mode than in second mode. However, no data were collected where the quality was good enough to determine whether the step in measured spike rate is due to a change in propagation mode or a change in the applied voltage.

No light, not in visible nor UV domain, was detected by the photomultiplier from any leading streamer head in fourth propagation mode, even though the reference camera detected intense light. There is most likely an experimental error preventing the emitted light from being detected by the photomultiplier. Due to this error, the hypothesis that UV is emitted frequently from fourth mode streamers, could not be tested in this work.

The amplitude of the detected UV light pulses does not differ significantly between second and third mode streamers in cyclohexane, but increase slightly with applied voltage. The intensity of emitted light pulses from second mode streamer heads could not be distinguished from that of their tails. In third propagation mode, however, mainly the streamer head was glowing.

It is important to note that the transmittance of the bandpass filter used in this experiment, is quite dependent of wavelength. Together with an unknown streamer emission spectrum, this makes it difficult to compare measured intensities even from streamers in the same liquid, as the electron energy and hence the excitation of the molecules is expected to increase with increasing applied voltage. That way the radiant power at different

modes and voltages, may be absorbed differently before entering the light detector (i.e. photomultiplier).

The radiant power has been estimated as an indication of how intense the streamer head glows when propagating in third mode. The radiant power is $\geq 9 \times 10^{-8}\,\mathrm{W}$ in the wavelength domain from 160 to $450]$ nm.

The breakdown velocity versus applied voltage for streamers of two, different experimental setups, have been compared. The results from the setup where streamers propagated along a glass surface, showed that fourth mode streamers appeared at a higher voltage than in the test cell of an earlier experiment, where streamers propagated in the bulk of cyclohexane. The main cause for this change is suspected to be the shielding effect of different components in this work's test cell.

Bibliography

[1] Erling Ildstad. *High Voltage Insultaion Materials*. Akademika forlag, Trondheim, August 2014. Compendium for TET4160.

[2] L. Lundgaard, D. Linhjell, G. Berg, and S. Sigmond. Propagation of positive and negative streamers in oil with and without pressboard interfaces. *Dielectrics and Electrical Insulation, IEEE Transactions on*, 5(3):388–395, Jun 1998.

[3] O. Lesaint and G. Massala. Positive streamer propagation in large oil gaps: experimental characterization of propagation modes. *Dielectrics and Electrical Insulation, IEEE Transactions on*, 5(3):360–370, Jun 1998.

[4] V. M. Atrazhev, V. S. Vorob'ev, I. V. Timoshkin, M. J. Given, and S. J. MacGregor. Mechanisms of impulse breakdown in liquid: The role of joule heating and formation of gas cavities. *IEEE Transactions on Plasma Science*, 38(10):2644–2651, Oct 2010.

[5] N. Davari, P.-O. Åstrand, S. Ingebrigtsen, and M. Unge. Excitation energies and ionization potentials at high electric fields for molecules relevant for electrically insulating liquids. *Journal of Applied Physics*, 113(14), 2013.

[6] N. Davari, P.-O. Åstrand, M. Unge, L. E. Lundgaard, and D. Linhjell. Field-dependent molecular ionization and excitation energies: Implications for electrically insulating liquids. *AIP Advances*, 4(3), 2014.

[7] Inge Madshaven. Modeling the propagation of streamers in liquids - the townsend-meek criterion and a novel model for photoionization. Master, NTNU, June 2015.

[8] Øystein L. G. Hestad. *Prebreakdown phenomena in solids and liquids stressed by fast transients: The effect of additives and phase*. PhD thesis, NTNU, Trondheim, 2010:243.

[9] Dung Van Nguyen. *Experimental studies of streamer phenomena in long oil gaps*. PhD thesis, Norwegian University of Science and Technology, Faculty of Information Technology, Mathematics and Electrical Engineering, Department of Electric Power Engineering, Trondheim, Norway, 2013.

[10] A. Beroual, M. Zahn, A. Badent, K. Kist, A. J. Schwabe, H. Yamashita, K. Yamazawa, M. Danikas, W. D. Chadband, and Y. Torshin. Propagation and structure of streamers in liquid dielectrics. *IEEE Electrical Insulation Magazine*, 14(2):6–17, March 1998.

[11] P Gournay and O Lesaint. A study of the inception of positive streamers in cyclohexane and pentane. *Journal of Physics D: Applied Physics*, 26(11):1966–1974, 1993.

[12] P. Gournay and O. Lesaint. On the gaseous nature of positive filamentary streamers in hydrocarbon liquids. ii: Propagation, growth and collapse of gaseous filaments in pentane. *Journal of Physics D: Applied Physics*, 27(10):2117–2127, 1994.

[13] Abderrahmane Beroual Thomas Aka-Ngnui. Determination of the streamers characteristics propagating in liquids using the electrical network computation. *IEEE Transactions on Dielectrics and Electrical Insulation*, 13(3):572–579, 2006.

[14] O. Lesaint and G. Massala. Transition to fast streamers in mineral oil in the presence of insulating solids. In *Conference Record of the 1996 IEEE International Symposium on Electrical Insulation*, volume 2, pages 737–740 vol.2, Jun 1996.

[15] N. L. Allen and P. N. Mikropoulos. Streamer propagation along insulating surfaces. *IEEE Transactions on Dielectrics and Electrical Insulation*, 6(3):357–362, June 1999.

[16] Isidor Sauers Loucas G. Christophorou, editor. *Gaseous Dielectrics VI*. Springer Science and Business Media, LLC, Oak Ridge National Laboratory, Tennessee, 1991. Proceedings of Sixth International Symposium on Gaseous Dielectrics.

[17] H. Rodrigo, B.H. Tan, and N.L. Allen. Negative and positive impulse corona development along cylindrical insulator surfaces. *Science, Measurement and Technology, IEE Proceedings* -, 152(5):201–206, Sept 2005.

[18] B.H. Bransden & C.J. Joachain. *Quantum Mechanics*. Pearson Education Limited, 2 edition, 2000.

[19] Ola Hunderi Egil Lillestøl and Jan R. Lien. *Generell fysikk for universiteter og høgskoler - Bind 2 Varmelære og electromagnetisme*. Universitetsforlaget, 2006. ISBN-13: 978-82-15-00006-0.

[20] Hamamatsu photomultiplier tubes 1986. Technical report, Hamamatsu Photonics K.K., Electron Tube Division, Japan, 1986. Published online: `https://archive.org/details/HamamatsuPhotomultiplierTubes1986`.

[21] Hamamatsu mcp pmt r2286u-02, 1985.

[22] R Coelho and J Debeau. Properties of the tip-plane configuration. *Journal of Physics D: Applied Physics*, 4(9):1266, 1971.

[23] Stian Ingebrigtsen. *The Influence of Chemical Composition on Streamer Initiation and Propagation in Dielectric Liquids*. PhD thesis, NTNU, Norway, 2008. 2008:264.

[24] Corning 7980 - glass type: Fused quartz silica. `http://www.sgpinc.com/corning.htm`, Mar 2008. Specialty Glass Products, Inc.

[25] Joseph Ladislas Wiza. Microchannel plate detectors. *Nuclear Instruments and Methods*, 162(1):587 – 601, 1979.

[26] Stanley Sobieski. Ultraviolet response of semitransparent multialkali photocathodes. *Appl. Opt.*, 15(10):2298–2299, Oct 1976.

[27] Calcium fluoride (caf2) windows. http://www.edmundoptics.com/optics/windows-diffusers/ultraviolet-uv-infrared-ir-windows/calcium-fluoride-caf2-windows/2676/, 2016. Edmund Optics.

[28] B. Halle. Uv-vis-ir apochromats. http://www.b-halle.de/EN/Catalog/Objectives/UV-VIS-IR_Achromats.php, march 2013. last modified 18.03.2016.

[29] Uv fused silica windows. http://www.edmundoptics.com/optics/windows-diffusers/ultraviolet-uv-infrared-ir-windows/1-wave-uv-fused-silica-windows/2076/, 2016. Edmund Optics Inc.

[30] Acton Research Corporation. Uv bandpass filter - deep uv, pn number 200-w-2d. Documentation submitted from Acton Optics & Coating.

[31] N-wg-280 25.4mm dia. longpass filter. http://www.edmundoptics.com/optics/optical-filters/longpass-edge-filters/longpass-glass-color-filters/64510/, 2016. Edmund Optics Inc.

[32] Nanocam operating instructions - proxitronic nca-c manual. www.Proxitronic.de - ProxiVision.

[33] Ch. Wohlfarth. *Supplement to IV/6*, chapter Dielectric constant of cyclohexane, pages 348–350. Springer Berlin Heidelberg, Berlin, Heidelberg, 2008.

[34] F.T. Mackenzie and J.A. Mackenzie. *Our changing planet*. Prentice-Hall, Upper Saddle River, NJ.

[35] Aif Lofthus and Paul H. Krupenie. The spectrum of molecular nitrogen. *Journal of Physical and Chemical Reference Data*, 6(1):113–307, 1977.

[36] Kenichi Watanabe, Edward C. Y Inn, Murray Zelikoff, and Air Force Cambridge Research Center (U.S.). Geophysics Research Directorate.

Absorption coefficients of several atmospheric gases. 1953. "Errata sheet" inserted.

[37] GroGlass. Sapphire semi-transparent mirror. http://www.groglass.com/img/media/Sapphire_Semi_Transparent.pdf, september 2015. Company: GroGlass.

[38] Jürgen H. Gross. *Field Ionization and Field Desorption*, pages 355–380. Springer Berlin Heidelberg, Berlin, Heidelberg, 2004.

Appendix A: Liquid absorption

The absorbance spectra of many liquids that are relevant when studying the streamer mechanism, are presented in Figure 6.1. The relevant liquid in this study is cyclohexane. It shows approximately zero absorption between 350 and 700 nm and an absorbance coefficient of 4 between 200 and 225 nm, approximately.

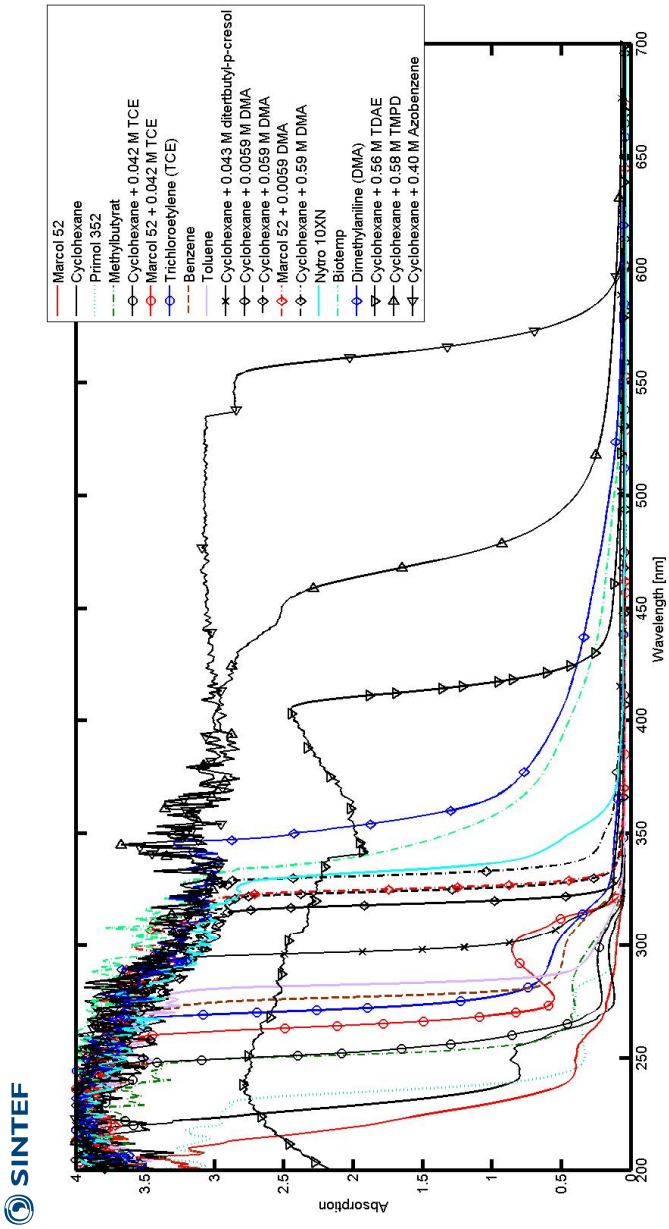

Figure 6.1: Sintef material and Chemistry AS have measured the absorbance spectra through 10 mm samples for different liquids relevant for the study of streamer mechanisms[unpublished, internal communication].

Appendix B: Recordings of detected streamer heads

The following figures depict the measurements that formed the basis for the intensity statistics presented in Figure 4.10, section **??**. These data where selected from series 23 because they meet the head detection criteria which are explained in section 3.4 where the data analysis is described. In short the figures show photomultiplier (PM) recordings where the data samples during the time frame called "passing time" (marked in grey), are regarded as light emitted from the leading streamer head. The corresponding reference images are presented along side. The time frame when the reference camera shutter was open, has been marked in the PM recordings.

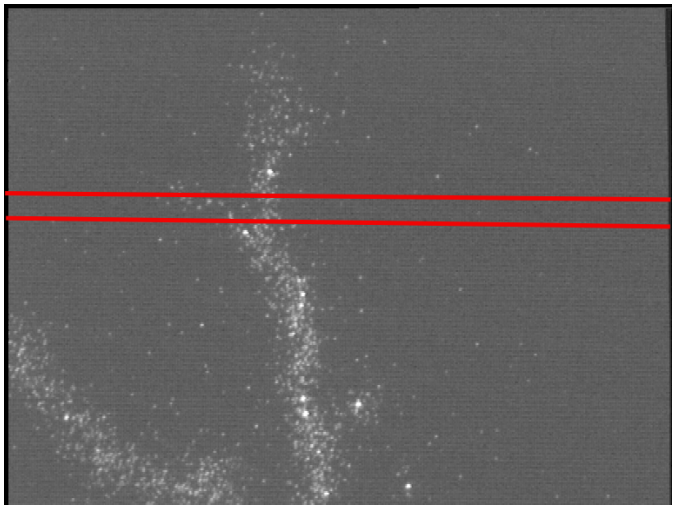

(a) Reference image: Red lines are located at PM's entrance window frames.

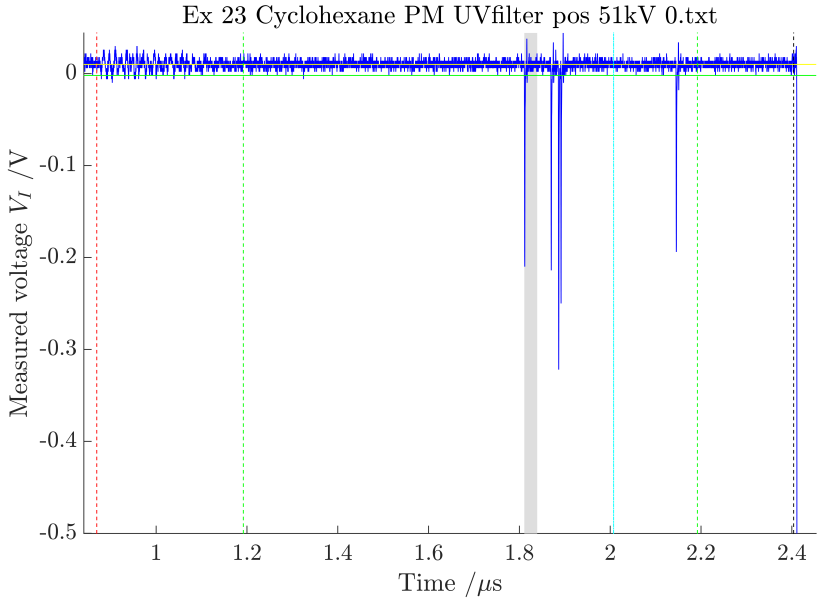

(b) Photomultiplier recording

Passing time: $[t_{fs}, t_{fs} + pt(v_{BD})]$
PM signal
Voltage triggered: $t_{10\%}$
Breakdown: t_{BD}
Offset
Max. background noise
Ref. Camera shutter open and close
$ETA(v_{BD})$
$ETA(v_{BD}/10)$

Figure 6.2: PM recording and reference image of streamer, AV=51 kV, series 23, v_{BD}= 2.7 mm/µs. Liquid: Cyclohexane. Filter: (F1) UV bandpass - peak at 200 nm.

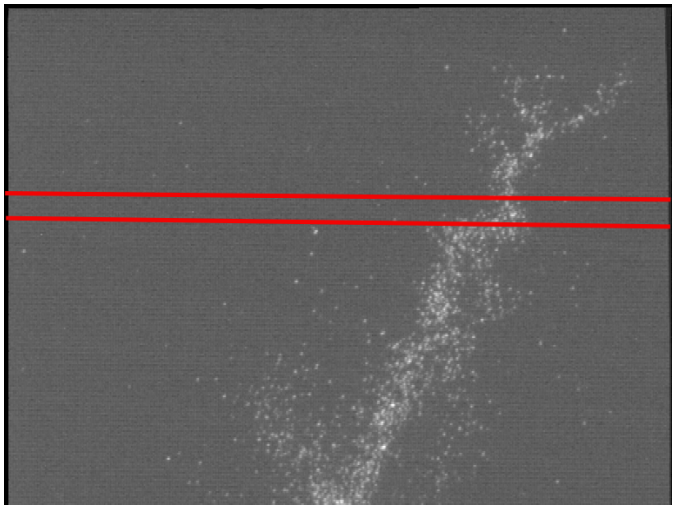

(a) Reference image: Red lines are located at PM's entrance window frames.

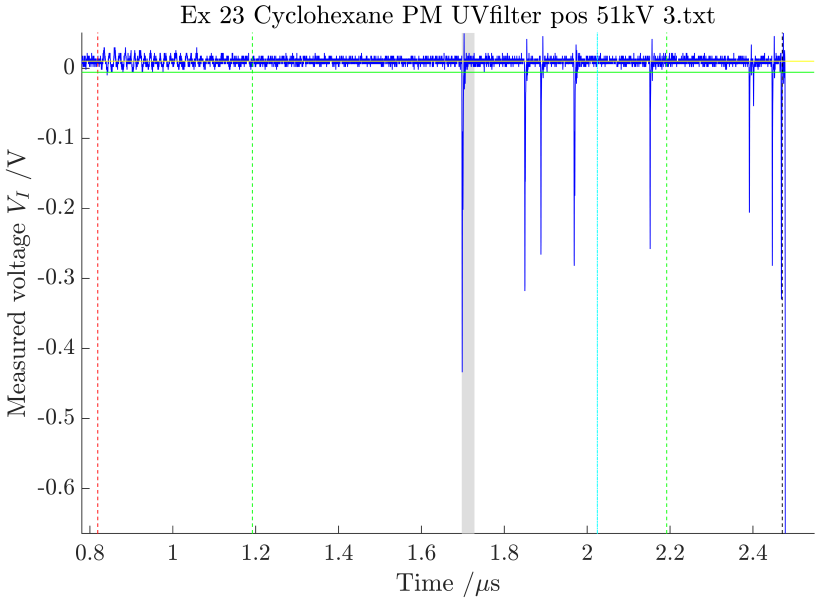

(b) Photomultiplier recording

Passing time: $[t_{fs}, t_{fs} + pt(v_{BD})]$
PM signal
Voltage triggered: $t_{10\%}$
Breakdown: t_{BD}
Offset
Max. background noise
Ref. Camera shutter open and close
$ETA(v_{BD})$
$ETA(v_{BD}/10)$

Figure 6.3: PM recording and reference image of streamer, AV=51 kV, series 23, v_{BD}= 2.5 mm/µs. Liquid: Cyclohexane. Filter: (F1) UV bandpass - peak at 200 nm.

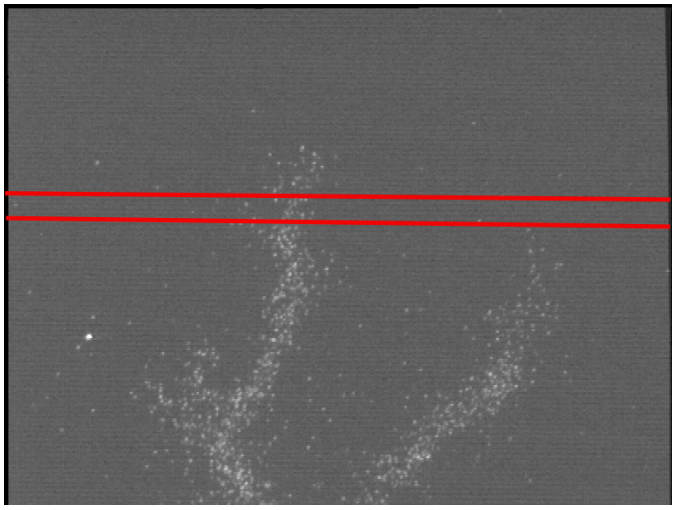

(a) Reference image: Red lines are located at PM's entrance window frames.

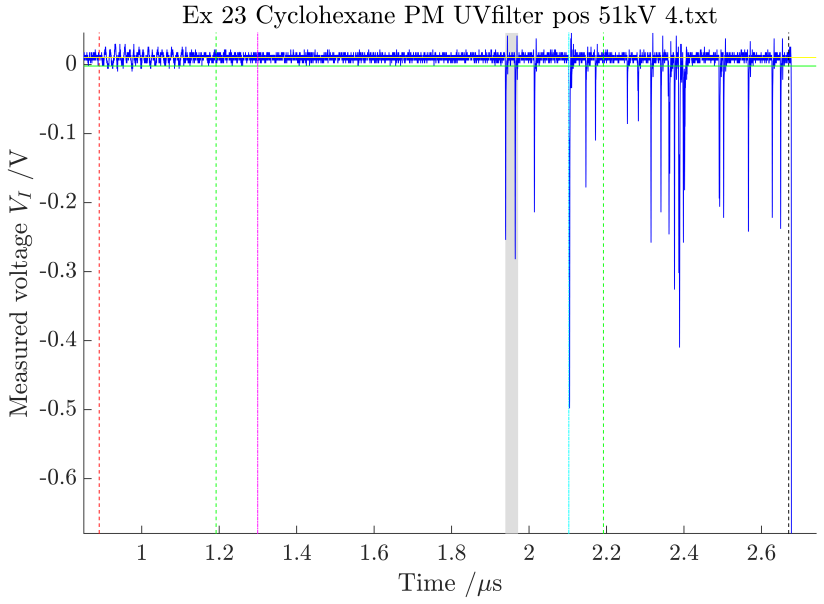

(b) Photomultiplier recording

Passing time: $[t_{fs}, t_{fs} + pt(v_{BD})]$
PM signal
Voltage triggered: $t_{10\%}$
Breakdown: t_{BD}
Offset
Max. background noise
Ref. Camera shutter open and close
$ETA(v_{BD})$
$ETA(v_{BD}/10)$

Figure 6.4: PM recording and reference image of streamer, AV=51 kV, series 23, v_{BD}= 2.3 mm/µs. Liquid: Cyclohexane. Filter: (F1) UV bandpass - peak at 200 nm.

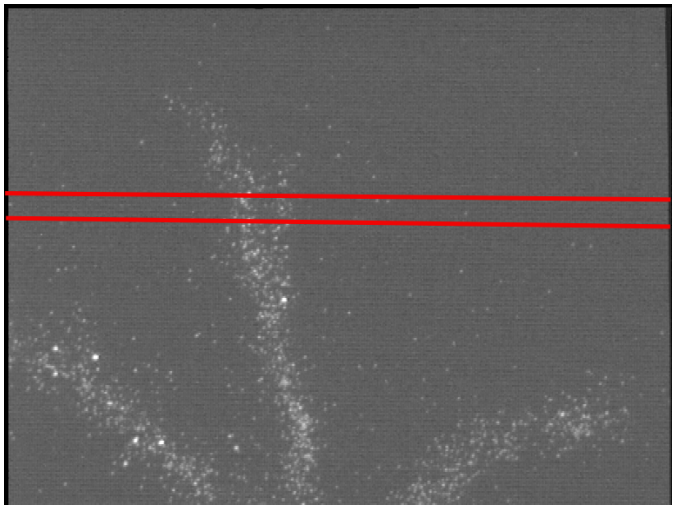

(a) Reference image: Red lines are located at PM's entrance window frames.

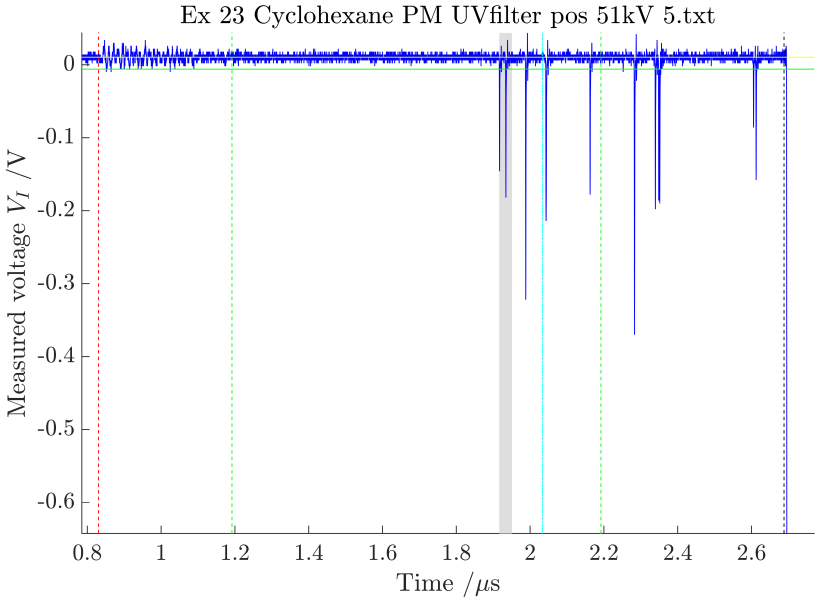

(b) Photomultiplier recording

Passing time: $[t_{fs}, t_{fs} + pt(v_{BD})]$
PM signal
Voltage triggered: $t_{10\%}$
Breakdown: t_{BD}
Offset
Max. background noise
Ref. Camera shutter open and close
$ETA(v_{BD})$
$ETA(v_{BD}/10)$

Figure 6.5: PM recording and reference image of streamer, AV=51 kV, series 23, v_{BD}= 2.2 mm/µs. Liquid: Cyclohexane. Filter: (F1) UV bandpass - peak at 200 nm.

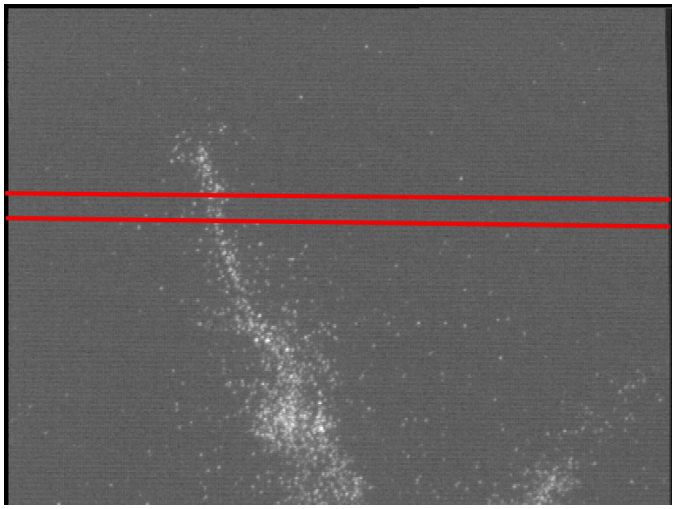

(a) Reference image: Red lines are located at PM's entrance window frames.

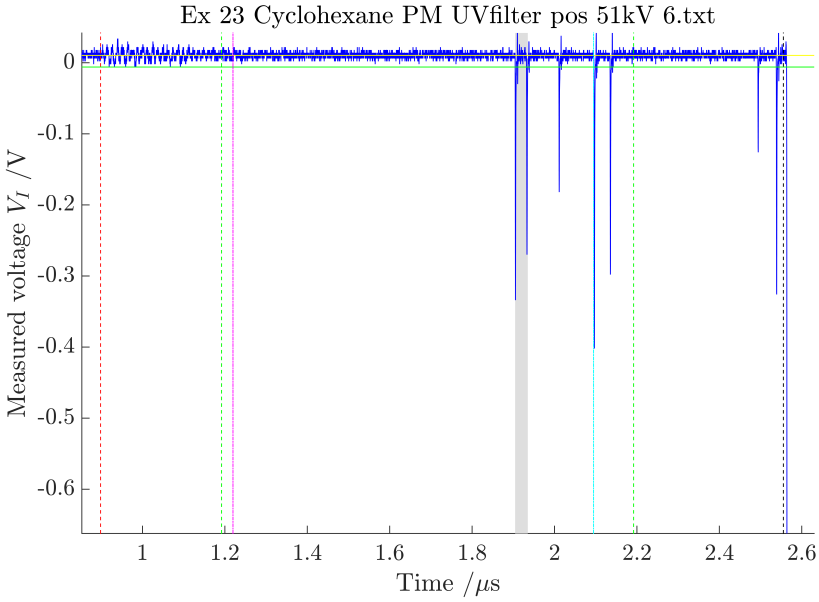

(b) Photomultiplier recording

Passing time: $[t_{fs}, t_{fs} + pt(v_{BD})]$
PM signal
Voltage triggered: $t_{10\%}$
Breakdown: t_{BD}
Offset
Max. background noise
Ref. Camera shutter open and close
$ETA(v_{BD})$
$ETA(v_{BD}/10)$

Figure 6.6: PM recording and reference image of streamer, AV=51 kV, series 23, v_{BD}= 2.5 mm/µs. Liquid: Cyclohexane. Filter: (F1) UV bandpass - peak at 200 nm.

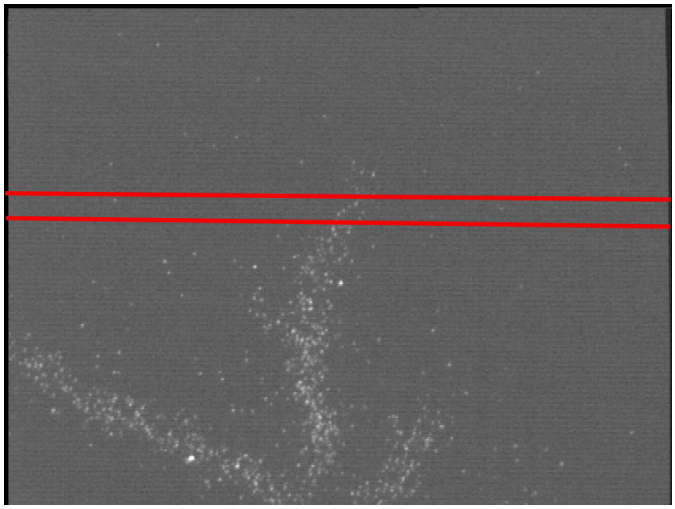

(a) Reference image: Red lines are located at PM's entrance window frames.

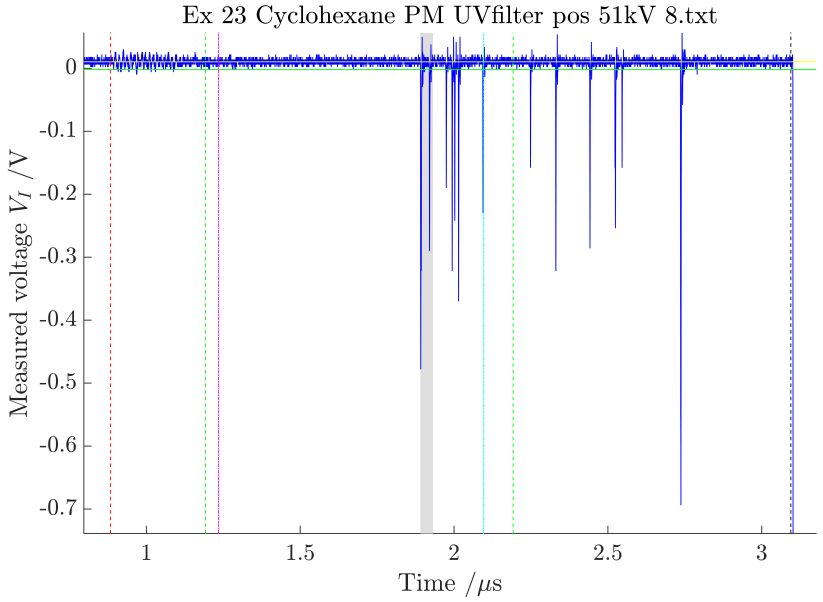

(b) Photomultiplier recording

Passing time: $[t_{fs}, t_{fs} + pt(v_{BD})]$
PM signal
Voltage triggered: $t_{10\%}$
Breakdown: t_{BD}
Offset
Max. background noise
Ref. Camera shutter open and close
$ETA(v_{BD})$
$ETA(v_{BD}/10)$

Figure 6.7: PM recording and reference image of streamer, AV=51 kV, series 23, v_{BD}= 1.9 mm/µs. Liquid: Cyclohexane. Filter: (F1) UV bandpass - peak at 200 nm.

(a) Reference image: Red lines are located at PM's entrance window frames.

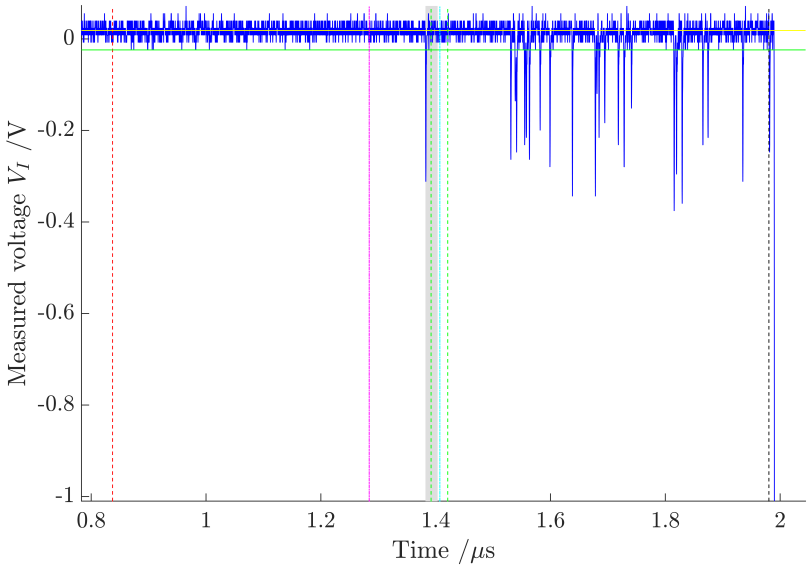

(b) Photomultiplier recording

Passing time: $[t_{fs}, t_{fs} + pt(v_{BD})]$
PM signal
Voltage triggered: $t_{10\%}$
Breakdown: t_{BD}
Offset
Max. background noise
Ref. Camera shutter open and close
$ETA(v_{BD})$
$ETA(v_{BD}/10)$

Figure 6.8: PM recording and reference image of streamer, AV=60 kV, series 23, v_{BD}= 3.6 mm/µs. Liquid: Cyclohexane. Filter: (F1) UV bandpass - peak at 200 nm.

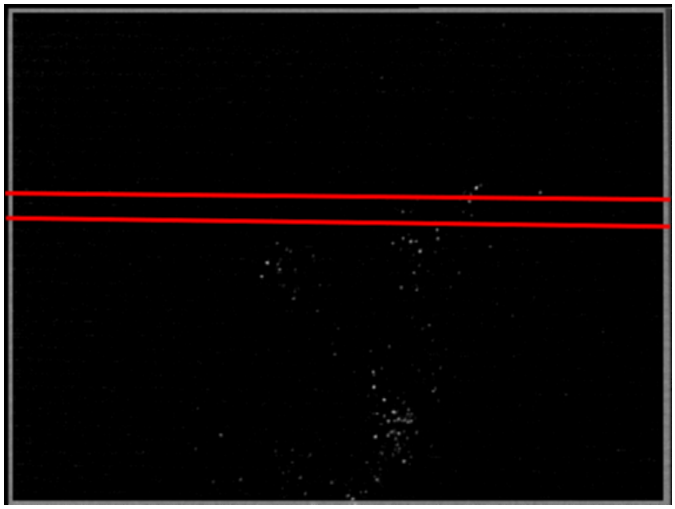

(a) Reference image: Red lines are located at PM's entrance window frames.

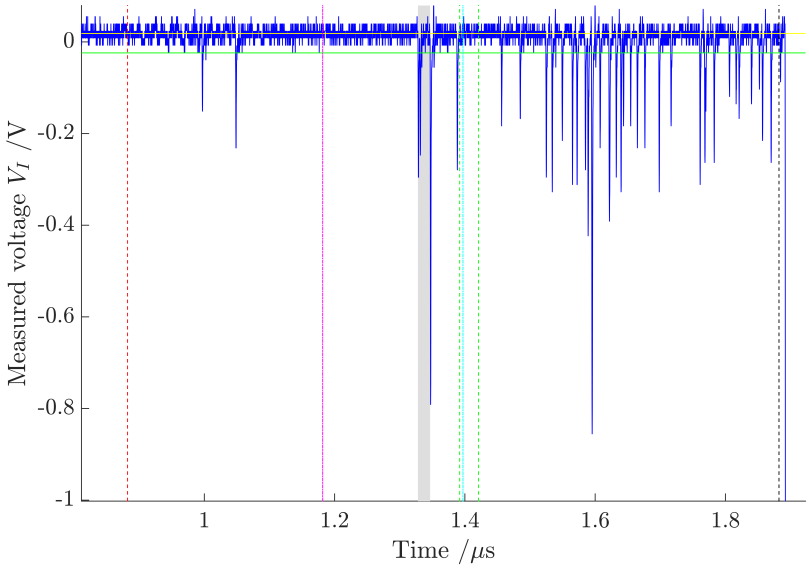

(b) Photomultiplier recording

Passing time: $[t_{fs}, t_{fs} + pt(v_{BD})]$
PM signal
Voltage triggered: $t_{10\%}$
Breakdown: t_{BD}
Offset
Max. background noise
Ref. Camera shutter open and close
$ETA(v_{BD})$
$ETA(v_{BD}/10)$

Figure 6.9: PM recording and reference image of streamer, AV=60 kV, series 23, v_{BD}= 4.1 mm/µs. Liquid: Cyclohexane. Filter: (F1) UV bandpass - peak at 200 nm.

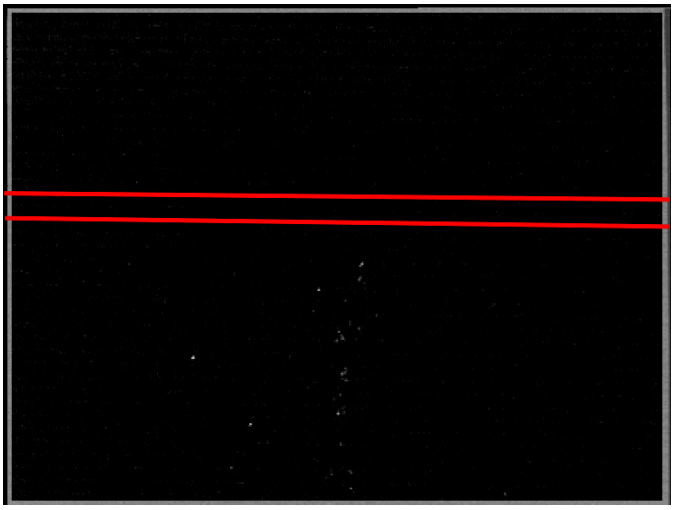

(a) Reference image: Red lines are located at PM's entrance window frames.

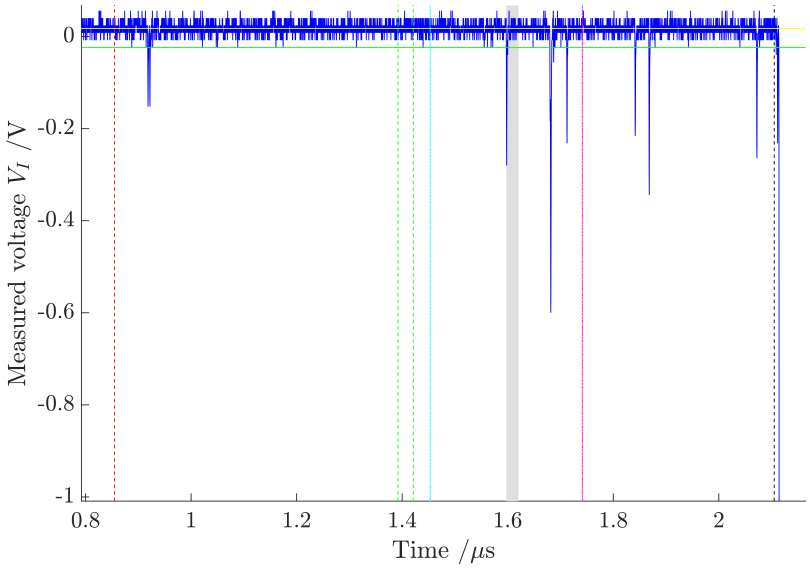

(b) Photomultiplier recording

Passing time: $[t_{fs}, t_{fs} + pt(v_{BD})]$
PM signal
Voltage triggered: $t_{10\%}$
Breakdown: t_{BD}
Offset
Max. background noise
Ref. Camera shutter open and close
$ETA(v_{BD})$
$ETA(v_{BD}/10)$

Figure 6.10: PM recording and reference image of streamer, AV=60 kV, series 23, v_{BD}= 3.3 mm/µs. Liquid: Cyclohexane. Filter: (F1) UV bandpass - peak at 200 nm.

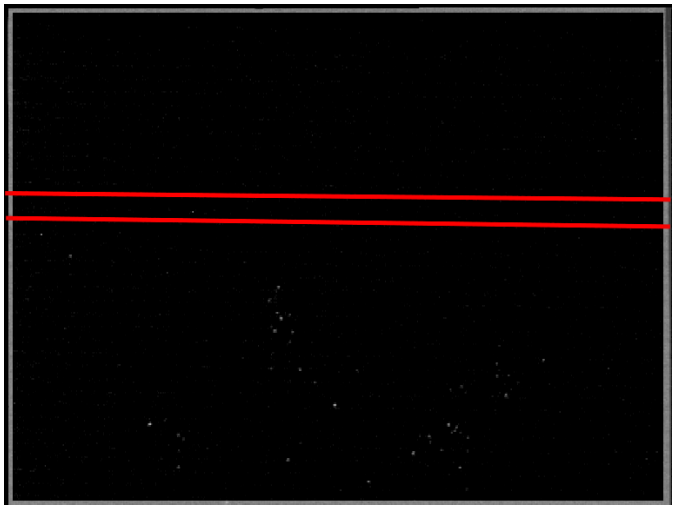

(a) Reference image: Red lines are located at PM's entrance window frames.

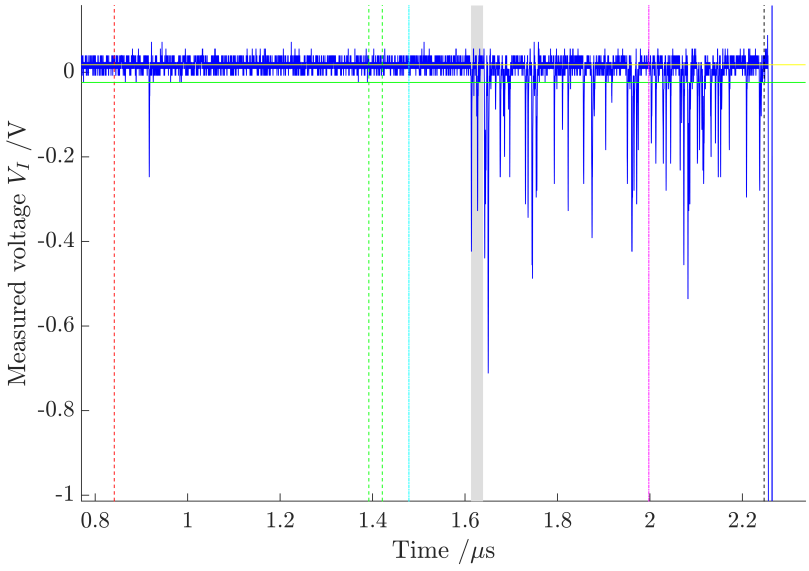

(b) Photomultiplier recording

Passing time: $[t_{fs}, t_{fs} + pt(v_{BD})]$
PM signal
Voltage triggered: $t_{10\%}$
Breakdown: t_{BD}
Offset
Max. background noise
Ref. Camera shutter open and close
$ETA(v_{BD})$
$ETA(v_{BD}/10)$

Figure 6.11: PM recording and reference image of streamer, AV=60 kV, series 23, v_{BD}= 2.9 mm/µs. Liquid: Cyclohexane. Filter: (F1) UV bandpass - peak at 200 nm.

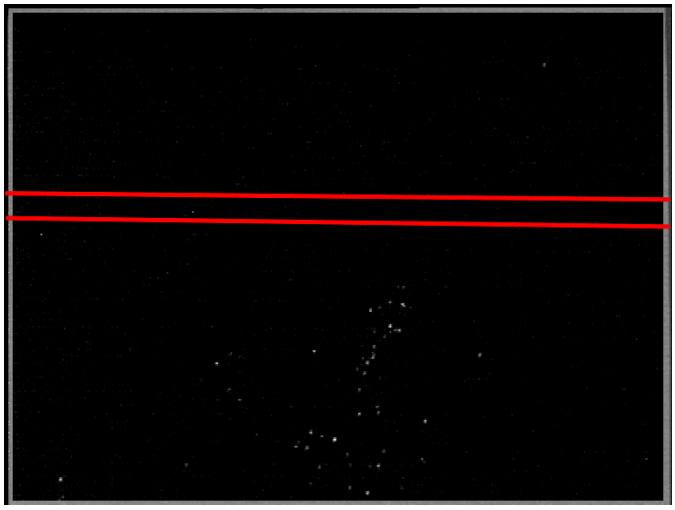

(a) Reference image: Red lines are located at PM's entrance window frames.

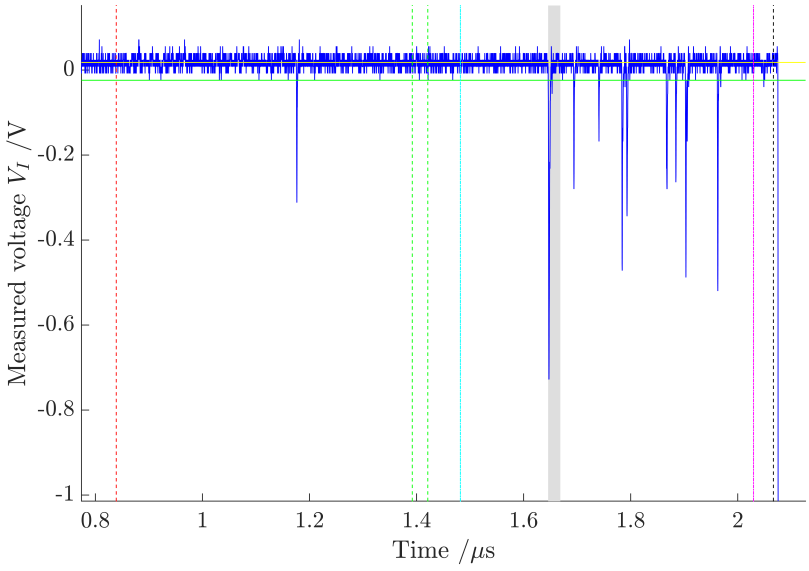

(b) Photomultiplier recording

Passing time: $[t_{fs}, t_{fs} + pt(v_{BD})]$
PM signal
Voltage triggered: $t_{10\%}$
Breakdown: t_{BD}
Offset
Max. background noise
Ref. Camera shutter open and close
$ETA(v_{BD})$
$ETA(v_{BD}/10)$

Figure 6.12: PM recording and reference image of streamer, AV=61 kV, series 23, v_{BD}= 3.4 mm/µs. Liquid: Cyclohexane. Filter: (F1) UV bandpass - peak at 200 nm.

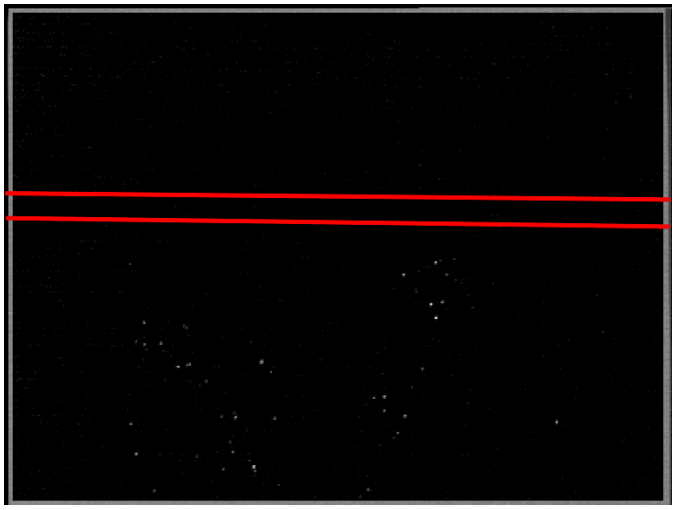

(a) Reference image: Red lines are located at PM's entrance window frames.

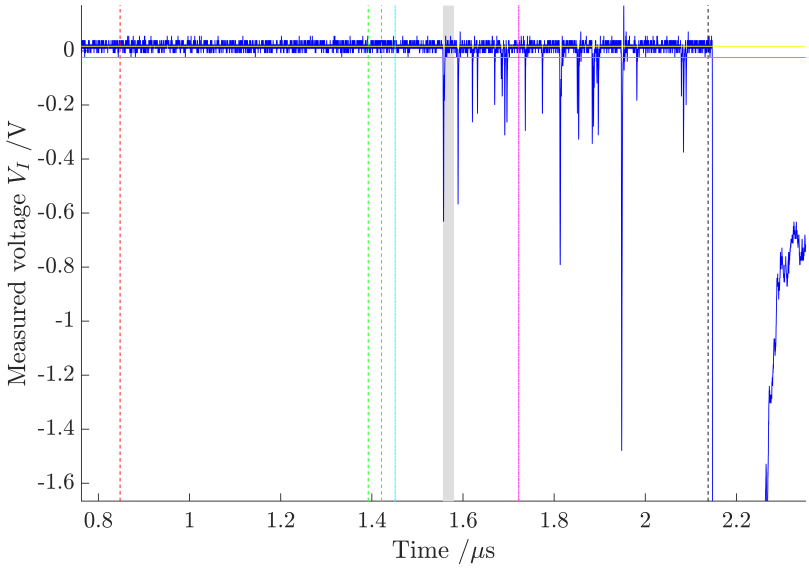

(b) Photomultiplier recording

Passing time: $[t_{fs}, t_{fs} + pt(v_{BD})]$
PM signal
Voltage triggered: $t_{10\%}$
Breakdown: t_{BD}
Offset
Max. background noise
Ref. Camera shutter open and close
$ETA(v_{BD})$
$ETA(v_{BD}/10)$

Figure 6.13: PM recording and reference image of streamer, AV=61 kV, series 23, v_{BD}= 3.2 mm/µs. Liquid: Cyclohexane. Filter: (F1) UV bandpass - peak at 200 nm.

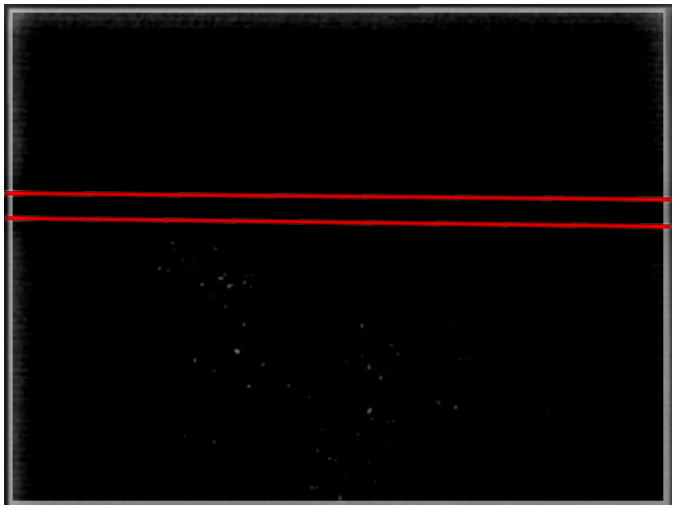

(a) Reference image: Red lines are located at PM's entrance window frames.

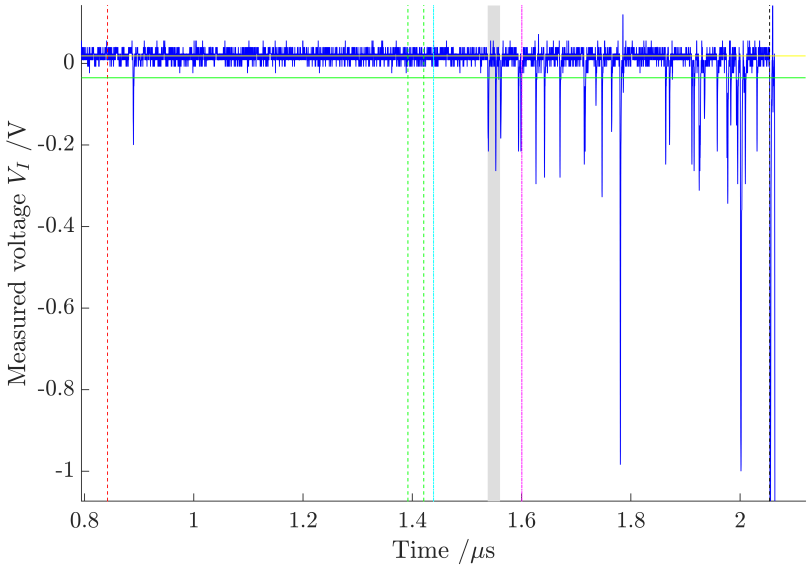

(b) Photomultiplier recording

Passing time: $[t_{fs}, t_{fs} + pt(v_{BD})]$
PM signal
Voltage triggered: $t_{10\%}$
Breakdown: t_{BD}
Offset
Max. background noise
Ref. Camera shutter open and close
$ETA(v_{BD})$
$ETA(v_{BD}/10)$

Figure 6.14: PM recording and reference image of streamer, AV=61 kV, series 23, v_{BD}= 3.4 mm/µs. Liquid: Cyclohexane. Filter: (F1) UV bandpass - peak at 200 nm.

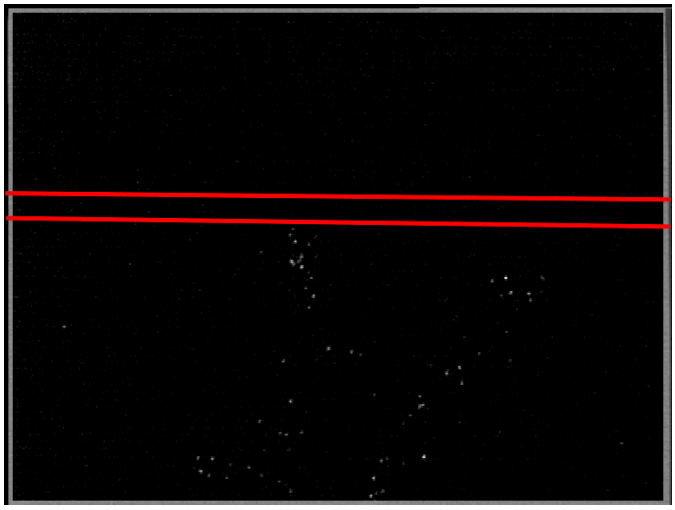

(a) Reference image: Red lines are located at PM's entrance window frames.

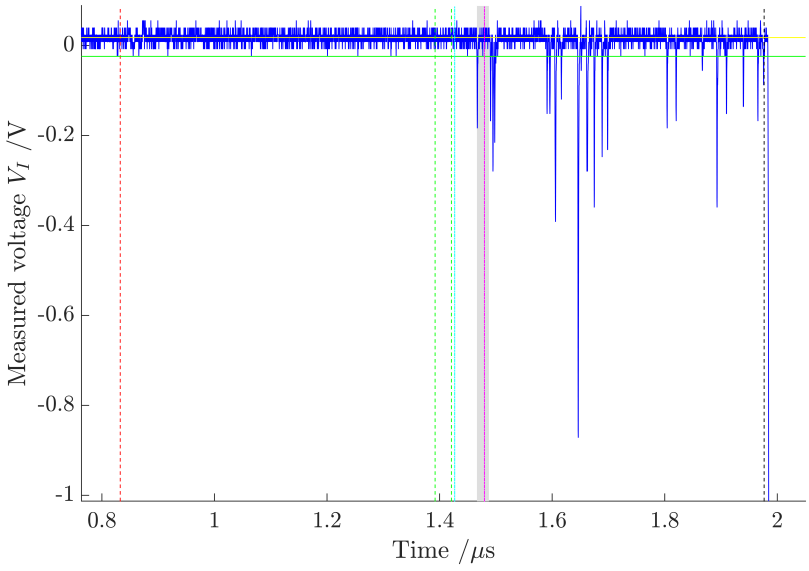

(b) Photomultiplier recording

Passing time: $[t_{fs}, t_{fs} + pt(v_{BD})]$
PM signal
Voltage triggered: $t_{10\%}$
Breakdown: t_{BD}
Offset
Max. background noise
Ref. Camera shutter open and close
$ETA(v_{BD})$
$ETA(v_{BD}/10)$

Figure 6.15: PM recording and reference image of streamer, AV=61 kV, series 23, v_{BD}= 3.6 mm/µs. Liquid: Cyclohexane. Filter: (F1) UV bandpass - peak at 200 nm.

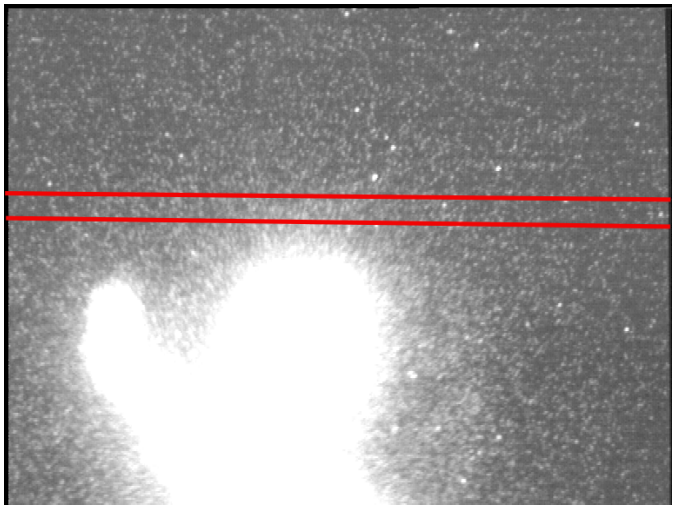

(a) Reference image: Red lines are located at PM's entrance window frames.

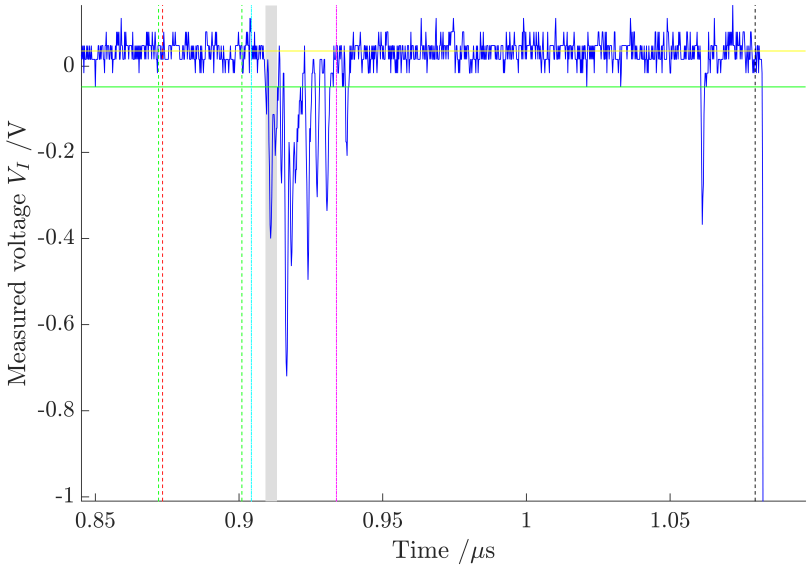

(b) Photomultiplier recording

Passing time: $[t_{fs}, t_{fs} + pt(v_{BD})]$
PM signal
Voltage triggered: $t_{10\%}$
Breakdown: t_{BD}
Offset
Max. background noise
Ref. Camera shutter open and close
$ETA(v_{BD})$
$ETA(v_{BD}/10)$

Figure 6.16: PM recording and reference image of streamer, AV=80 kV, series 23, v_{BD}= 20.0 mm/µs. Liquid: Cyclohexane. Filter: (F1) UV bandpass - peak at 200 nm.

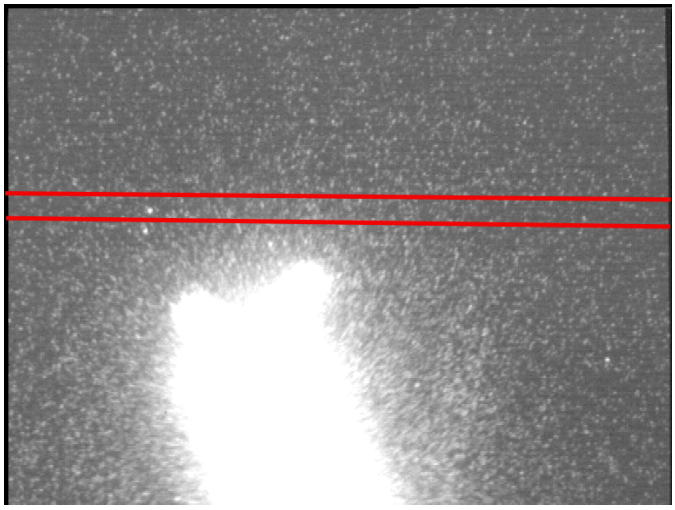

(a) Reference image: Red lines are located at PM's entrance window frames.

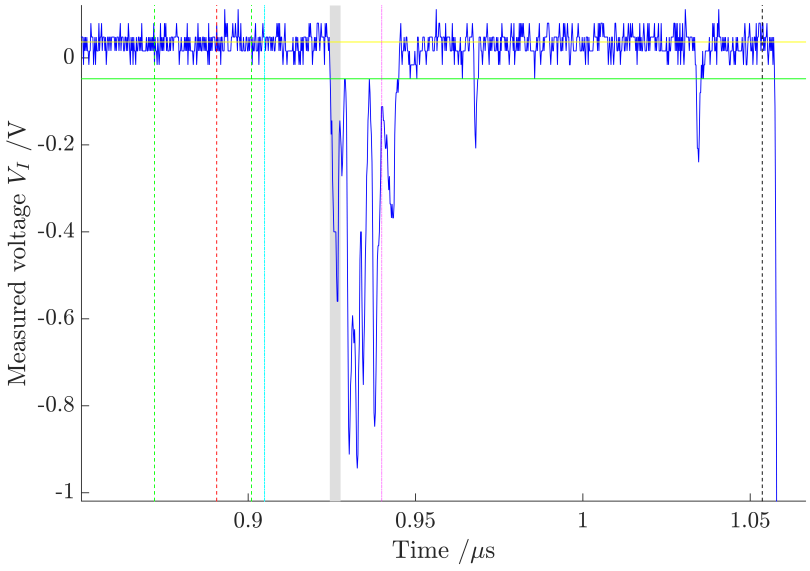

(b) Photomultiplier recording

Passing time: $[t_{fs}, t_{fs} + pt(v_{BD})]$
PM signal
Voltage triggered: $t_{10\%}$
Breakdown: t_{BD}
Offset
Max. background noise
Ref. Camera shutter open and close
$ETA(v_{BD})$
$ETA(v_{BD}/10)$

Figure 6.17: PM recording and reference image of streamer, AV=80 kV, series 23, v_{BD}= 25.3 mm/µs. Liquid: Cyclohexane. Filter: (F1) UV bandpass - peak at 200 nm.

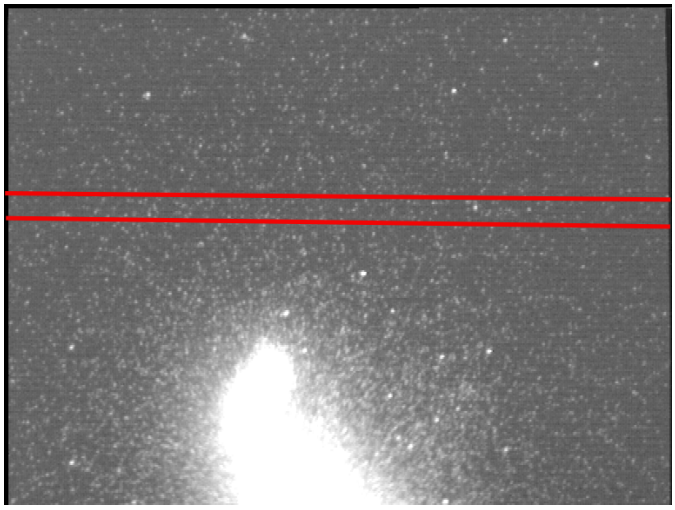

(a) Reference image: Red lines are located at PM's entrance window frames.

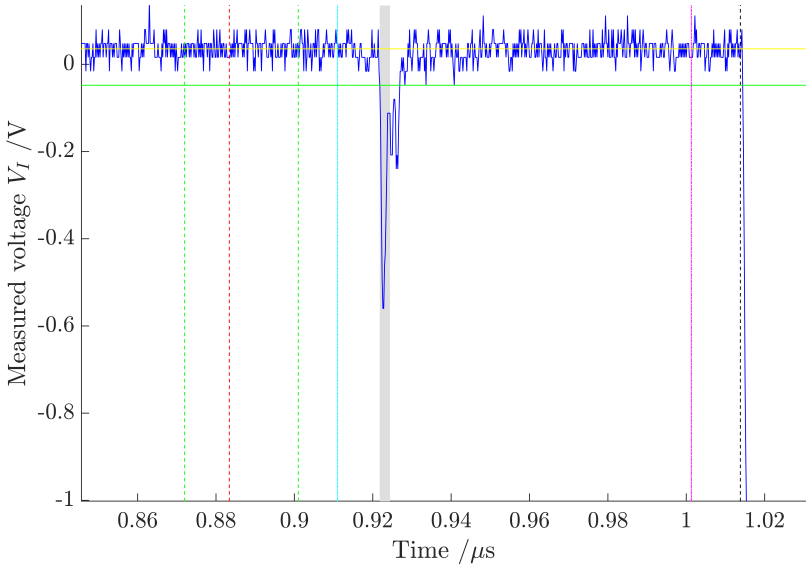

(b) Photomultiplier recording

Passing time: $[t_{fs}, t_{fs} + pt(v_{BD})]$
PM signal
Voltage triggered: $t_{10\%}$
Breakdown: t_{BD}
Offset
Max. background noise
Ref. Camera shutter open and close
$ETA(v_{BD})$
$ETA(v_{BD}/10)$

Figure 6.18: PM recording and reference image of streamer, AV=80 kV, series 23, v_{BD}= 31.7 mm/µs. Liquid: Cyclohexane. Filter: (F1) UV bandpass - peak at 200 nm.

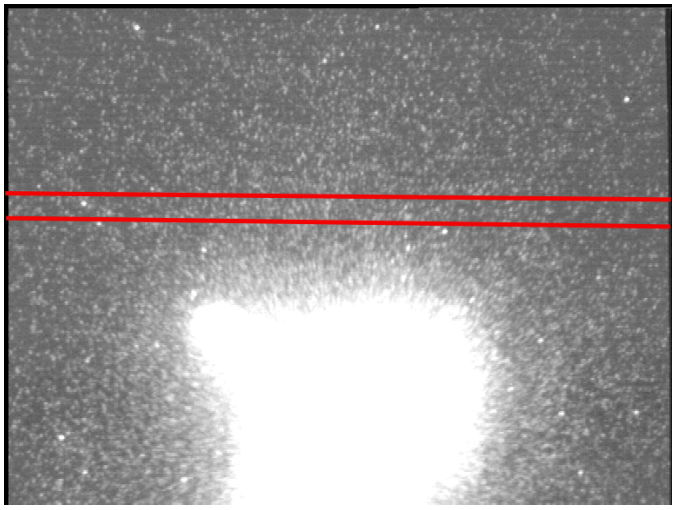

(a) Reference image: Red lines are located at PM's entrance window frames.

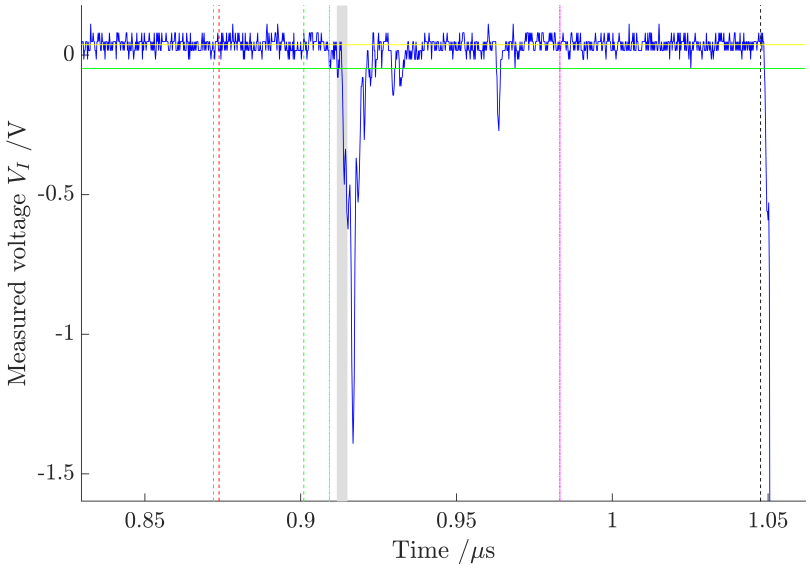

(b) Photomultiplier recording

Passing time: $[t_{fs}, t_{fs} + pt(v_{BD})]$
PM signal
Voltage triggered: $t_{10\%}$
Breakdown: t_{BD}
Offset
Max. background noise
Ref. Camera shutter open and close
$ETA(v_{BD})$
$ETA(v_{BD}/10)$

Figure 6.19: PM recording and reference image of streamer, AV=81 kV, series 23, v_{BD}= 23.8 mm/µs. Liquid: Cyclohexane. Filter: (F1) UV bandpass - peak at 200 nm.

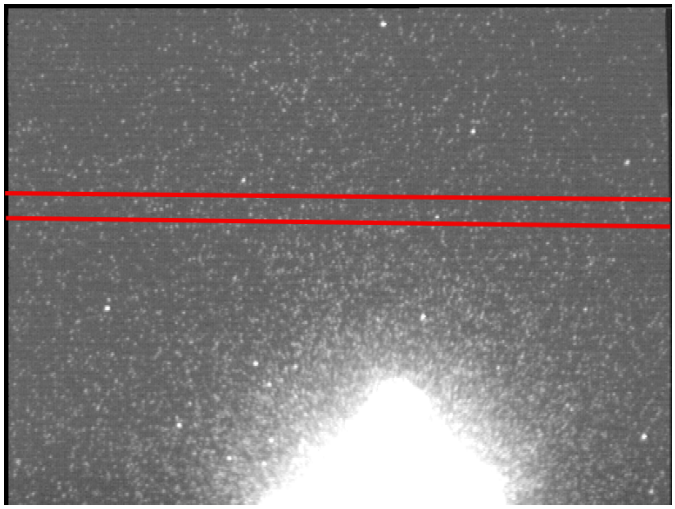

(a) Reference image: Red lines are located at PM's entrance window frames.

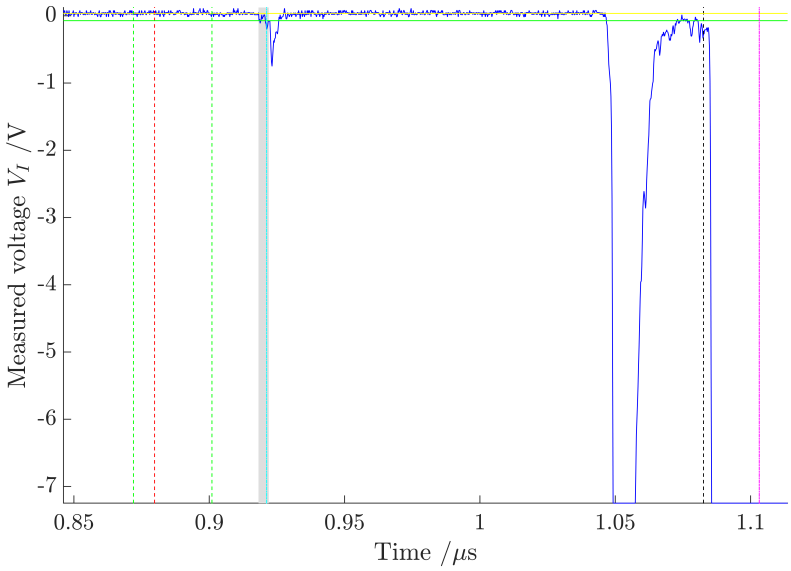

(b) Photomultiplier recording

Passing time: $[t_{fs}, t_{fs} + pt(v_{BD})]$
PM signal
Voltage triggered: $t_{10\%}$
Breakdown: t_{BD}
Offset
Max. background noise
Ref. Camera shutter open and close
$ETA(v_{BD})$
$ETA(v_{BD}/10)$

Figure 6.20: PM recording and reference image of streamer, AV=81 kV, series 23, v_{BD}= 20.4 mm/µs. Liquid: Cyclohexane. Filter: (F1) UV bandpass - peak at 200 nm.

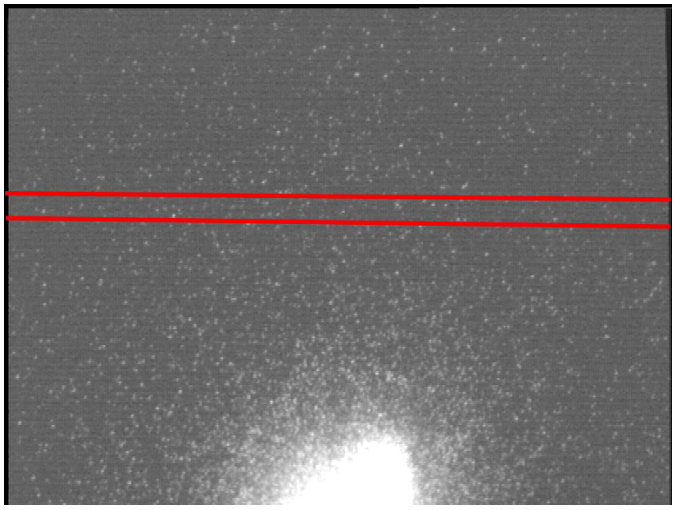

(a) Reference image: Red lines are located at PM's entrance window frames.

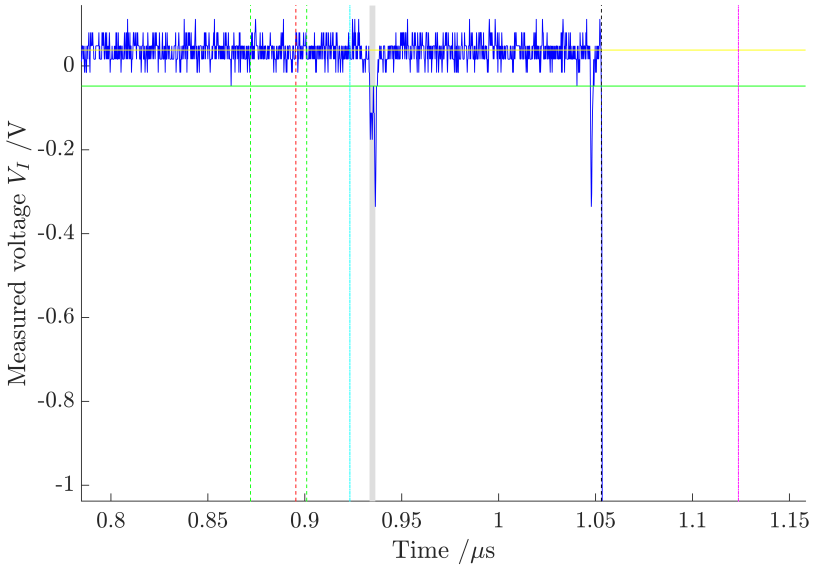

(b) Photomultiplier recording

Passing time: $[t_{fs}, t_{fs} + pt(v_{BD})]$
PM signal
Voltage triggered: $t_{10\%}$
Breakdown: t_{BD}
Offset
Max. background noise
Ref. Camera shutter open and close
$ETA(v_{BD})$
$ETA(v_{BD}/10)$

Figure 6.21: PM recording and reference image of streamer, AV=81 kV, series 23, v_{BD}= 26.2 mm/µs. Liquid: Cyclohexane. Filter: (F1) UV bandpass - peak at 200 nm.

Appendix C: Ionisation, excitation and photon emittance

Ionisation of a molecule is the process where an electron is set free from bound state. Figure 6.22 illustrates how ionisation may happen: impact, field or photo-ionisation, or a combination of these mechanisms[1, 5].

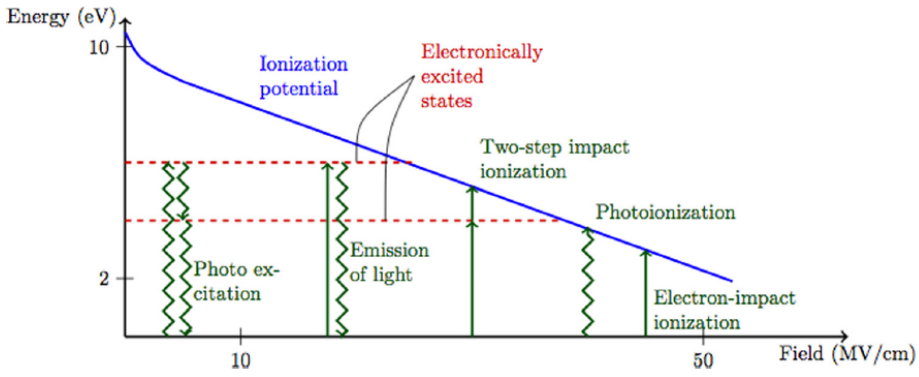

Figure 6.22: Impact, field and photo-ionisation is illustrated. The sketch is copied from [5].

An atom A is excited to A^* when it absorbs the energy equal to the energy difference between the two states. Excitation processes can be described by the following reactions:

$$A + \gamma \rightarrow A^* \tag{6.1}$$
$$A + e^- \rightarrow A^* + e^- \tag{6.2}$$
$$A + B \rightarrow A^* + B \tag{6.3}$$

Case (6.1) is the absorption of a photon γ. Case (6.2) shows excitation as a free electron e^- collides inelastically with A. In case (6.3) thermal

energies excites molecule A as it collides inelastically with an arbitrary molecule B. In streamers the most dominant energy is the high electric current. The electrons are able to transfer a lot of their energy to the heavier molecules[1].

If the absorbed energy is greater than or equal to the ionisation potential IP, then an electron is liberated from its bound state at the molecule A. Then the reactions are either of the following

$$A + \gamma \rightarrow A^+ + e^- \tag{6.4}$$
$$A + e^- \rightarrow A^+ + e^- + e^- \tag{6.5}$$
$$A + B \rightarrow A^+ + e^- + B \tag{6.6}$$

Ions can also be excited, either in a separate reaction from a new collision or combined with the ionisation process. Any absorbed energy exceeding IP will excite the ion into the state $(A^+)^*$. The final reactions would be as in (6.4)-(6.6), but with A^+ swapped by $(A^+)^*$.

Field ionisation is caused by an enhanced probability of tunnelling when the ionisation potential is reduced[38].

Energy is released as electrons become more bound to a molecule, mainly as light or heat [5]. This happens either by de-excitation, i.e. the reversed reaction of (6.1), or as a free electron gets trapped by an ion, like reaction (6.4) reversed. If a photon is emitted, its energy becomes $E_{A^*} - E_A = hf$. The molecule may also de-excite stepwise, causing one photon to be emitted per step.

Appendix D: Photomultiplier noise sources

In this appendix the causes for possible noise and offset in the anode current from a photomultiplier, are described. These noises are present also in the dark current, which is the current through the anode when the tube operates in complete darkness [20]. Noise and offset may be caused by the high voltage supplied, thermionic emission of electrons, glass scintillation, ionisation of residual gases, ohmic leakage and/or field emission.

Dark current increases exponentially with supplied voltage[20]. This will cause an offset when the voltage is fixed.

Thermionic emission of electrons is the effect where thermal energy excites the electrons higher than the work function of the photocathode and MCP materials[20]. This occurs even at room temperature. Hence dark current increases with temperature. It is a predominant factor in dark current.

A photomultiplier tube is designed to be at vacuum inside. However, if residual gases are present, they can be ionised by photoelectrons[20, 25]. Then, later, they collide with the photocathode ore MCP so that secondary electrons are emitted. This would result in relatively large noise in terms of pulses in the output signal, and may be relevant for old photomultiplier tubes, as they are more worn out. One reason that these gases are present, is desorption from the microchannel walls when bombarded with electrons [25].

Glass scintillation occur when electrons deviates from the desired trajectory and strikes the glass envelope[20]. This results in dark pulses[20]. This noise is eliminated by coating the glass with conductive paint and by setting the cathode at ground potential[20].

If the insulation of the tube is imperfect, ohmic leakage may cause dark current [20]. This is predominant at low voltage and temperature.

When operating at maximum voltage rated for the PM, the electric field may be so strong at electrodes that they emit electrons [20]. Therefore the

user manual recommends to operate at least 200 V below the maximum rating. [1]

The photomultiplier tube can become saturated with space charge at high incident light intensities. The ratio between output current and incident light flux is constant up to a certain point where the ratio increases before converging to zero. Hamamatsu Photonics K.K. reports the output current of pulsed peaks to deviate with $5\,\%$ from its linearity at $130\,\mathrm{mA}$ for PMT R2286U-02 [21]. This corresponds to 6.5 V across a $50\,\Omega$ resistor.

Another effect of high incident light intensity, is dead time. Dead time is the time required for the MCP to recover from charge depletion due to large numbers of secondary emissions [25]. This implies that high current pulses in the output are followed by dead time. During dead time, the MCP gain will be reduced. This is a source of error.

Wiza deduces that a typical MCP with channel capacitance $C = 7.4 \times 10^{-17}\,\mathrm{F}$ and resistance $R = 2.75 \times 10^{14}\,\Omega$, will have channel recovery time of the order $1 \times 10^{-2}\,\mathrm{s}$[25], i.e. the RC time constant of a the DC circuit across this channel alone. The effective dead time of an entire MCP is however more proportional to a set of parallel channels. Given 10^5 channels in a plate operating almost independently, the effective dead time is of the order $100\,\mathrm{ns}$.

[1] The maximum rated voltage for the photomultiplier PMT R2286U-02 used in present experiment, is 4200 V.